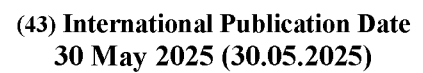
(12) INTERNATIONAL APPLICATION PUBLISHED UNDER THE PATENT COOPERATION TREATY (PCT)

(19) World Intellectual Property Organization

International Bureau







(10) International Publication Number WO 2025/111491 A1

(51) International Patent Classification:

B01D 69/14 (2006.01) **B01D 69/10** (2006.01) **B01D 71/02** (2006.01) **B01D 69/12** (2006.01)

B01D 71/38 (2006.01)

(21) International Application Number:

PCT/US2024/056939

(22) International Filing Date:

21 November 2024 (21.11.2024)

(25) Filing Language: English

(26) Publication Language: English

(30) Priority Data:

63/601,542 21 November 2023 (21.11.2023) US

(71) Applicants: THE RESEARCH FOUNDATION FOR THE STATE UNIVERSITY OF NEW YORK [US/US]; Technology Transfer, University at Buffalo, UB Commons, 520 Lee Entrance, Suite 109, Amherst, New York 14228 (US). BROOKHAVEN SCIENCE ASSOCIATES, LLC

[US/US]; 40 Brookhaven Avenue, Building 460, Upton, New York 11973 (US).

- (72) Inventors: LIN, Haiqing; 386 N. Rockingham Way, Amherst, New York 14228 (US). HU, Leiqing; 316 Furnas Hall, Buffalo, New York 14260 (US). BUI, Vinh; 4280 Chestnut Ridge Road, Apartment E4, Buffalo, New York 14228 (US). SUBRAMANIAN, Ashwanth; 8900 SW Sweek Drive, Apartment 1413, Tualatin, Oregon 97062 (US). LEE, Won-II; 85 Artist Lake Drive, Middle Island, New York 11953 (US). KISSLINGER, Kim; 48 Vista Drive, Manorville, New York 11949 (US). NAM, Chang-Yong; 6 Spaulding Lane, Stony Brook, New York 11973 (US).
- (74) Agent: ROMAN, JR., Paul J. et al.; Hodgson Russ LLP, 140 Pearl Street, Suite 100, BUFFALO, New York 14202-4040 (US).
- (81) Designated States (unless otherwise indicated, for every kind of national protection available): AE, AG, AL, AM, AO, AT, AU, AZ, BA, BB, BG, BH, BN, BR, BW, BY, BZ, CA, CH, CL, CN, CO, CR, CU, CV, CZ, DE, DJ, DK, DM,

(54) Title: POLYMER-BASED MEMBRANES, METHODS OF MAKING SAME, AND USES THEREOF

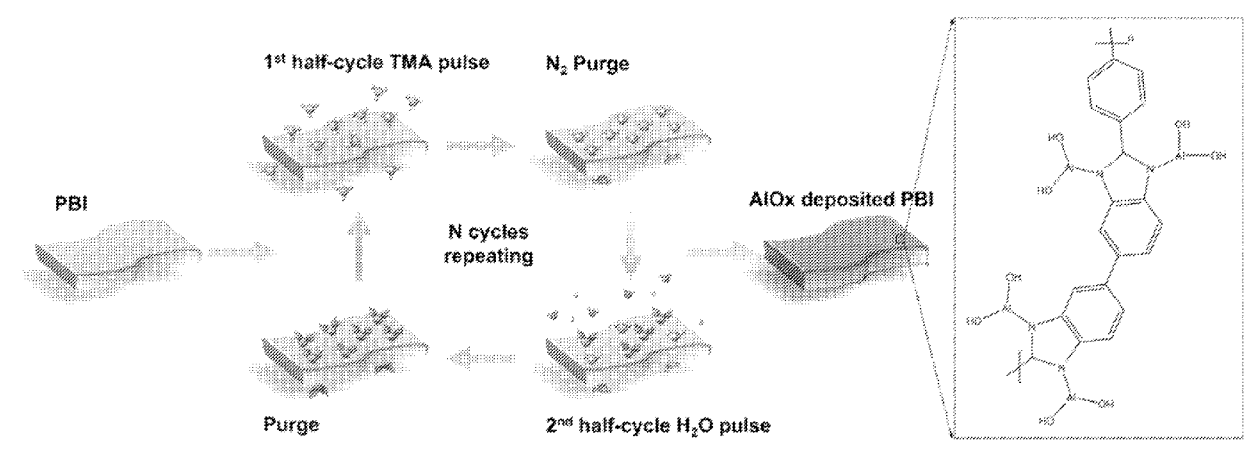


FIG. 5

(57) Abstract: Polymer-based membranes and methods of making and uses of polymer-based membranes. In various examples, a polymer-based membrane comprises a polymer film and a metal oxide layer, where the polymer chains of the polymer film are crosslinked by metal oxide groups or a carbonized polymer film comprising a plurality of micropores or a polyorganosilica film comprising a plurality of ultramicropores and a plurality of a metal oxide domains disposed on at least a portion of an exterior surface of at least a portion of the micropores or ultramicropores. In various examples, a polymer-based membrane is produced by contacting a polymer film or a carbonized polymer film or a polyorganosilica film with one or more vapor-phase precursor(s) and optionally, water vapor, such as, for example, in an atomic layer deposition process. In various examples, a polymer-based membrane or system comprising a polymer-based membrane is used in a gas, such as, for example, hydrogen or carbon dioxide, separation and/or enrichment process.

DO, DZ, EC, EE, EG, ES, FI, GB, GD, GE, GH, GM, GT, HN, HR, HU, ID, IL, IN, IQ, IR, IS, IT, JM, JO, JP, KE, KG, KH, KN, KP, KR, KW, KZ, LA, LC, LK, LR, LS, LU, LY, MA, MD, MG, MK, MN, MU, MW, MX, MY, MZ, NA, NG, NI, NO, NZ, OM, PA, PE, PG, PH, PL, PT, QA, RO, RS, RU, RW, SA, SC, SD, SE, SG, SK, SL, ST, SV, SY, TH, TJ, TM, TN, TR, TT, TZ, UA, UG, US, UZ, VC, VN, WS, ZA, ZM, ZW.

(84) Designated States (unless otherwise indicated, for every kind of regional protection available): ARIPO (BW, CV, GH, GM, KE, LR, LS, MW, MZ, NA, RW, SC, SD, SL, ST, SZ, TZ, UG, ZM, ZW), Eurasian (AM, AZ, BY, KG, KZ, RU, TJ, TM), European (AL, AT, BE, BG, CH, CY, CZ, DE, DK, EE, ES, FI, FR, GB, GR, HR, HU, IE, IS, IT, LT, LU, LV, MC, ME, MK, MT, NL, NO, PL, PT, RO, RS, SE, SI, SK, SM, TR), OAPI (BF, BJ, CF, CG, CI, CM, GA, GN, GQ, GW, KM, ML, MR, NE, SN, TD, TG).

Published:

— with international search report (Art. 21(3))

POLYMER-BASED MEMBRANES, METHODS OF MAKING SAME, AND USES THEREOF

CROSS REFERENCE TO RELATED APPLICATIONS

[0001] This application claims the benefit of U.S. Provisional Application No.

5 63/601,542, filed November 21, 2023; the contents of the above-identified application are hereby fully incorporated herein by reference in their entirety.

STATEMENT REGARDING FEDERALLY SPONSORED RESEARCH OR DEVELOPMENT

[0002] This invention was made with government support under grant numbers 2044623 awarded by National Science Foundation and DE-FE0031636, DE-FE0032209, and DE-SC0012704 awarded by Department of Energy. The government has certain rights in the invention.

BACKGROUND

10

15

20

25

30

[0003] The separation of CO₂ from mixtures with H₂ is one of the most important gas separations, producing 94 million metric tons of H₂ worldwide, valued at \$170 billion in 2021. The need of CO₂ removal will grow tremendously if the Integrated Gasification Combined Cycle (IGCC) processes to produce power gains wider acceptance. Considering the enormous amount of hydrogen produced in this process, any improvement in H₂/CO₂ separation efficiency would lead to significant savings in H₂ production and power production.

[0004] Membranes offer an approach for hydrogen purification and CO₂ capture due to their simplicity of operation and high energy efficiency. The existing H₂-selective membrane materials have rigid polymer chains with strong size-sieving ability to maximize the diffusivity selectivity. However, the rigid polymer chains often lead to low diffusion coefficient and low permeability, which prevents the ready adoption of this energy efficient technology. On the other hand, conventional polymer engineering, such as cross-linking and blending, is always subject to the trade-off between permeability and selectivity.

[0005] The removal of CO₂ from mixtures with hydrogen is often achieved using adsorption and absorption (such as Selexol[™] absorption) processes, which operate at 10 °C or below. There is intensive research on H₂-selective membranes for H₂/CO₂ separation, though no commercial membrane products have been developed yet, due to the lack of the materials with high performance at temperatures up to 150 °C.

10

15

20

30

[0006] Functional surface plays a critical role in a variety of applications, and the ability to uniformly deposit angstrom (Å)-scale thin layers is desirable. Atomic layer deposition (ALD) has emerged as an attractive approach, as it utilizes reactions between alternative gaseous precursors, depositing dense thin layers with well-controlled thicknesses. It can effectively modify the hydrophilicity and chemistries of the dense surface, fine-tune the pore size and porosity at a molecular level for porous substrates, and improve the resistance to solvents. As such, ALD has demonstrated the potential to improve polymer performance, such as water treatment, membrane liquid separations, energy storage, and catalysts. ALD holds promise to precisely fine-tune the pore size and thus size-sieving ability in polymeric membranes to improve gas separation performance in a scalable way, partially because commercial membranes comprise very thin selective layers and any modification at nanoscales exerts a significant impact on the overall performance. However, ALD has been conventionally used to generate AlOx layers to improve barrier properties for gases and vapors, with a few studies on gas separation focused on a polymer of intrinsic microporosity (PIM-1). For instance, PIM-1 was treated with ALD using trimethylaluminum (TMA) and water, and 6-cycle AlO_x deposition decreased the pore size from 6.5–8.5 to 6.2 Å and increased CO₂/CH₄ selectivity by 260% from 15.7 to 56.2. However, the reduced pore size decreased CO₂ permeability by more than one order of magnitude from 8287 to 624 Barrer (1 Barrer = 10^{-10} cm³(STP) cm cm⁻² s⁻¹ cmHg⁻¹). On the other hand, an enormous amount of functional polymers have been developed for societally important gas separations, such as H₂/CO₂ separation for clean H₂ purification and pre-combustion CO₂ capture. There is a substantial gap in understanding how ALD nanotechnology may impact the nanostructures of functional polymers and thus gas separation performance, limiting the application of ALD on polymeric membranes for industrial gas separations.

25 SUMMARY OF THE DISCLOSURE

[0007] The present disclosure provides, *inter alia*, polymer-based membranes. The present disclosure also provides methods of making and uses of polymer-based membranes. [0008] In an aspect, the present disclosure provides polymer-based membranes. In various examples, a polymer-based membrane is a gas separation and/or gas enrichment membrane or the like. In various examples, a polymer-based membrane is made by a method of the present disclosure. In various examples, a polymer-based membrane comprises a polymer film (which may be a free-standing polymer film or the like) and a metal oxide layer disposed on at least a portion or all an exterior surface or surfaces of the polymer film. In

10

15

20

25

30

various examples, a polymer-based membrane comprises a carbonized polymer film or a polyorganosilica film or the like; and a plurality of metal oxide domains, disposed on at least a portion or all of the exterior surface or surfaces of at least a portion, substantially all, or all the micropores or ultramicropores. In various examples, a polymer-based membrane or membranes are be used for hydrogen separation, such as, for example, hydrogen purification and CO₂ capture, for example, in hydrogen production plants and power plants, hydrogen recovery from refinery off-gas and natural gas liquid production, hydrogen recovery from mixtures with nitrogen in ammonia plants, hydrogen removal from syngas for methanol plants, hydrogen separation from mixtures with helium, and the like.

[0009] In an aspect, the present disclosure provides methods of making polymer-based membranes. In various examples, a method produces one or more polymer-based membrane(s) of the present disclosure. In various examples, a method of making a one or more polymer-based membrane(s) comprises forming a polymer film or forming a polymer film on at least a portion of, substantially all, or all the exterior surfaces of a substrate or an interlayer disposed on a substrate; optionally, drying the polymer film; optionally, carbonizing the polymer film or optionally, plasma treating the polymer film; and contacting the polymer film with one or more vapor-phase metal oxide precursor(s) (e.g., in (or as part of) an atomic layer deposition (ALD) method or the like), and, optionally, water vapor, optionally, repeating the contacting a desired number of times, where the polymer-based membrane(s) is/are formed. The method may comprise one or more (e.g., a plurality of) contacting(s). In various examples, multiple contactings are carried out sequentially.

[0010] In an aspect, the present disclosure provides systems. In various examples, a

system comprises one or more polymer-based membrane(s) of the present disclosure and/or one or more polymer-based membrane(s) made by a method of present disclosure. In various examples, the system is a gas separation and/or gas enrichment system or the like. In various examples, the system is configured as gas separation and/or gas enrichment system or the like. In various examples, one or more polymer-based membrane(s) is/are disposed in a housing or the like. In various examples, the system further comprises one or more additional component(s) typically used in a gas separation and/or enrichment system. In various examples, the system is configured for normal flow, tangential flow filtration, or the like, or any combination thereof.

[0011] In an aspect, the present disclosure provides uses of polymer-based membrane(s) of the present disclosure. In various examples, a polymer-based membrane or polymer-based membranes (or a system comprising polymer-based membrane(s)) is/are used in a gas

15

separation and/or enrichment process or the like. In various examples, a method of separating one or more gas(es) from a mixture comprising the one or more gas(es) and at least one other gas and/or enriching one or more gas(es) in a mixture comprising at least one other gas comprises: contacting the mixture or the like) with one or more polymer-based membrane(s) of the present disclosure and/or a polymer-based membrane/polymer-based membranes made by a method of present disclosure and/or a system of the present disclosure; and optionally, repeating the contacting with contacted mixture or a portion thereof a desired number of times (such as, for example, until a desired separation and/or enrichment is achieved, where one or more of the gas(es) in the mixture is separated from the mixture (or the contacted mixture) and/or enriched in the mixture (or the contacted mixture).

[0012] In various examples, the present disclosure provides polymer-based membranes that are a scalable platform to engineer a membrane surface at an atomic level. This approach can, in various examples, effectively tune chain packing and surface chemistry of the polymeric materials, thus leading to enhanced separation properties of the polymer-based membranes for various separations and/or enrichments.

BRIEF DESCRIPTION OF THE FIGURES

- [0013] For a fuller understanding of the nature and objects of the disclosure, reference should be made to the following detailed description taken in conjunction with the accompanying figures.
- 20 **[0014]** FIGS. 1A–1K show an ALD schematic and morphology for PBI-xC. FIG. 1A shows the reactions. FIG. 1B shows three phases including AlO_x, PBI/AlO_x hybrid, and PBI bulk doped by TMA. FIG. 1C shows AlO_x thickness on Si wafers and PBI films as a function of ALD cycles. Cross-sectional HAADF TEM micrographs of PBI-3C are shown in FIG. 1D and of PBI-17C are shown in FIG. 1F. EDS elemental mapping of PBI-3C is shown in FIG.
- 1E and of PBI-17C s shown FIG. 1G. SEM cross-sectional images and in-situ Al EDS mappings of PBI-1C is shown in FIG. 1H, of PBI-3C is shown in FIG. 1I, of PBI-11C is shown in FIG, 1J, and of PBI-17C is shown in FIG. 1K.
- [0015] FIGS. 2A–2F show physicochemical properties of the PBI-xC samples. FIG. 2A shows surface roughness determined from AFM images. FIG. 2B shows high-resolution XPS spectra of Al 2p. FIG. 2C shows the molar ratios of Al/C and Al/N. FIG. 2D shows the WAXD patterns. FIG. 2E shows the glass transition temperature (*T_g*). FIG. 2F shows tensile stress-strain curves.

- [0016] FIGS. 3A–3D show pure-gas H₂/CO₂ separation properties of PBI-xC at 35 °C. H₂/CO₂ separation properties for PBI-xC as a function of ALD cycles at 7.8 atm (FIG. 3A), and PBI-3C as a function of feed gas pressure (FIG. 3B). FIG. 3C shows CO₂ and C₂H₆ solubility at 7.8 atm and FIG. 3D shows CO₂ diffusivity as a function of feed gas pressure.
- 5 [0017] FIGS. 4A–4E show mixed-gas H₂/CO₂ separation performance with H₂/CO₂ of 50:50 in PBI-xC. FIG. 4A shows H₂ permeability as a function of temperature. FIG. 4B shows H₂/CO₂ selectivity as a function of temperature. FIG. 4C shows a comparison with Robeson's upper bound at 200 °C. FIG. 4D shows long-term stability of PBI-1C in dry-wet-dry conditions at 7.8 atm and 200 °C for 100 h (h = hour(s)). FIG. 4E shows comparison with state-of-the-art polymeric materials (Table 5), including PBI-(H₃PO₄)-0.16, PBI-TCL-6H, PBI-SCA4-17, PBI-SCA8-10, PBI-TMA-0.22, PBI-TaA-0.32, PBI-NiT-0.17, CPAM-15, PBI-TBB-0.213, P84-BuDA-6H, IP PA, IP PBDI, and IP BILPs. The last number in the sample names represents the testing temperatures (°C).
 - [0018] FIG. 5 shows a schematic of a full ALD deposition cycle on PBI film.
- 15 [0019] FIGS. 6A–6F show 3-Dimensional (3D) surface images of PBI (FIG. 6A), PBI-1C (FIG. 6B), PBI-3C (FIG. 6C), PBI-11C (FIG. 6D), and PBI-17C (FIG. 6E) detected using AFM. FIG. 6F shows surface maximum height (R_{max}) and root-mean-squared average of the height (R_q) analyzed from their AFM images.
 - [0020] FIG. 7 shows survey scan spectra of PBI and PBI-xC using XPS.
- 20 [0021] FIGS. 8A–8F show images of water contact angles (WCAs) for PBI (FIG. 8A), PBI-1C (FIG. 8B), PBI-3C (FIG. 8C), PBI-11 C (FIG. 8D), and PBI-17 C (FIG. 8E). FIG. 8F shows the water contact angle as a function of ALD cycles.
 - [0022] FIG. 9A shows a comparison of the density of PBI-xC and PBI-TMA-xC as a function of cycles. FIG. 9B shows WAXD patterns of PBI, PBI-TMA-3C, and PBI-TMA-
- 25 17C. FIG. 9C shows TGA curves of the PBI-xC films. FIG. 9D shows DTA curves of the PBI-xC films. FIG. 9E shows DSC curves of the PBI-xC films. FIG. 9F shows refined DSC curves of the PBI-xC films.
 - [0023] FIG. 10A shows pure-gas permeability and selectivity as a function of TMA pulsing cycles, and FIG. 10B shows pure-gas permeability and selectivity as a function of the feed pressure in PBI. FIG. 10C shows CO₂ and FIG. 10D shows C₂H₆ sorption isotherms of PBI, PBI-3C, and PBI-17C at 35 °C. FIG. 10E shows mixed-gas CO₂ permeability as a function of temperature.
 - [0024] FIGS. 11A–11E show sequential low-temperature carbonization and VPI of PBI to obtain PBI*T_c-t* for H₂/CO₂ separation. FIG. 11A shows a schematic of VPI nanoengineering.

10

15

permeability.

FIG. 11B shows bright-field scanning transmission electron microscopy (STEM) images of the bulk area, and FIG. 11C shows STEM images of the area beneath the surface for the cross-section of PBI600-100×3C. STEM-energy dispersive spectroscopy (EDS) elemental mappings of PBI600-100×3C are shown in FIGS. 11D and 11E including Al, O, and C (FIG. 11D), and Al only (FIG. 11E).

[0025] FIGS. 12A–12F show nanostructures of PBI*T_c-t* as a function of the TMA exposure time (*t*, s). FIG. 12A shows high-resolution x-ray photoelectron spectroscopy (XPS) spectra of Al 2p, and FIG. 12B shows molar ratios of Al/C and Al/N. FIG. 12C shows tensile stress-strain curves. FIG. 12D shows the *d*-spacing of PBI600-*t*. FIG. 12E shows pore volume and surface area, and FIG. 12F shows pore size distribution obtained by non-local density functional theory (NLDFT) from N₂ sorption at –196 °C.

[0026] FIGS. 13A–13F show pure-gas H₂/CO₂ separation properties of PBI*T_c-t* at 100 °C. FIG. 13A shows the effect of the TMA exposure time (*t*) for PBI600-*t* on gas permeability. FIG. 13B shows a comparison of H₂ permeability, and FIG. 13C shows a comparison of H₂/CO₂ selectivity in PBI*T_c* and PBI*T_c*-100. FIG. 13D shows CO₂ and C₂H₆ sorption isotherms of PBI600 and PBI600-100. FIG. 13E shows CO₂ solubility and diffusivity of PBI600-*t*. FIG. 13F shows comparison with the 2008 Robeson's upper bound at 100 °C. For PBI*T_c-t* samples, increasing *t* from 0 to 100 s increases selectivity and decreases H₂

20 [0027] FIGS. 14A–14E show H₂/CO₂ separation performance of PBI550-100. FIG. 14A shows the effect of CO₂ partial pressure, and FIG. 14B shows the effect of temperature. FIG. 14C shows the long-term stability in dry-wet-dry conditions at 150 °C. FIG. 14D shows a comparison of PBI500-100 and PBI550-100 with the leading CMS materials with T_c < 700 °C, including PBI-PPA600, PBI600, cellophane600, Torlon675, MTI aramide675,</p>

cellulose600, metal oxide-PFA525, Matrimid500, and PPG-Cellulose550. FIG. 14E shows a comparison with CMS*T_c* with *T_c* ≥ 700 °C (including polyimide700, cellulose700, PBI900, Torlon925, MTI aramide925, CANAL-TB900, PABZ-6FDA850, and polyester800) and other ALD-engineered materials (including Pd/Al₂O₃, PBI/Al₂O₃, ZIF-8, PIM-1/Al₂O₃, and SSZ-13). The values after @ represent testing temperature, and P and M represent pure-gas and mixed-gas permeation, respectively. The details are also summarized in Table 12.

[0028] FIGS. 15A–15D show the morphology and H₂/CO₂ separation performance of PBI550-100 TFC membranes. FIG. 15A shows a photo of a polymer-based membrane and FIG. 15B shows a SEM cross-section image. FIG. 15C shows pure-gas permeance and H₂/CO₂ selectivity as a function of temperature. FIG. 15D shows a comparison with other

15

20

25

leading CMS membranes with T_c < 700 °C (including Torlon675, MTI aramide675, cellulose550, metal oxide-PFA525, and Matrimid500) and those with $T_c \ge 700$ °C (including polyimide700, Torlon925, MTI aramide925, cellulose850, and polyester800). The upper bound was estimated assuming 1 μ m-thick selective layers. The details are summarized in Table 14.

[0029] FIGS. 16A and 16B shows cross-sectional bright-field scanning transmission electron micropore (STEM) images of PBI600 (FIG. 16A) and PBI600-100 (FIG. 16B).

[0030] FIG. 17A show Raman spectra and FIG. 17B shows XPS spectra of PBI600-*t* samples (with 1 cycle). FIG. 17C shows XPS spectrum of PBI600-100×3C. FIGS. 17D and 17E show WAXD patterns of PBI600-*t* (FIG. 17D), and PBI, PBI500, PBI550, and their VPI-treated samples (FIG. 17E). FIG. 17F shows the skeletal density, bulk density, and porosity of PBI600-*t* films.

[0031] FIGS. 18A–18D show SEM surface (left) and cross-sectional (right) images of PBI600 (FIG. 18A), PBI600-40 (FIG. 18B), PBI600-70 (FIG. 18C), and PBI600-100 (FIG. 18D).

[0032] FIGS. 19A and 19B show HAADF-STEM EDS mappings and corresponding element compositions of bulk area (FIG. 19A) and surface area of PBI600-100×3C (FIG. 19B): C (an example of which is identified with an arrow), Al (an example of which is identified with an arrow), and N (an example of which is identified with an arrow). Cross-sectional high-angle annular dark field scanning transmission electron microscopy (HAADF-STEM) (left) and STEM-energy dispersive spectroscopy (EDS) elemental maps (right) are shown, specifically of PBI600 (FIG. 19C), PBI600-40 (FIG. 19D), PBI600-70 (FIG. 19E), and PBI600-100 (FIG. 19F): C (an example of which is identified with an arrow). N (an example of which is identified with an arrow), and Pt (an example of which is identified with an arrow).

[0033] FIG. 20 shows N_2 adsorption isotherms of PBI600 and PBI600-t at -196 °C.

[0034] FIGS. 21A and 21B show SEM surface images of PBI550-100 TFC membrane with intact PDMS layer (FIG. 21A) and scratched PDMS layer (FIG. 21B).

30 [0035] FIGS. 22A-22C show physical properties and C₃H₆/C₃H₈ separation properties of 6FDA-DAM500-x. FIG. 22A shows WAXD, FIG. 22B shows Raman, and FIG. 22C C₃H₆/C₃H₈ separation.

[0036] FIG. 23A shows a schematic of chemical structure changes from rubbery polysiloxane to POSi and AlOx-POSi. FIGS. 23B-23D show SEM cross-sectional images of

20

25

30

POSi membrane (FIG. 23B), POSi-3C (FIG. 23C), and SEM surface of POSi-3C (FIG. 23D). FIG. 23E shows surface roughness values of POSi membranes at different ALD cycle, obtained from AFM characterization.

[0037] FIG. 24A shows gas transport properties of POSi membranes with different number of ALD cycle at 150°C and 60 psi. FIG. 24B shows an ideal H₂/gas selectivity of POSi-AlOx membranes.

[0038] FIG. 25A shows the temperature effect on the H₂/CO₂ separation performance of POSi-1C. FIG. 25B shows the effect of feed concentrations on the H₂/CO₂ separation performance of POSi-3C. FIG. 25C shows the long-term stability of POSi-3C.

10 DETAILED DESCRIPTION OF THE DISCLOSURE

[0039] Although subject matter of the present disclosure is described in terms of certain embodiments and examples, other embodiments and examples, including embodiments and examples that do not provide all the benefits and features set forth herein, are also within the scope of this disclosure. For example, various structural, logical, and process step changes may be made without departing from the scope of the disclosure.

As used herein, unless otherwise indicated, "about", "substantially", or "the like", [0040] when used in connection with a measurable variable (such as, for example, a parameter, an amount, a temporal duration, or the like) or a list of alternatives, is meant to encompass variations of and from the specified value including, but not limited to, those within experimental error (which can be determined by, e.g., a given data set, an art accepted standard, etc. and/or with, e.g., a given confidence interval (e.g., 90%, 95%, or more confidence interval from the mean), such as, for example, variations of +/-10% or less, +/-5% or less, +/-1% or less, and +/-0.1% or less of and from the specified value), insofar such variations in a variable and/or variations in the alternatives are appropriate to perform in the instant disclosure. As used herein, the term "about" may mean that the amount or value in question is the exact value or a value that provides equivalent results or effects as recited in the claims or taught herein. That is, it is understood that amounts, sizes, compositions, parameters, and other quantities and characteristics are not and need not be exact, but may be approximate and/or larger or smaller, as desired, reflecting tolerances, conversion factors, rounding off, measurement error, or the like, or other factors known to those of skill in the art such that equivalent results or effects are obtained. In general, an amount, size, composition, parameter, or other quantity or characteristic, or alternative is "about" or "the like," whether or not expressly stated to be such. It is understood that where "about," is used before a

15

20

25

30

quantitative value, the parameter also includes the specific quantitative value itself, unless specifically stated otherwise.

[0041] Ranges of values are disclosed herein. The ranges set out a lower limit value and an upper limit value. Unless otherwise stated, the ranges include the lower limit value, the upper limit value, and all values between the lower limit value and the upper limit value, including, but not limited to, all values to the magnitude of the smallest value (either the lower limit value or the upper limit value) of a range. It is to be understood that such a range format is used for convenience and brevity, and thus, should be interpreted in a flexible manner to include not only the numerical values explicitly recited as the limits of the range, but also to include all the individual numerical values or sub-ranges encompassed within that range as if each numerical value and sub-range is explicitly recited. To illustrate, a numerical range of "0.1% to 5%" should be interpreted to include not only the explicitly recited values of 0.1% to 5%, but also, unless otherwise stated, include individual values (e.g., 1%, 2%, 3%, and 4%) and the sub-ranges (e.g., 0.5% to 1.1%; 0.5% to 2.4%; 0.5% to 3.2%, and 0.5% to 4.4%, and other possible sub-ranges) within the indicated range. It is also understood (as presented above) that there are a number of values disclosed herein, and that each value is also herein disclosed as "about" that particular value in addition to the value itself. For example, if the value "10" is disclosed, then "about 10" is also disclosed. Ranges can be expressed herein as from "about" one particular value, and/or to "about" another particular value. Similarly, when values are expressed as approximations, by use of the antecedent "about", it will be understood that the particular value forms a further disclosure. For example, if the value "about 10" is disclosed, then "10" is also disclosed.

[0042] As used herein, unless otherwise stated, the term "structural analog" refers to any polymer, precursor, gas, or the like that can be envisioned to arise from an original polymer, precursor, gas, or the like, if one atom or group of atoms, functional groups, or substructures of the original polymer, precursor, gas, or the like is replaced with another atom or group of atoms, functional groups, substructures, or the like. In various examples, the term "structural analog" refers to any group that is derived from an original any polymer, precursor, gas, or the like, for example, by a chemical reaction or the like, where the polymer, precursor, gas, or the like is modified or partially substituted, such that at least one structural feature of the original polymer, precursor, gas, or the like is retained.

[0043] As used herein, unless otherwise stated, the term "group" refers to a chemical entity that is monovalent (i.e., has one terminus that can be (is) covalently bonded to other chemical species), divalent, or polyvalent (i.e., has two or more termini that can be (are)

15

20

25

30

covalently bonded to other chemical species). The term "group" also includes radicals (e.g., monovalent radicals and multivalent radicals, such as, for example, divalent radicals, trivalent radicals, and the like). Illustrative examples of groups include:

$$-\xi$$
-CH₃ $-\xi$ -CH₂- ξ - ξ -, and the like.

5 **[0044]** The present disclosure provides, *inter alia*, polymer-based membranes. The present disclosure also provides methods of making and uses of polymer-based membranes.

[0045] In an aspect, the present disclosure provides polymer-based membranes. In various examples, a polymer-based membrane is a gas separation and/or gas enrichment membrane (such as, for example, a H₂/CO₂ separation membrane or the like) or the like. In various examples, a polymer-based membrane is made by a method of the present disclosure. Non-limiting examples of polymer-based membrane layers are disclosed herein.

[0046] In various examples, a polymer-based membrane comprises (or consists essentially of or consists of) a polymer film (which may be a free-standing polymer film or the like) (which may be referred to as a polymer layer) and a metal oxide layer (such as, for example, an Al Ox (aluminum oxide) layer or the like) disposed on at least a portion or all an exterior surface or surfaces of the polymer film. In various examples, at least a portion of the polymer chains are immobilized and/or crosslinked by metal oxide group(s) (such as, for example, AlOx group(s) or the like). In various examples, a polymer-based membrane comprising a polymer film does not comprise any material, structure, or the like that materially affects the use of the polymer-based membranes in gas separation, gas enrichment, or the like (such as, for example, materials, structures, or the like used in biological applications).

[0047] In various examples, a polymer-based membrane comprises a carbonized polymer film (which may be a free-standing carbonized polymer film or the like) or a polyorganosilica film (which may be a free-standing polyorganosilica film or the like) (e.g., comprising a porous silica-like POSi structure or the like); and a plurality of metal oxide domains (such as, for example, AlOx (aluminum oxide) domains or the like, which may comprise stoichiometric aluminum oxide, sub-stoichiometric aluminum oxide, or the like, or any combination thereof, or the like), disposed on at least a portion or all the an exterior surface or surfaces of at least a portion, substantially all, or all the micropores or ultramicropores. In various examples, at least a portion, substantially all, or all of the metal oxide domains are infiltrated into at least a portion, substantially all, or all of the surface micropores (which may

10

15

20

25

30

result in molecular sieving behavior, such as, for example, molecular sieving behavior that increases H₂/CO₂ selectivity without significant loss of H₂ permeability at elevated temperatures or the like). In various examples, a polymer-based membrane comprising the carbonized polymer film is a carbon molecular sieve (CMS) membrane or the like. In various examples, a carbonized polymer-based membrane comprising a carbonized polymer film or a polyorganosilica-based membrane does not comprise any material, structure, or the like that materially affects the use of the polymer-based membranes in gas separation, gas enrichment, or the like (such as, for example, materials, structures, or the like used in biological applications).

[0048] In various examples, a polymer-based membrane (e.g., a gas separation membrane or the like) comprises: (i) optionally, a substrate (which may be a porous substrate); optionally, an interlayer disposed on the substrate (on which the polymer film is disposed); and a polymer film (which may be a free-standing polymer film or the like) comprising a plurality of polymer chains; and a metal oxide layer (such as, for example, an AlOx (aluminum oxide) layer or the like), which may comprise a stoichiometric metal oxide (such as, for example, a stoichiometric aluminum oxide or the like), a sub-stoichiometric metal oxide (such as, for example, a sub-stoichiometric aluminum oxide, or the like) or the like, or any combination thereof, disposed on at least a portion or all of an exterior surface or surfaces of the polymer film, wherein at least a portion of the polymer chains are immobilized and/or crosslinked by metal oxide groups (such as, for example, AlOx groups or the like), or (i) optionally, a substrate (which may be a porous substrate); optionally, an interlayer disposed on the substrate (on which the polymer film is disposed); a carbonized polymer film (which may be a free-standing carbonized polymer film or the like) comprising a plurality of micropores or a polyorganosilica film (which may be a free-standing polyorganosilica film or the like) comprising a plurality of ultramicropores; and a plurality of a metal oxide domains (such as, for example, AlOx (aluminum oxide) domains or the like), which may comprise stoichiometric aluminum oxide, sub-stoichiometric aluminum oxide, or the like, or any combination thereof, disposed on at least a portion or all of an exterior surface or surfaces of at least a portion, substantially all, or all of the micropores or ultramicropores.

[0049] Various substrates can be used. A substrate can have various forms, compositions, etc. In various examples, a substrate is a porous substrate or non-porous substrate. In various examples, a substrate is planar (e.g., a planar substrate). In various examples, a substrate is an ultrafiltration membrane, a microfiltration membrane, or the like. In various examples, a substrate is a cylindrical (e.g., a tube, such as, for example, a ceramic tube or the like) or the

15

20

25

30

like. In various examples, a fiber is a hollow fiber comprising a hollow wall (or at least a portion of a wall is hollow), and the hollow wall or the hollow portion of a wall comprises a plurality of pores (such as, for example a plurality of pores comprising at least one linear dimension (which may be a cross-sectional dimension, such as, for example, a diameter, or the like) (which may be average pore dimension(s) of from about 1 nm to about 100 nm, including all 0.1 nm values and ranges therebetween (e.g., about 5 nm to about 50 nm, about 5 nm, about 10 nm, about 10 nm, or about 50 nm)). In various examples, a substrate is aluminum oxide (AAO) (such as, for example, flat AAO (e.g., anodic flat AAO or the like)), cylindrical α-alumina hollow fiber (HF) or a plurality thereof, or the like.

[0050] In various examples, a substrate is (or comprises) one or more polymer material(s), one or more inorganic material(s) (such as, for example, metal(s), ceramic material(s), or the like, or any combination thereof), or the like, or any combination thereof. In various examples, a substrate is (or comprises) a metal chosen from stainless steel, titanium, zirconium, tin, tungsten, and the like, and any combination thereof and/or a ceramic material chosen from aluminum oxide, titanium oxide, zirconium oxide, tin oxide, tungsten oxide, and the like, and any combination thereof. In various examples, a substrate is (or comprises) a polymer chosen from polysulfones, polyethersulfones, polyacrylonitriles, polyvinylidene fluorides, polysiloxanes, structural analogs thereof, and the like, and any combination thereof.

[0051] A polymer-based membrane may comprise an interlayer. In various examples, in the case of a porous substrate, an interlayer prevents (e.g., substantially prevents) penetration of polymer into surface pores of the porous substrate. An interlayer is disposed on at least a portion of, substantially all, or all of a surface or surfaces of a substrate and is disposed between a polymer film or carbonized polymer film or a polyorganosilica film. In various examples, (in the case where the interlayer is present) an interlayer is disposed on at least a portion, substantially all, or all of a surface (such as, for example, exterior surface or the like) or all the surfaces (such as, for example, exterior surfaces or the like) of the substrate.

[0052] In various examples, an interlayer is gutter layer. Without intending to be bound by any particular theory, it is considered the interlayer provides a desirable surface for forming a polymer film. In various examples, an interlayer is dense layer. In various examples, an interlayer is dense layer comprising desirable (e.g., high) gas permeance (e.g., the interlayer does not adversely affect gas flow thru the polymer film.

[0053] In various examples, an interlayer is an intermediate layer. In various examples, a polymer-based membrane comprises an intermediate layer (comprising metal oxide groups

10

15

20

25

30

covalently bound to polymer groups) disposed between a bulk polymer film and a bulk metal oxide layer.

[0054] In various examples, an interlayer comprises one or more linear dimension(s) (e.g., a linear dimension substantially perpendicular or perpendicular to a longest linear dimension of the interlayer (or perpendicular to a plane defined by the interlayer), such as, for example, a thickness, a cross-sectional dimension, or the like, or the like) of about 10 nm to about 1,000 nm, including all 0.1 nm values and ranges therebetween. In various examples, an interlayer is (or comprises) one or more polymer material(s) (, one or more inorganic material(s) (such as, for example, metal(s), ceramic material(s), or the like, or any combination thereof), or the like, or any combination thereof.

[0055] An interlayer can comprise various polymers materials, inorganic layers, or the like, or any combination thereof. Non-limiting examples of polymer materials and inorganic layers include substrate materials as described herein. In various examples, an interlayer is (or comprises) a material chosen from zeolites, alumina, zirconia, titania, polymer materials (such as, for example, polydimethylsiloxane and poly(1-trimethylsilyl-1-propyne and the like), and the like, and any combination thereof.

[0056] A polymer-based membrane can comprise various polymer films. In various examples, a polymer film is disposed on at least a portion, substantially all, or all of a surface (such as, for example, exterior surface or the like) or all the surfaces (such as, for example, exterior surfaces or the like) of the substrate (in the case where the interlayer is not present). In various examples, a polymer film is disposed at least a portion, substantially all, or all of a surface (such as, for example, an exterior surface or the like) of the interlayer (in the case where the interlayer is present).

[0057] A polymer film can have various shapes. In various examples, a polymer film is tubular, a hollow fiber, flat (e.g., substantially flat sheet), or the like.

[0058] In various examples, a polymer film comprises one or more polymer(s). A polymer film may be referred to as a selective layer. In various examples, a polymer is a homopolymer, a copolymer (such as, for example, a block copolymer, a random copolymer, or the like, or any combination thereof), or the like. In various examples, a polymer is not crosslinked or is crosslinked. In various examples, a polymer comprises a plurality of oxygen-containing groups, nitrogen-containing groups, sulfur-containing groups, or the like). In various examples, these groups can react with a metal oxide precursor to form interchain and/or intrachain crosslinking groups formed from a metal oxide precursor. In various examples, a polymer film comprises one or more elastomer(s) (such as, for example,

15

20

25

30

thermoplastic elastomer(s) or the like). Non-limiting examples of polymers include polybenzimidazoles, polyimides, polyamides, polysulfones, polycarbonates, cellulose acetates, Pebax polymers, PolyActive polymers, polyethers, polysiloxanes, structural analogs thereof, or the like, copolymers thereof (such as, for example copolymers comprising polyetheroxide or the like), or any combination thereof. Non-limiting examples of polymer films include films of (or films comprising) Pebax® (a block copolymer variation of PEBA (polyether block amide): a block copolymer obtained by polycondensation of a carboxylic acid polyamide with an alcohol termination polyether), a block copolymer comprising a soft block/segment or soft blocks/segments and a hard block/segment or hard blocks/segments (such as, for example, PolyActive (polyethylene oxide (soft block/segment)/ polybutylene terephthalate (PBT) (hard block/segment) or the like), or the like or any combination thereof. [0059] A polymer can have various molecular weights. In various examples, a polymer has a molecular weight (Mw and/or Mn or about 10,000 to about 1,000,000 g/mol, including all 0.1 g/mol values and ranges therebetween.

[0060] A polymer film can have various sizes. In various examples, a polymer film comprises one or more linear dimension(s) (e.g., a linear dimension substantially perpendicular or a longest linear dimension of the polymer film (or perpendicular to a plane defined by the polymer film), such as, for example, a thickness, a cross-sectional dimension, or the like, or the like) of about 10 nm to about 10,000 nm, including all 0.1 nm values and ranges therebetween.

[0061] A polymer-based membrane can comprise various metal oxide layers. In various examples, a metal oxide group of a metal oxide layer immobilize and/or crosslink polymer chains (e.g., intrachain and/or intrachain immobilize and/or crossklink) of a polymer film. In various examples, the metal oxide layer (such as, for example, AlOx layer or the like) is continuous or discontinuous and/or the AlOx layer complexes (e.g., forms one or more covalent bond(s) with the polymer film). In various examples, a metal oxide is chosen from stoichiometric aluminum oxide, sub-stoichiometric aluminum oxide (AlOx), and the like, stoichiometric titanium oxide, sub-stoichiometric titanium oxide (SiOx), and the like, stoichiometric zinc oxide, sub-stoichiometric zinc oxide (ZnOx), and the like, stoichiometric tin oxide, sub-stoichiometric zinc oxide (ZnOx), and the like, structural analogs thereof, and any combination thereof.

[0062] A metal oxide layer can have various sizes. In various examples, a metal oxide layer (such as, for example, AlOx layer or the like) comprises one or more linear

10

15

20

25

30

dimension(s) (e.g., a linear dimension substantially perpendicular or a longest linear dimension of the polymer film (or perpendicular to a plane defined by the polymer film), such as, for example, a thickness, a cross-sectional dimension, or the like, or the like) of about 10 nm to about 10,000 nm, including all 0.1 nm values and ranges therebetween.

[0063] A polymer-based membrane can comprise various carbonized polymer films. In various examples, a polymer-based membrane comprises a carbonized polymer film comprising a plurality of micropores (such as, for example, surface micropores or the like). In various examples, at least a portion, substantially all, or all of the micropores comprise a size (e.g., a linear dimension (such as, for example, a diameter or the like) of about 2 nm to about 100 nm, including all 0.1 nm values and ranges therebetween), which may be an average size; and/or the porosity is about 1 volume percent to about 20 volume percent (based on the total volume of the polymer -based membrane or carbonized polymer film), including all 0.1 percent values and ranges therebetween.

[0064] A polymer-based membrane can comprise various polyorganosilica films. In various examples, a polymer-based membrane comprises a polyorganosilica film comprising a plurality of ultramicropores (such as, for example, surface ultramicropores or the like). In various examples, at least a portion, substantially all, or all of the ultramicropores comprise a size (e.g., a linear dimension (such as, for example, a diameter or the like) of about 0.3 nm to about 1 nm, including all 0.01 nm values and ranges therebetween), which may be an average size; and/or the porosity is about 1 volume percent to about 20 volume percent (based on the total volume of the polymer -based membrane or polyorganosilica film), including all 0.1 percent values and ranges therebetween.

[0065] A carbonized polymer film or polyorganosilica film can comprise various metal oxide layers and/or metal oxide domains. In various examples, a metal oxide layer or metal oxide domain is a stoichiometric metal oxide domain, a sub-stoichiometric metal oxide domain, or the like, or any combination thereof. In various examples, a metal oxide layer or metal oxide domains is/are chosen from AlOx layers or domains (e.g., a stoichiometric AlOx layer or domain, a sub-stoichiometric AlOx layer or domain, and the like, and any combination thereof), SiOx layers or domain, and the like, and any combination thereof), TiOx layers or domains (e.g., a stoichiometric TiOx layer or domain, a sub-stoichiometric TiOx layer or domain, and the like, and any combination thereof), ZnOx layers or domains (e.g., a stoichiometric ZnOx layer or domain, and the like, and any combination thereof), SnOx layers or domain, and the like, and any combination thereof), SnOx layers or domains (e.g., a stoichiometric SnOx

15

20

25

30

layer or domain, a sub-stoichiometric SnOx layer or domain, and the like, and any combination thereof), and the like, and structural analogs thereof, and any combination thereof.

[0066] A polymer-based membrane may comprise nanoparticles. In various examples, a polymer film or a carbonized polymer film or a polyorganosilica film also comprises a plurality of nanoparticles. In various examples, a combination of two or more structurally and/or compositionally different nanoparticles. In various examples, at least a portion, substantially all, or all of the nanoparticles are metal-organic fragments or the like. In various examples, the nanoparticles are chosen from zeolitic imidazolate framework-8 (ZIF-8) (e.g., comprising a size of about 30 nm to about 200 nm, including all 0.1 nm values and ranges therebetween), ZIF-7 (e.g., comprising a size of about 20 nm to about 100 nm, including all 0.1 nm values and ranges therebetween), ZIF-67 (e.g., having a size of about 30 nm to about 200 nm, including all 0.1 nm values and ranges therebetween), UiO-66 (e.g., having a size of about 50 nm to about 200 nm, including all 0.1 nm values and ranges therebetween), UiO-66-NH₂ (e.g., having a size of about 50 nm to about 50 nm, including all 0.1 nm values and ranges therebetween).

[0067] Nanoparticles can have various sizes. In various examples, at least a portion, substantially all, or all of the nanoparticles have a size (e.g., a linear dimension (such as, for example, a diameter or the like) of about 10 nm to about 100 nm, including all 0.1 nm values and ranges therebetween) and/or are present in the polymer film at about 0 to about 40 percent by weight (based on the total weight of the polymer film), including all 0.1 weight percent values and ranges therebetween (e.g., about 1 weight percent to about 40 weight percent).

[0068] A polymer-based membrane can have various shapes. In various examples, a polymer-based membrane is tubular, a hollow fiber, flat (e.g., substantially flat sheet), or the like.

[0069] The size (area or the like) and/or form of a polymer-based membrane is not particularly limited. Processing methods/equipment that can be used to fabricate polymer-based membranes of a wide-range of areas and/or forms are known in the art. In various examples, the area of a polymer-based membrane is an area typically used in membrane gas separation and/or gas enrichment process or the like.

[0070] A polymer-based membrane can have various uses or can be configured for various uses. In various examples, a polymer-based membrane or membranes are be used for hydrogen separation, such as, for example, hydrogen purification and CO₂ capture, for

20

25

example, in hydrogen production plants and power plants, hydrogen recovery from refinery off-gas and natural gas liquid production, hydrogen recovery from mixtures with nitrogen in ammonia plants, hydrogen removal from syngas for methanol plants, hydrogen separation from mixtures with helium, and the like. In various examples, a membrane is configured for normal flow modes, tangential flow modes, or the like.

[0071] A polymer-based membrane can exhibit desirable properties. In various examples, a polymer-based membrane exhibits one or more or all of the following: desirable H₂ permeability (e.g., an H₂ permeability of about 1 to about 1000 Barrer), which may be up to about 200 °C or about 300 °C;

desirable H₂/CO₂ selectivity (e.g., an H₂/CO₂ selectivity of about 10 to about 200); which may be up to about 200 °C or about 300 °C; or desirable thermal stability (e.g., thermal stability to about at least about 200 °C or about 300 °C).

[0072] In an aspect, the present disclosure provides methods of making polymer-based membranes. In various examples, a method produces one or more polymer-based membrane(s) of the present disclosure. Non-limiting examples of methods of making polymer-based membranes are disclosed herein.

[0073] In various examples, a method of making a one or more polymer-based membrane(s) comprises forming a polymer film (e.g., a free-standing polymer film) or forming a polymer film on at least a portion of, substantially all, or all the exterior surfaces of a substrate (which may be a porous substrate) or an interlayer disposed on a substrate; optionally, drying the polymer film; optionally, carbonizing (e.g., at least partially, substantially, or completely carbonizing) the polymer film (e.g., such that a carbonized polymer film comprising a plurality of micropores (such as, for example, surface micropores or the like) is formed) or optionally, plasma treating the polymer film; and contacting the polymer film (e.g., the layer) with one or more vapor-phase metal oxide precursor(s) (such as, for example, one or more vapor-phase AlOx precursor(s) or the like) (e.g., in (or as part of) an atomic layer deposition (ALD) method or the like), and, optionally, water vapor, optionally, repeating the contacting a desired number of times, where the polymer-based membrane(s) is/are formed.

In various examples, a method of making a one or more polymer-based membrane(s) comprises contacting a polymer film (e.g., a layer) (such as, for example, a free-standing polymer film or a polymer film disposed on at least a portion of, substantially all, or all the exterior surfaces of a substrate (which may be a porous substrate), or an interlayer disposed on a substrate, or the like) (which may be a preformed polymer film) with

10

15

20

25

30

one or more vapor-phase metal oxide precursor(s) (such as, for example, one or more vapor-phase AlOx precursor(s) or the like) (e.g., in (or as part of) an atomic layer deposition (ALD) method or the like), and, optionally, water vapor, optionally, repeating the contacting a desired number of times, where the polymer-based membrane(s) is/are formed.

[0075] In various examples, a method of making a one or more polymer-based membrane(s) comprises, contacting a carbonized polymer film (e.g., a layer) or polyorganosilica film with one or more vapor-phase metal oxide precursor(s) (such as, for example, one or more vapor-phase AlOx precursor(s) or the like) (e.g., in (or as part of) an atomic layer deposition (ALD) method or the like), and, optionally, water vapor, optionally, repeating the contacting a desired number of times, where the polymer-based membrane(s) is/are formed. In various examples, the method further comprises carbonizing a polymer film (such as, for example, a free-standing polymer film or a polymer film disposed on at least a portion of, substantially all, or all the exterior surfaces of a substrate (which may be a porous substrate), or an interlayer disposed on a substrate, or the like) (which may be a preformed polymer film).

[0076] Various polymer films can be used. In various examples, a polymer film is formed as part of a method. In various examples, a polymer film is a pre-formed polymer film. A polymer film can be formed in a variety of manners, processes, and the like. Suitable polymer processes are known in the art. In various examples, a polymer film is formed by casting (such as, for example, solvent casting, spin casting, or the like), extrusion, coating, or the like. Non-limiting examples of polymers that comprise a polymer film or can be used to form a polymer film include polymers as described herein (e.g., with respect to the polymer-based membranes). In various examples, a polymer film comprises hydroxyl group(s) (which may be intrinsic hydroxyl groups or hydroxyl groups formed as a result of contacting a polymer film with water.

[0077] A method may comprise plasma treating a polymer film. In various examples, a method further comprises plasma treating (such as, for example, oxygen plasma treating or the like) a polymer film (e.g., a polysiloxane film or the like) before the polymer film is contacted with a vapor-phase metal oxide precursor(s). In various examples, a polymer film (e.g., a polysiloxane film or the like) is oxygen plasma treated using an ICP-RIE plasma chamber or the like. In various examples, plasma treatment of a polysiloxane film provides a plasma-treated film with a porous (e.g., ultramicroporous or the like) silica-like POSi structure with hydroxyl groups (-OH).

[0078] A polymer film or a carbonized polymer film or polyorganosilica film may comprise nanoparticles. In various examples, a polymer film or a carbonized polymer film comprises a plurality of nanoparticles. Non-limiting examples of nanoparticles include nanoparticles as described herein (e.g., with respect to the polymer-based membranes). 5 [0079] A method can use various metal oxide precursor(s). Without intending to be bound by any particular theory, it is considered a vapor-phase metal oxide precursor (such as, for example, a vapor-phase AlOx precursor) reacts to form at least a portion of or all the metal oxide in a metal oxide layer (such as, for example, an AlOx layer) or a metal oxide domain (such as, for example, an AlOx domain), or the like, in and/or on a polymer film. In 10 various examples, a vapor-phase metal oxide precursor is (or all vapor-phase metal oxide precursors are) stable at a temperature and/or pressure at which the precursor(s) exhibit(s) desirable vapor pressure. Non-limiting examples of vapor-phase metal oxide precursor(s) include vapor-phase AlOx precursors, vapor-phase SiOx precursors, vapor-phase TiOx precursors, vapor-phase ZnOx precursors, vapor-phase SnOx precursors, or the like, 15 structural analogs thereof, or any combination thereof. Non-limiting examples of vapor-phase AlOx precursor(s) include trialkyl aluminum compounds (such as, for example, trimethyl aluminum (TMA), or the like, structural analogs thereof, or any combination thereof) or any combination thereof; and/or the vapor-phase SiOx precursor(s) is/are chosen from silicon tetrahalide compounds (such as, for example, silicon tetrachloride, and the like, structural 20 analogs thereof, and any combination thereof), tris(dialkyl amino)silane compounds (such as, for example, tris(dimethylamino)silane, and the like, structural analogs thereof, and any combination thereof), and the like, structural analogs thereof, and any combination thereof; and/or the vapor-phase TiOx precursor(s) is/are chosen from titanium alkoxide compounds (such as, for example, titanium isopropoxide (TTIP), and the like, structural analogs thereof, 25 and any combination thereof), titanium halide compounds (such as, for example, titanium tetrachloride, and the like, structural analogs thereof, and any combination thereof), and the like, structural analogs thereof, and any combination thereof; and/or the vapor-phase ZnOx precursor(s) is/are chosen from dialkyl zinc compounds (such as, for example, diethyl zinc, and the like, and any combination thereof), or the like, structural analogs thereof, or any 30 combination thereof) or any combination thereof and/or the vapor-phase SnOx precursor(s) is/are chosen from stannic halide compounds (such as, for example, stannic chloride, and the like, structural analogs thereof, and any combination thereof), and the like, and any combination thereof.

15

20

25

30

[0080] A vapor-phase precursor or precursors can be used at various pressures. In various examples, contacting the polymer film with one or more vapor-phase precursor(s) is carried out in (or as part of) an atomic layer deposition (ALD) process or the like. In various examples, the pressure of the vapor-phase metal oxide precursor(s) (such as, for example, vapor-phase AlOx precursor(s) or the like) and/or water vapor is in the range typically used for processes such as, for example, ALD or the like.

[0081] A method may comprise one or more (e.g., a plurality of) contacting(s). In various examples, a contacting may be referred to as a cycle). In various examples, a contacting comprises a vapor phase infiltration (VPI) process. As an illustrative example, a polymer film or a carbonized polymer film or a polyorganosilica film is contacted with one or more vaporphase precursor(s) (such as, for example, AlOx precursor(s) or the like) and then contacted with water vapor (the combination of which may be referred to a cycle). In various examples, the atmosphere in which the film is disposed is purged with nitrogen after each contacting.

[0082] In various examples, multiple contactings are carried out sequentially. In various examples, a contacting is repeated 1, 2, 3, 4, 5, 6, 7, 8, 9, 10, 11, 12, 13, 14, 15, 16, 17, 18, 19, 20, or more times, where the vapor-phase precursor(s) is/are the same or at least one or more of the vapor-phase precursor(s) is different for one or more or all of the contacting(s).

[0083] In various examples, each contacting with one or more vapor-phase metal oxide precursor(s) (such as, for example, vapor-phase AlOx precursor(s) or the like) and/or water vapor and/or nitrogen gas is carried out in discrete (or separate) steps (such as, for example, pulses or the like). In various examples, each contacting with one or more vapor-phase metal oxide precursor(s) (such as, for example, vapor-phase AlOx precursor(s) or the like) and/or water vapor and/or nitrogen gas is carried out in pulse (such as, for example, pulses independently having a duration of about 5 to about20 seconds, including all 0.1 second values and ranges therebetween (e.g., about 5 seconds, about 10 seconds, or about 15 seconds).

[0084] In various examples, one or more metal oxide domain(s) (such as, for example, AlOx domain(s) or the like) are formed in at least a portion of, substantially all, or all of the micropores of the carbonized polymer film or the ultramicropores of the polyorganosilica film as a result of the contacting. In various examples, the contacting forms metal oxide (such as, for example, AlOx or the like), which may be in the form of one or more metal oxide domain(s) (such as, for example, AlOx domain(s) or the like) that is/are infiltrated in a micropore or micropores (such as, for example, a surface micropore or micropores or the like) of the carbonized polymer film or an ultramicropore or ultramicropores (such as, for

15

20

25

30

example, a surface ultramicropore or ultramicropores or the like) of the polyorganosilica film. In various examples, at least a portion of the polymer chains are immobilized and/or crosslinked by metal oxide group(s) (such as, for example, AlOx group(s) or the like) formed as a result of the contacting.

5 **[0085]** The methods comprise various reactions and processes. A reaction or process can be performed under various reaction conditions (e.g., time, temperature, pressure, or the like, or any combination thereof).

[0086] A reaction can be carried out for various times. The reaction time can depend on factors such as, for example, temperature, atmosphere, pressure, presence and/or reactivity of the vapor-phase metal oxide precursor(s), presence and/or intensity of an applied energy source, or the like, any a combination thereof.

[0087] In an aspect, the present disclosure provides systems. In various examples, a system comprises one or more polymer-based membrane(s) of the present disclosure and/or one or more polymer-based membrane(s) made by a method of present disclosure. Non-limiting examples of systems are disclosed herein.

[0088] In various examples, a system is a gas separation and/or gas enrichment system or the like. In various examples, a system is configured as gas separation and/or gas enrichment system or the like.

[0089] In various examples, one or more polymer-based membrane(s) is/are disposed in a housing, the housing comprising one or more orafic(es) (e.g., orifice(es) independently configured for introduction, control, or the like of gas(es) into the housing or removal of gas(es) from the housing). In various examples, a system further comprises one or more additional component(s) typically used in a gas separation and/or enrichment system (such as, for example, pump(s), mass/flow controller(s), reservoir(s), tank(s), pressure gauges, or the like, or any combination thereof, which may or may not be in gas contact with one or more of the polymer-based membrane(s). In various examples, the polymer-based membrane(s) is/are disposed in a housing, the housing comprising one or more orafic(es), which may be in gas contact with one or more mixtures. In various examples, a system comprises one or more or all the features of a system described herein. In various examples, a system is configured for normal flow, tangential flow filtration, or the like, or any combination thereof.

[0090] In an aspect, the present disclosure provides uses of polymer-based membrane(s) of the present disclosure. Non-limiting examples of uses of polymer-based membrane(s) layers are disclosed herein.

15

20

25

[0091] In various examples, a polymer-based membrane or polymer-based membranes (or a system comprising polymer-based membrane(s)) is/are used in a gas separation and/or enrichment process or the like. In various examples, a polymer-based membrane or polymer-based membranes (or a system comprising polymer-based membrane(s)) is/are used in a hydrogen purification and/or carbon dioxide capture process.

[0092] In various examples, a gas separation and/or enrichment process (such as, for example, a hydrogen purification and/or carbon dioxide capture process or the like) is carried out under pressure. In various examples, the contacting(s) is/are carried out under pressure. A separation and/or enrichment process can be carried out at various temperatures and/or pressures.

[0093] In various examples, a method of separating one or more gas(es) from a mixture comprising the one or more gas(es) and at least one other gas and/or enriching one or more gas(es) in a mixture comprising at least one other gas comprises: contacting the mixture or the like) with one or more polymer-based membrane(s) of the present disclosure and/or a polymer-based membranes made by a method of present disclosure and/or a system of the present disclosure; and optionally, repeating the contacting with contacted mixture or a portion thereof a desired number of times (such as, for example, until a desired separation and/or enrichment is achieved (e.g., observed), where one or more of the gas(es) in the mixture is separated from the mixture (or the contacted mixture) and/or enriched in the mixture (or the contacted mixture).

[0094] Various gases can be separated and/or enriched. Non-limiting examples of gases include H₂, CO₂, N₂, O₂, He, hydrocarbons (such as, for example, alkanes (e.g., C₁, C₂, C₃, C₄, C₅, C₆, C₇, and C₈ alkanes, such as, for example, methane and the like), alkenes (e.g., C₁, C₂, C₃, C₄, C₅, C₆, C₇, and C₈ alkenes), aromatic compounds (e.g., C₅ and C₆ aromatic compounds, such as, for example, benzene, toluene, xylenes, and the like) and the like, and structural analogs thereof, and any combination thereof. As illustrative examples, H₂ is separated from or enriched in a mixture comprising H₂ and CO₂ or CO₂ is separated from or enriched in a mixture comprising H₂ and CO₂. In various example, a method is a hydrogen gas purification and/or a carbon dioxide capture process, or the like.

Joseph Jo

20

25

30

[0096] In various examples, a method provides a gas or gases (such as, for example, H₂, CO₂, N₂, or the like, or a structural analog thereof, or a combination thereof) at a purity of about 60 mol% or weight% or greater, about 70 mol% or weight% or greater, about 80 mol% or weight% or greater, about 90 mol% or weight% or greater, about 98.5 mol% or weight% or greater, about 99 mol% or weight% or greater, about 99.5 mol% or weight% or greater, about 99.9 mol% or weight% or greater, or about 100 mol% or weight % (based on the total amount of gas(es) in the mixture) (e.g., wherein the mixture initially (e.g., before the contacting(s)) comprises the gas(es) at a lower (e.g., substantially lower) concentration and/or other gas(es).

[0097] A polymer-based membrane or one or more or all of the membranes may be reused. In various examples, polymer-based membrane(s) is/are reused in a subsequent separation and/or enrichment (such as, for example, a second separation and/or enrichment, a third separation and/or enrichment, etc.). In various examples, polymer-based membranes(s) is/are cleaned prior to use in each of the subsequent separation(s) and/or enrichment(s).

[0098] The following Statements describe various examples of polymer-based membranes, methods of making polymer-based membranes and uses thereof of the present disclosure and are not intended to be in any way limiting:
 Statement 1. A polymer-based membrane (e.g., a gas separation membrane or the like)

Statement 1. A polymer-based membrane (e.g., a gas separation membrane or the like) comprising: (A) optionally, a substrate (which may be a porous substrate); optionally, an interlayer disposed on the substrate (on which the polymer film/layer is disposed); and a polymer film (which may be a free-standing polymer film or the like) comprising a plurality of polymer chains; and a metal oxide layer (such as, for example, an AlOx (aluminum oxide) layer or the like), which may comprise a stoichiometric metal oxide (such as, for example, a stoichiometric aluminum oxide or the like), a sub-stoichiometric metal oxide (such as, for example, a sub-stoichiometric aluminum oxide, or the like) or the like, or any combination thereof, disposed on at least a portion or all of an exterior surface or surfaces of the polymer film, where at least a portion of the polymer chains are immobilized and/or crosslinked by metal oxide groups (such as, for example, AlOx groups or the like), or (B) optionally, a substrate (which may be a porous substrate); optionally, an interlayer disposed on the

substrate (on which the polymer film/layer is disposed); a carbonized polymer film (which may be a free-standing carbonized polymer film or the like) comprising a plurality of micropores or a polyorganosilica film (which may be a free-standing polyorganosilica film or the like) comprising a plurality of ultramicropores; and a plurality of a metal oxide domains (such as, for example, AlOx (aluminum oxide) domains or the like), which may comprise

20

25

30

stoichiometric aluminum oxide, sub-stoichiometric aluminum oxide, or the like, or any combination thereof, disposed on at least a portion or all of an exterior surface or surfaces of at least a portion, substantially all, or all of the micropores or ultramicropores.

Statement 2. A polymer-based membrane according to Statement 1, where the polymer film comprises polybenzimidazole, polyimides, polyamides, polysulfones, polycarbonates, cellulose acetates, Pebax polymers, PolyActive polymers, polyethers, polysiloxanes, structural analogs thereof, or the like, copolymers thereof (such as, for example copolymers comprising polyetheroxide or the like), or any combination thereof.

Statement 3. A polymer-based membrane according to Statement 1 or 2, where the polymer film comprises one or more linear dimension(s) (e.g., a linear dimension substantially perpendicular or a longest linear dimension of the polymer film (or perpendicular to a plane defined by the polymer film), such as, for example, a thickness, a cross-sectional dimension, or the like, or the like) of about 10 nm to about 10,000 nm, including all 0.1 nm values and ranges therebetween.

Statement 4. A polymer-based membrane according to any one of the preceding Statements, where the metal oxide layer (such as, for example, AlOx layer or the like) comprises one or more linear dimension(s) (e.g., a linear dimension substantially perpendicular or a longest linear dimension of the polymer film (or perpendicular to a plane defined by the polymer film), such as, for example, a thickness, a cross-sectional dimension, or the like, or the like) of about 10 nm to about 10,000 nm, including all 0.1 nm values and ranges therebetween. Statement 5. A polymer-based membrane according to any of the preceding Statements, where the polymer-based membrane comprises a carbonized polymer film comprising a plurality of micropores (such as, for example, surface micropores or the like) where, at least a portion, substantially all, or all of the micropores comprise a size (e.g., a linear dimension (such as, for example, a diameter or the like) of about 2 nm to about 100 nm, including all 0.1 nm values and ranges therebetween) or a polyorganosilica film comprising a plurality of ultramicropores (such as, for example, surface ultramicropores or the like) where, at least a portion, substantially all, or all of the ultramicropores comprise a size (e.g., a linear dimension (such as, for example, a diameter or the like) of about 0.3 nm to about 1 nm, including all 0.01 nm values and ranges therebetween), which may be an average size; and/or the porosity of the carbonized polymer film or polyorganosilica film) is about 1 volume percent to about 20 volume percent (based on the total volume of the polymer -based membrane (e.g., the carbonized polymer film or polyorganosilica film), including all 0.1 percent values and ranges therebetween.

Statement 6. A polymer-based membrane according to any of the preceding Statements, where the film/layer further comprises a plurality of nanoparticles.

Statement 7. A polymer-based membrane according to Statement 6, where at least a portion, substantially all, or all of the nanoparticles have a size (e.g., a linear dimension (such as, for example, a diameter or the like) of about 10 nm to about 100 nm, including all 0.1 nm values and ranges therebetween) and/or are present in the polymer film at about 0 to about 40 percent by weight (based on the total weight of the polymer film), including all 0.1 weight percent values and ranges therebetween (e.g., about 1 weight percent to about 40 weight percent).

- Statement 8. A polymer-based membrane according to any of the preceding Statements, where the metal oxide layer or metal oxide domains is/are chosen from AlOx layers or domains, SiOx layers or domains, TiOx layers or domains, ZnOx layers or domains, SnOx layers or domains, and the like, and structural analogs thereof, and any combination thereof. Statement 9. A polymer-based membrane according to any of the preceding Statements,
- where the polymer-based membrane exhibits one or more or all of the following: desirable H2 permeability (e.g., an H2 permeability of about 1 to about 1000 Barrer), which may be up to about 200 °C or about 300 °C; desirable H2/CO2 selectivity (e.g., an H2/CO2 selectivity of about 10 to about 200); which may be up to about 200 °C or about 300 °C; desirable thermal stability (e.g., thermal stability to about at least about 200 °C or about 300 °C).
- Statement 10. A method of making a polymer-based membrane of the present disclosure (e.g., a polymer-based membrane of any one of Statements 1 to 9), the method comprising forming a polymer film (e.g., a free-standing polymer film) or forming a polymer film on at least a portion of, substantially all, or all of the exterior surfaces of a substrate (which may be a porous substrate); optionally, drying the polymer film; optionally, at least partially,
- substantially, or completely (depending on the carbonizing conditions) carbonizing the polymer film (e.g., such that a carbonized polymer film comprising a plurality of micropores (such as, for example, surface micropores or the like) is formed) or plasma treating the polymer film (e.g., such that a polyorganosilica film comprising a plurality of ultramicropores (such as, for example, surface ultramicropores or the like) is formed); and contacting the polymer film or the carbonized polymer film (e.g., the layer) or the plasma treated polymer film with one or more vapor-phase metal oxide precursor(s) (such as, for example, vapor-phase AlOx precursor(s), structural analogs thereof, or the like) and, optionally, water vapor, optionally, repeating the contacting a desired number of times, where

the polymer-based membrane is formed.

Statement 11. A method according to Statement 10, the contacting is carried out sequentially (such as, for example, in sequential contactings).

Statement 12. A method according to Statement 10 or 11, where the contacting is repeated 1, 2, 3, 4, 5, 6, 7, 8, 9, 10, 11, 12, 13, 14, or 15 times.

- Statement 13. A method according to any one of Statements 10 to 12, where the vapor-phase metal oxide precursor(s) is/are chosen from vapor-phase AlOx precursors, vapor-phase SiOx precursors, vapor-phase TiOx precursors, vapor-phase ZnOx precursors, vapor-phase SnOx precursors, and the like, and structural analogs thereof, and any combination thereof.

 Statement 14. A method according to Statement 13, where the vapor-phase AlOx precursor(s)
 - is/are chosen from trialkyl aluminum compounds (such as, for example, trimethyl aluminum (TMA), and the like, structural analogs thereof, and any combination thereof) and any combination thereof; and/or the vapor-phase SiOx precursor(s) is/are chosen from silicon tetrahalide compounds (such as, for example, silicon tetrachloride, and the like, structural analogs thereof, and any combination thereof), tris(dialkyl amino)silane compounds (such as,
- for example, tris(dimethylamino)silane, and the like, structural analogs thereof, and any combination thereof) and combination thereof; and/or the vapor-phase TiOx precursor(s) is/are chosen from titanium alkoxide compounds (such as, for example, titanium isopropoxide (TTIP), and the like, structural analogs thereof, and any combination thereof), titanium halide compounds (such as, for example, titanium tetrachloride, and the like,
- structural analogs thereof, and any combination thereof), and any combination thereof; and/or the vapor-phase ZnOx precursor(s) is/are chosen from dialkyl zinc compounds (such as, for example, diethyl zinc), and the like, structural analogs thereof, and any combination thereof) and any combination thereof and/or the vapor-phase SnOx precursor(s) is/are chosen from stannic halide compounds (such as, for example, stannic chloride, and the like, structural analogs thereof, and any combination thereof), and the like, and any combination thereof. Statement 15. A method according to any one of Statements 10 to 14, where the film/layer

comprises a plurality of nanoparticles.

Statement 16. A system (e.g., a system for gas isolation, gas concentration/enrichment, or the like, or any combination thereof) comprising one or more polymer-based membrane(s) of the present disclosure (such as, for example, a polymer-based membrane/polymer-based membranes of any of Statements 1 to 9 and/or a polymer-based membrane/polymer-based membranes made by a method of present disclosure, such as, for example, a method of any of Statements 10 to 15).

15

20

25

30

enrichment(s).

Statement 17. A system according to Statement 16, where the polymer-based membrane(s) is/are disposed in a housing, the housing comprising one or more orafic(es) configured for introduction, control, or the like of gas(es) into the housing.

Statement 18. A system according to Statement 16 or 17, the system where the system is configured for gas separation and/or gas enrichment.

Statement 19. A system according to any one of Statements 16 to 18, the system further comprising one or more components suitable for use in gas separation and/or gas enrichment. Statement 20. A method of separating one or more gas(es) (such as, for example, H₂, CO₂, N₂, He, or the like, or a structural analog thereof, or any combination thereof) from a mixture comprising the one or more gas(es) and at least one other gas and/or enriching one or more gas(es) (such as, for example, H₂, CO₂, N₂, He, or the like, or a structural analog thereof, or any combination thereof) in a mixture comprising at least one other gas, the method comprising: contacting the mixture or the like) with one or more polymer-based membrane(s) of the present disclosure (such as, for example, a polymer-based membrane/polymer-based membranes substrate/substrates of any of Statements 1 to 9) and/or a polymer-based membrane/polymer-based membranes made by a method of present disclosure (such as, for example, a method of any of Statements 10 to 15) and/or a system of the present disclosure

contacting with contacted mixture or a portion thereof a desired number of times; where one or more of the gas(es) in the mixture is separated from the mixture (or the contacted mixture) and/or enriched in the mixture (or the contacted mixture).

(such as, for example, a system of any of Statements 16 to 19); and optionally, repeating the

Statement 21. A method according to Statement 20, where the mixture is an effluent from a fossil fuel power plant, an industrial gas effluent (such as, for example, a refinery gas effluent, natural gas liquid production effluent, ammonia plant effluent, methanol plant effluent, or the like), mixture from syngas processing, or the like.

Statement 22. A method according to Statements 20 or 21, where the polymer-based membrane(s) is/are reused in a subsequent separation and/or enrichment (such as, for example, a second separation and/or enrichment, a third separation and/or enrichment, etc.). Statement 23. A method according to any one of Statements 20 to 22, where the polymer-based membranes(s) are cleaned prior to use in each of the subsequent separation(s) and/or

[0099] The steps of the methods described in the various embodiments and examples disclosed herein are sufficient carry out the methods making polymer-based membranes and methods of using polymer-based membranes of the present disclosure. Thus, in an

10

15

20

25

30

embodiment or example, a method consists essentially of a combination of the steps of the methods disclosed herein. In another embodiment or example, a method consists of such steps.

[0100] The following Examples are presented to illustrate the present disclosure. They are not intended to be limiting in any manner.

EXAMPLE 1

[0101] This example describes polymer-based membranes of the present disclosure, methods of making same, and uses thereof.

[0102]Few-Cycle Atomic Layer Deposition to Nanoengineer Polybenzimidazole. Atomic layer deposition (ALD) creates uniform sub-nanometer films on a variety of surfaces and nanopore walls and has been used to modify polymers to improve surface affinity towards specific molecules, solvent resistance, and barrier properties to gases and vapors. This example describes that few-cycle ALD can be used to engineer functional polymers at a sub-nanometer scale to improve both molecular size-sieving ability and counterintuitively, gas permeability. Particularly, 1-cycle ALD treatment of polybenzimidazole (PBI) by sequential exposure to trimethylaluminum (TMA) and water vapor remarkably increases H₂ permeability by 120% - 270% and H₂/CO₂ selectivity by 30% at 35 - 200 °C. The ALD not only deposits an AlO_x layer on the surface but also enables the TMA to infiltrate and react with the bulk PBI to form an AlO_x network, disrupting polymer chain packing and increasing chain rigidity. The membrane remains stable when challenged with simulated syngas, overcoming the permeability/selectivity tradeoff for H₂/CO₂ separation. This example showcases a facile and scalable way of engineering polymeric membranes at a sub-nanometer level to improve molecular separation performance.

[0103] This example reports the synergistic effect of the ALD treatment of polybenzimidazole (PBI, a leading polymer for H₂/CO₂ separation) to increase H₂ permeability and H₂/CO₂ selectivity simultaneously. An ALD cycle includes four steps (FIG. 5). First, TMA vapor is introduced and adsorbed onto the PBI film surface, enabling the TMA to diffuse into the film subsurface. Second, the TMA is purged by N₂ flow to remove the TMA from the chamber. Third, water vapor is introduced to bind to the Al atoms on the surface and in the films forming hydroxyl groups, which act as growth sites for AlO_x. Fourth, the N₂ is used to purge out the by-products and residual reactants. By repeating the cycles, an AlO_x layer can grow on the PBI film with a precisely controlled thickness. More importantly, the Lewis-acidic TMA vapor diffuses into the film and reacts with the Lewis-basic amine

15

20

25

30

groups on the PBI chains (FIG. 1A), inducing new Al-N bonds and an AlOx network inside the PBI film (i.e., vapor-phase infiltration (VPI)), disrupting the chain packing and influencing the free volumes. Consequently, the ALD-treated PBI films comprise three phases (FIG. 1B), including an AlO_x layer on the surface, a dense AlO_x/PBI hybrid layer beneath the surface, and the bulk PBI doped by TMA (i.e., AlO_x). These samples are named PBI-xC, where x represents the number of ALD cycles (x = 1 - 17 in this example). This example investigated the effect of the ALD cycles on both the morphology and H₂/CO₂ separation properties of the PBI membranes. It was found that one ALD cycle increases pure-gas H₂ permeability by 270% from 2.3 to 8.4 Barrer while retaining H₂/CO₂ selectivity of 12 at 35 °C, and increasing the temperature from 35 to 200 °C increases H₂ permeability of PBI-1C by more than on order of magnitude to 110 Barrer and H₂/CO₂ selectivity by 58% to 19. The PBI-1C exhibits stable H₂/CO₂ separation performance when challenged with simulated syngas containing water vapor up to 200 °C, surpassing Robeson's upper bound. The significant improvement of H₂/CO₂ separation performance by relatively simple, only a few ALD cycles convincingly demonstrate its potential for industrial applications.

[0105] Experimental. Materials. Celazole PBI powder was procured from PBI Performance Products, Inc. (Charlotte, NC). Dimethylformamide (DMF) was acquired from Sigma-Aldrich Corporation (St. Louis, MO). Gas cylinders of N₂, H₂, and CO₂ with ultrahigh purity were purchased from Airgas Inc. (Buffalo, NY).

casting a solution containing 6 mass% PBI in DMF followed by 48-hour drying under vacuum at 150 °C. ALD was conducted using a Veeco Savannah S200 at 85 °C and 0.4 Torr under N2 environment. Each cycle of depositions includes 15-ms pulsation of TMA as an Al precursor, 10-s N2 purging, 15-ms pulsation of water vapor as an oxidizer, and 10-s N2 purging. Multi-cycles can be used to obtain a desired AlO_x thickness on PBI films. For TMA only infiltration, each cycle includes 15-ms pulsation of TMA separated by 10-s N2 purging. [0107] Characterization. An M-2000FI ellipsometer (J.A. Woollam Co., Lincoln, NE) was used to determine the AlO_x thickness after various ALD cycles on Si wafers. The spectral reflectance data were collected with incidence angles from 50° to 80° at an angle step size of 10° and wavelengths from 200 to 1600 nm. The thickness was analyzed by the WVASE32 data acquisition and analysis software based on a three-layer model (AlO_x/native SiO₂:Si) and the optical constants of each layer provided by the software.

PCT/US2024/056939

10

15

20

25

30

[0108] A dimension icon atomic force microscopy (AFM, Bruker, Germany) was used to record the roughness of the samples in air tapping mode with a probe of TESPA-V2 (Bruker, Germany). A goniometer (Ramé-hart Instrument, Succasunna, NJ) was used to measure the surface hydrophilicity using water drops of 2 µL. A dynamic mechanical analyzer (DMA) (Q800 TA Instrument) was employed to investigate mechanical properties using static tensile loading. The uniaxial tensile loading on the sample started from 0.1% and increased by 1.0 %/min until the sample fractured. Three areas of each sample were measured, and average Young's modulus (from the elastic deformation region), tensile strength, and fracture strain were obtained from the stress-strain curves. The curves of thermogravimetric analysis (TGA) and differential scanning calorimetry (DSC) were obtained from an SDT Q600 (TA Instruments, New Castle, DE) from 100 to 800 °C at a ramping rate of 10 °C min⁻¹ under a N₂ flow. A Focused Ion Beam Scanning Electron Microscopy (FIB-SEM, Carl Zeiss Auriga CrossBeam, Germany) was used to observe the cross-section, and an EDS (Oxford Instruments, Abingdon, UK) was used to analyze the elemental distribution. The PBI-xC samples were characterized using Transmission electron microscope (TEM, FEI Talos, 200 kV), and the cross-sectional samples were prepared using a standard in situ FIB lift-out procedure and Ga ion milling with FEI Helios 600 Nanolab. The elemental compositions were characterized by x-ray photoelectron spectroscopy (XPS) on a custom-built XPS system equipped with a hemispherical electron energy analyzer (SPECS) and Al Ka X-ray source (1486.6 eV).

[0109] Pure-gas permeability was determined using a constant-volume and variable-pressure apparatus at 35 and 150 °C. Pure-gas sorption isotherms of CO₂ and C₂H₆ at 35 °C were determined using a gravimetric sorption analyzer of IGA 001 (Hiden Isochema Ltd., Warrington, UK). The uncertainty for gas permeability and solubility is estimated to be <10% using an error propagation method. Mixed-gas permeation was performed using a constant-pressure and variable-volume apparatus from 100 to 200 °C.

[0110] Results and Discussion. Membrane Fabrication and Characterization
[0111] To determine the growth rate of deposited AlO_x layer on the surface, a control experiment was conducted on Si wafers with ALD cycles of 2 – 40, and their thicknesses were determined using ellipsometry. FIG. 1C shows that the AlO_x layer thickness increases linearly at 0.09 nm/cycle.

[0112] FIGS. 1D-1G show the cross-sectional high angle annular dark-field (HAADF) scanning transmission electron microscopy (STEM) and energy-dispersive X-ray

15

20

25

30

spectroscopy (EDS) elemental mapping for PBI-3C and PBI-17C, which show an Alcontaining layer with a thickness of 7.5 and 22 nm, respectively. These layers are much thicker than pure AlO_x deposited on the Si wafers (0.25 nm at 3 cycles and 1.5 nm at 17 cycles, FIG. 1C) because a significant amount of TMA can infiltrate into PBI, thus forming a dense, AlOx-infiltrated PBI layer, as evidenced by the sparse, yet uniformly distributed Al signals within the bulk PBI from the EDS mappings (FIGS, 1E and 1G) and the Al EDS mappings from SEM (FIGS. 1H-IK). The results are consistent with the ALD treatment of PIM-1, where 6 cycles deposited <1 nm AlO_x on the surface but achieved an infiltration depth of 3-5 µm, though PIM-1 has much higher fractional free volume (FFV, 0.26) than PBI (0.16). FIG. 5 compares the surface morphology of PBI and PBI-1C using AFM. The PBI film exhibits smooth surface with a height deviation ranging from -7.6 to 8.2 nm with an arithmetic height average (Ra) of 1.8 nm (FIG. 2A). The 1-cycle ALD dramatically increases R_a to 12 nm likely because the TMA reacts with the amine groups on the surface and etches the surface. The maximum height (R_{max}) and root-mean-squared average of the height (R_{q}) also increase significantly (FIG. 6F). However, further increase in the number of ALD cycles decreases the surface roughness (FIGS. 6A-6E) because of the uniform deposition of the AlO_x layer via true ALD mode (as opposed to VPI) and the planarization of the surface. Surface chemistry of the PBI-xC films was characterized using XPS. All samples exhibit characteristics peaks of C 1s (285 eV), N 1s (399 eV), and O 1s (532 eV) (FIG. 7). The abnormally high O content in the samples can be ascribed to the -OH groups formed on the surface and water molecules adsorbed on the surface. The ALD treatment increases the Al 2p peak at 75 eV and decreases the N 1s peak at ~400 eV (FIG. 2B). The 17-cycle treatment increases the Al/C molar ratio from 0 to 0.19 and the Al/N ratio from 0 to 1.3 and decreases the N/C from 0.23 to 0.15 (Table 1), confirming the formation of the AlO_x layer on the surface. Additionally, the PBI-xC surface shows similar water contact angles (WCAs) at \approx 90° (FIGS. 8A-8F), indicating that the ALD has a negligible impact on the hydrophilicity because of the thin AlO_x layers produced in this study. FIG. 2C shows the molar ratios of Al/C and Al/N. FIG. 2D compares the wideangle X-ray diffraction (WAXD) patterns of PBI-xC samples. There is an absence of sharp peaks for crystalline structures probably because the crystalline AlOx layer is too thin to

calculated using Bragg's law. The d-spacing decreases slightly with increasing ALD cycles,

determine. The broad peak on the PBI pattern at 23.2° corresponds to a d-spacing

(representing an average intersegmental distance between the polymer chains) of 3.8 Å

as the TMA (<5.4 Å) interacts with the amine groups, narrows the free volume at the

15

20

25

30

subnanometer scale, and tightens the polymer nanostructures. The results are also consistent with the increased density with increasing ALD cycles (FIG. 9A).

[0114] The TGA curves of the PBI-xC films almost overlap that of the pristine PBI (FIG. 9C), indicating that the ALD has a negligible effect on the thermal stability. The glass transition temperature (T_g) can be determined from the DSC curves (FIGS. 2E and 9D). The pristine PBI exhibits a T_g value of 448 °C, consistent with the literature data. Interestingly, one and three cycles of ALD treatment increase the T_g significantly to 490 and 519 °C, respectively, indicating the enhanced chain rigidity throughout the bulk, confirming the TMA infiltration of the bulk PBI (FIGS. 1E and 1G). Since normal ALD would add only <10 nm AlO $_x$ layers on the surface of the 8- μ m films, the increased T_g value further confirms that in the disclosed ALD process, TMA is not only adsorbed on the surface but also penetrates into the bulk films via VPI mode, reacting with the polymer chains.

[0115] FIG. 2F compares the stress-strain curves of PBI, PBI-1C, and PBI-3C. The AlO_x deposition has a minimal effect on Young's modulus but decreases tensile strength, fracture strain, and toughness (Table 2), which are similar to the ALD-treated PIM-1. This result suggests the increased chain rigidity, validating the TMA infiltration and reaction with the bulk PBI. Notably, 3-cycle ALD significantly decreases the fracture strain from 18% to 8.1% and toughness from 2600 to 760 MJ/m³, consistent with the dramatic change in gas permeation properties.

[0116] Gas Transport Properties and Separation Mechanism. FIG. 3A exhibits pure-gas H_2 and CO_2 permeability of PBI-xC of $\approx 8.0~\mu m$ ($\mu m = micrometer(s)$) at 7.8 atm and 35 °C. PBI shows H_2 permeability of 2.3 Barrer and H_2/CO_2 selectivity of 12, consistent with the literature. 1-cycle ALD increases H_2 permeability by 270% to 8.4 Barrer while retaining H_2/CO_2 selectivity. As a comparison, the PBI films were also treated with TMA pulsing only and a similar trend of increasing gas permeability (FIG. 10A) was observed, suggesting the importance of the reaction between TMA and PBI. The dramatic TMA sorption during initial ALD cycles has also been reported for other polymers, such as polymethylmethacrylate (PMMA), polypropylene (PP), and poly(vinyl chloride) (PVC). On the other hand, both PBI and PBI-1C exhibit the same d-spacing value (FIG. 2D), suggesting that the TMA may impact the free volume distribution increasing gas permeability, rather than increase free volume. Further increase in ALD cycles decreases gas permeability and increases H_2/CO_2 selectivity because the decreasing d-spacing becomes more dominant. For instance, PBI-17C exhibits H_2 permeability of 0.62 Barrer and H_2/CO_2 selectivity of 20. The decreased

permeability can also be partially ascribed to the increased thickness of the AlO_x layer on the surface and the increased resistance to gas transport.

[0117] FIG. 3B illustrates the pressure dependency of H₂/CO₂ separation properties of PBI-3C at 35 °C. Gas permeability decreases with increasing feed pressure, which can be described by the dual-mode sorption model, where the Langmuir sorption sites become saturated at high pressures. In contrast, this behavior differs from that of the pristine PBI (FIG. 10B), presumably because the PBI-3C has lower free volumes and is easier to be saturated than PBI. Additionally, H₂/CO₂ selectivity remains almost unchanged with increasing pressure in PBI-3C.

10 [0118] Gas permeability can be decoupled into solubility and diffusivity to elucidate the transport mechanism. As H₂ sorption in PBI is too low to determine using the apparatus described herein, C₂H₆ is chosen as its surrogate, as neither has specific interactions with PBI or AlO_x. The CO₂ and C₂H₆ sorption isotherms at 35 °C can be satisfactorily described using the dual-mode sorption model (Equation 1) (FIGS. 10C and 10D) with the adjustable 15 parameters recorded in Table 3. The ALD decreases CO_2 solubility by 30% and C'_H values regardless of the cycle number, indicating a decreased Langmuir sorption capacity caused by the reduced free volume. It was observed that the C'_H value for C_2H_6 decreases significantly from 26 to 1.0 cm³(STP) cm⁻³ with increasing ALD cycles, indicating that the Langmuir cavities gradually become inaccessible to C₂H₆ because of the reduced free volume size. As 20 such, CO₂/C₂H₆ solubility selectivity increases with increasing ALD cycles. The sorption behavior further validates the TMA infiltration and commensurate decrease in free volumes of the bulk PBI.

[0119] FIG. 3C shows CO₂ and C₂H₆ solubility at 7.8 atm. FIG. 3D depicts that 3-cycle ALD increases CO₂ diffusivity by 170% from 3.5 × 10⁻¹⁰ to 9.5 × 10⁻¹⁰ cm²/s at 35 °C, but a further increase to 17 cycles decreases CO₂ diffusivity to 8.6 × 10⁻¹¹ cm²/s, reflecting the competing effects of the disrupted chain packing by the infiltrated TMA and the reduced free volume by the AlO_x network and TMA cross-linking. The ALD treatment mainly affects CO₂ diffusivity, instead of CO₂ solubility. Such an effect is expected to be similar for H₂ transport, though it cannot be directly validated because of the lack of H₂ sorption data.

30 **[0120]** H₂/CO₂ Separation Performance. PBI-*x*C samples are further evaluated with a H₂/CO₂ (50/50 vol%) mixture at 100 - 200 °C. Both H₂ permeability (FIG. 4A) and CO₂ permeability (FIG. 10E) increase with increasing temperature, which can be described using the Arrhenius equation (Equation 2) with the fitting parameters recorded in Table 4. The activation energy for permeation (*E_P*) slightly decreases before increasing with increasing

15

20

25

30

ALD cycle, consistent with the trend of gas permeability. Surprisingly, different from the pristine PBI, the PBI-xC exhibits E_P values higher for H₂ than for CO₂ probably because of the enhanced polymer chain rigidity, leading to an increased H₂/CO₂ selectivity with increasing temperature (FIG. 4B). For instance, PBI-1C exhibits H₂ E_P of 18 kJ/mol (higher than CO₂ E_P of 11 kJ/mol), leading to an increased H₂/CO₂ selectivity from 12 at 35 °C to 19 at 200 °C.

[0121] FIG. 4C compares mixed-gas performance of PBI, PBI-1C, and PBI-17C at 200 $^{\circ}$ C with Robeson's upper bound. PBI-1C has an excellent combination of H₂ permeability and H₂/CO₂ selectivity, surpassing the upper bound. Therefore, it was chosen to investigate the long-term stability using simulated syngas containing water vapor up to 1.8 mol% at 200 $^{\circ}$ C. PBI-1C exhibits stable mixed-gas H₂ permeability of \approx 100 Barrer and H₂/CO₂ selectivity of 20 at both dry and wet conditions for 100 h (FIG. 4D), which is the same as the initial H₂/CO₂ separation performance (FIGS. 4A and 4B), indicating its robustness against physical aging and water vapor. The results also indicate that the deposited AlO_x layer is stable under the high-temperature humid condition.

[0122] FIG. 4E compares PBI-1C and PBI-17C with the leading polymeric materials for H₂/CO₂ separation. PBI-1C shows superior H₂/CO₂ separation performance due to the fine-tuned polymer chain structures by AlO_x deposition and TMA cross-linking. With only 1 ALD cycle but significantly improved separation performance, the ALD technology is facile and scalable and holds great potential for industrial H₂/CO₂ separation.

[0123] This example demonstrated a facile and scalable ALD approach to improve H₂/CO₂ selectivity and unexpectedly enhanced H₂ permeability in PBI. In addition to the deposition of AlO_x on the surface, the ALD allows the infiltration of the TMA into the films and reaction with the PBI chains synergistically to modify the free volumes at a subnanometer scale. Specifically, the infiltrated TMA reacts with the amine groups on the PBI chains, forming AlOx networks and disrupting the chain packing (increasing gas diffusivity) and reducing the free volume (increasing size-sieving ability). Impressively, one ALD cycle increases H₂ permeability by 120% from 50 to 110 Barrer and H₂/CO₂ selectivity by 30% from 15 to 19 at 200 °C. PBI-1C demonstrates stable and excellent H₂/CO₂ separation performance against high temperatures, water vapor, and physical aging, and it surpasses most state-of-the-art polymeric membranes and the permeability/selectivity upper bound. This example also demonstrates that the few-cycle ALD can be an effective strategy to nanoengineer polymeric membranes for various molecular separations. The scalable yet

15

20

effective fine-tuning of nanopores by few-cycle ALD may be used to manipulate porous materials for other applications, such as adsorption, catalysts, and energy storage.

[0124] To compare the full cycle of AlO_x deposition, TMA pulsing without the water vapor pulsing was conducted on the PBI film. Those films were named as PBI-TMA-xC, where x represents the number of TMA pulsing cycles (x = 1 - 17). The TMA pulsing slightly increases the film density (FIG. 9A). On the other hand, FIG. 9B exhibits WAXD patterns of PBI, PBI-TMA-3C, and PBI-TMA-17C. Those three samples exhibit the same d-spacings at 0.38 nm, indicating that only TMA pulsing is incapable of enhancing the chain packing. Increasing the TMA pulsing cycles increases gas permeability before decreasing (FIG. 10A), consistent with the ALD-treated PBI films. At the TMA pulsing cycles above 11, further increasing the cycles exerts little effect on gas permeability probably because TMA has saturated the free volumes in the PBI.

[0125] All PBI-xC films exhibit thermal degradation behaviors similar to the pristine PBI (FIG. 9C). Particularly, all samples exhibit mass losses of 2 - 4 % before 400 °C because of the evaporation and degradation of residue impurities. However, the films are stable from 400 to 550 °C, as confirmed by their derivative thermogravimetric analysis (DTA) curves (FIG. 9D). The T_g can be estimated from their DSC curves (FIGS. 9E and 9F).

[0126] Table 1. Elemental molar composition on the surfaces of PBI-xC samples analyzed using XPS.

Samples	Elen	nental comp	Mola	Molar ratio		
Samples	С	N	O	Al	N/C	Al/C
PBI	68.4	15.6	16.0	0	0.23	0
PBI-1C	63.9	14.0	21.3	0.83	0.22	0.013
PBI-3C	52.1	5.91	40.4	1.65	0.11	0.032
PBI-11C	34.1	6.00	56.0	3.85	0.18	0.11
PBI-17C	26.7	4.04	64.1	5.13	0.15	0.19

[0127] Table 2. Young's modulus, tensile strength, fracture strain, and toughness of PBI, PBI-1C, and PBI-3C.

Samples	Young's modulus (MPa)	Tensile strength (MPa)	Failure strain (%)	Toughness (MJ/m³)
PBI	3900 ± 550	180 ± 19	18 ± 5	2600 ± 1000
PBI-1C	3900 ± 140	140 ± 8	12 ± 4	1100 ± 410
PBI-3C	4000 ± 630	140 ± 37	8.1 ± 0.2	760 ± 190

[0128] Table 3. Parameters of the dual-mode sorption model for CO₂ and C₂H₆ sorption in PBI, PBI-3C, and PBI-17C at 35 °C. The units for k_D , b, and C'_H are cm³(STP) cm⁻³·atm⁻¹, and cm³(STP) cm⁻³, respectively.

Comples		CO_2			C_2H_6	
Samples	$-k_D$	b	C'_H	k_D	b	C'_H
PBI	0.74	0.52	31	0.88	0.36	26
PBI-3C	0.56	0.37	22	1.1	028	6.4
PBI-17C	0.61	0.32	23	1.5	0.25	1.0

5 **[0129]** Table 4. Values of $E_{P,A}$ and $P_{A,\theta}$ for mixed-gas H₂ and CO₂ permeation in PBI-xC films.

Samples	E_{PA} ((kJ/mol)	$P_{A,\theta}$ (×	10 ³ Barrer)
Samples	H_2	CO_2	H_2	CO_2
PBI	21 ± 0.2	21 ± 0.5	9.9 ± 0.07	0.70 ± 0.016
PBI-1C	18 ± 1.1	11 ± 1.4	9.9 ± 0.35	0.10 ± 0.009
PBI-3C	20 ± 2.2	17 ± 1.3	15 ± 0.94	0.34 ± 0.019
PBI-11C	21 ± 1.7	18 ± 1.5	15 ± 0.66	0.41 ± 0.029
PBI-17C	31 ± 0.19	27 ± 0.14	100 ± 0.51	1.5 ± 0.009

[0130] Table 5. H₂/CO₂ separation properties in selected membrane materials for comparison (cf. FIG. 4E). Mixed-gas contains 50% CO₂ and 50% H₂.

	Materials		Mixed- or pure- gas	Temp.	H ₂ permeability (Barrer)	H ₂ /CO ₂ selectivity
This	1	PBI-1C	Mixed	200	110	20
study	2	PBI-17C	Mixed	200	38	24
	3	PBI- (H ₃ PO ₄)- 0.16	Mixed	180	19	32
	4	PBI-TCL- 6H	Mixed	200	38	17
	5	PBI- SCA4-17	Mixed	150	16	45
T 1:	6	PBI- SCA8-10	Mixed	150	37	23
Leading polymeric	7	PBI-TMA- 0.22	Mixed	150	16	28
materials	8	PBI-TaA- 0.32	Mixed	150	20	29
	9	PBI-NiT- 0.17	Mixed	175	130	14
	10	CPAM-15	Mixed	200	50	24
	11	PBI-TBB- 0.213	Mixed	150	9.6	24
	12	P84- BuDA-6H	Pure	100	47	14

15

25

30

13	IP PA	Mixed	140	7.0	50
14	IP PBDI	Mixed	150	69	22
15	IP BILPs	Pure	150	14	32

EXAMPLE 2

- [0131] This example describes polymer-based membranes of the present disclosure, methods of making same, and uses thereof.
- 5 [0132] This example describes vapor phase infiltrated carbon molecular sieve membranes for efficient H₂/CO₂ separation.
 - [0133] Materials. Celazole PBI powder was purchased from PBI Performance Product Inc. (Charlotte, NC). N, N-dimethylformamide (DMF) were provided from Sigma-Aldrich Corporation (St. Louis, MO). Gas cylinders of N₂, H₂, CO₂, CH₄ and C₂H₆ with ultrahigh purity were obtained from Airgas Inc. (Buffalo, NY).
 - [0134] Fabrication of polybenzimidazole (PBI) and derived carbon molecular sieve (CMS) membranes. The PBI membrane was fabricated using a reported method. Shortly, commercial m-PBI powders were added in DMF and dissolved under 160 °C overnight. The obtained solution was filtered through a 1- μ m glass fiber filter, and then casted into a glass petri dish. The solution was dried at 60 °C with a N₂ flow overnight. The obtained film membrane was peeled off from the petri dish and then dried under vacuum at 200 °C for 48 hours. The final membrane has a uniform thickness around 45 ~ 55 μ m.
- [0135] The as-prepared PBI membrane was sandwiched between two ceramic plates and carbonized in a tube furnace (MTI Corporation, Richmond, CA) with a N₂ flow of 200
 20 mL/min. The temperature was then ramped up from ≈ 23 °C to the carbonization temperature (*T_c*) by 10 °C/min and the films were soaked at *T_c* for 2 h. Finally, the furnace was naturally cool down to ≈ 23 °C with the N₂ flow.
 - [0136] Vapor phase infiltration on PBI and its CMS membranes. A single AlO_x infiltration cycle is consisted of 4 protocols. First, TMA is dosed in the chamber by 100 s exposure time under a static vacuum (~10 Torr), followed by chamber purging with nitrogen at 100 sccm for 100 s. Water vapor is then injected under a static vacuum (~35 Torr) by 100 s exposure time, followed by chamber purging with nitrogen at 100 sccm for 100 s.
 - [0137] Characterization. Wide-angle x-ray diffraction (WAXD) patterns were obtained using a Rigaku Ultima IV X-ray diffractometer with a 1.54 Å wavelength of Cu Kα x-ray source. A Renishaw inVia Raman Microscope (Renishaw plc, UK) was employed to achieve Rman spectra of pristine CMS600 and Al2O3-infiltrated CMS600 samples. The bulk density

15

of the CMS film was calculated based on corresponded mass and volume. The skeletal density of the CMS films was measured using a Micromeritics Accu-Pyc II 1340 Gas Pycnometer (Micromeritics Instrument Corporation, Norcross, GA). Sample mass and volume were measured to determine the bulk density. A Micromeritics Accu-Pyc II 1340 Gas Pycnometer (Micromeritics Instrument Corporation, Norcross, GA) was used to measure skeletal density.

[0138] Pure-gas permeability was determined using a constant-volume and variable-pressure system. Pure-gas sorption was determined using a gravimetric sorption analyzer (IGA 001, Hiden Isochema, UK). Mixed-gas H₂/CO₂ separation performance was demonstrated on a constant-pressure and variable-volume apparatus. During the test, N₂ was employed as the sweep gas on the permeate side. Water vapor concentration at the feed side was controlled via adjusting the temperature of the water bubbler, where the H₂/CO₂ mixture passed through before entering to the cell.

[0139] Table 6 presents parameters related to porous structure properties of those CMS membranes, including skeletal and bulk densities, and estimated porosity based on those two densities, as well as d-spacing (or average distance between polymer chains or carbon stackings) from WAXD, and pore volume and surface determined from CO₂ adsorption at 273 K or N₂ adsorption at 77 K.

[0140] Table 6. Skeletal and bulk densities, porosity, *d*-spacing, pore volume and surface area of all samples.

Samples	Skeletal density (g/cm ³)	Bulk density (g/cm ³)	Porosity (%)	d- spacing (Å)	Pore volume (cm ³ /g) [†]	Surface area (cm²/g) [†]	Pore volume (cm ³ /g) [‡]	Surface area (cm ² /g) ²
sMMM	1.353 ± 0.008	1.325 ± 0.005	2.1 ± 0.4	3.5	0.0090	11	0.041	17
sMMM400	1.306 ± 0.008	1.160 ± 0.020	11 ± 2	4.9	N/A **	N/A	N/A	N/A
sMMM450	1.283 ± 0.013	1.120 ± 0.029	13 ± 2	N/A	0.016	17	0.054	23
sMMM500	1.344 ± 0.030	1.162 ± 0.018	14 ± 2	4.5	N/A	N/A	N/A	N/A
sMMM550	1.441 ± 0.010	1.187 ± 0.038	18 ± 3	4.1	0.049	43	0.064	27

Note: $^{\dagger}V$ alues are obtained from CO_2 adsorption at 0 $^{\circ}C$; $^{\ddagger}v$ alues are obtained from N_2 adsorption at -196 $^{\circ}C$; $^{\ddagger}N/A$ means data is not available.

10

15

30

EXAMPLE 3

[0141] The following is an example of polymer-based membranes of the present disclosure, methods of making same, and uses thereof.

Described are polymer-based membranes with high H₂/CO₂ selectivity using surface nanoengineering, achieving the separation at low cost and higher energy efficiency. This approach overcomes the inherent roadblocks in polymers to obtain both high permeability and selectivity consists of starting with strongly size-sieving polymers. Two approaches using atomic layer deposition (ALD) technology were demonstrated. Approach 1 is the AlO_x deposition on polymer surface using ALD with 1 to 17 cycles, as demonstrated on polybenzimidazole (PBI) in FIG. 5. The ALD precursor trimethylaluminium (TMA) vapor can penetrate into the PBI film, reacting with imidazole rings on PBI chains, thus immobilizing and cross-linking PBI chains simultaneously. As such, both gas diffusion and size-sieving ability were be enhanced, leading to increased H₂ permeability and H₂/CO₂ selectivity up to 200 °C. Approach 2 includes two steps. Firstly, PBI film was carbonized from 500 °C to 700 °C to create micropores that enhance gas transport and then gas permeability. Then AlO_x was infiltrated into the surface micropores of carbonized PBI films using ALD with 1 to 7 cycles. The surface micropores can be tuned by the infiltrated AlO_x to obtain strong molecular sieving behavior that increases H₂/CO₂ selectivity without significant loss of H₂ permeability at elevated temperatures.

20 **[0143]** The thermally stable membranes developed have high H₂ permeability and high H₂/CO₂ selectivity, leading to a low cost and energy efficient separation of hydrogen purification and CO₂ capture from fossil fuel derived power plants. Additionally, the ALD-engineered membranes can operate at the syngas processing temperature (150°C). Unlike the conventional absorption or adsorption technology operating near ambient temperatures, the membrane technology developed here shows high energy efficiency and low operating cost.

EXAMPLE 4

[0144] The following is an example of polymer-based membranes of the present disclosure, methods of making same, and uses thereof.

[0145] Atomically fine-tuning organic-inorganic carbon molecular sieve (CMS) membranes for green hydrogen production. The following example discloses a facile approach to tailor the microporous structures of CMS materials using a vapor phase infiltration (VPI) process derived from atomic layer deposition (ALD), as shown in FIG.

11A. As a scalable interfacial engineering technique, VPI allows the metalorganic precursor vapor to diffuse into the micropores and form atomic layers on the pore wall. VPI has never been demonstrated to achieve sub-3.3 Å micropores for selective H₂ permeation while rejecting CO₂.

5 [0146] This example shows that hybrid organic-inorganic CMS materials can be prepared from polybenzimidazole (PBI) with moderate H₂/CO₂ selectivity at low T_c to retain good mechanical properties, followed by VPI processes to atomically engineer ultramicropores to achieve a precise cut-off at 3.3 Å and thus excellent H₂/CO₂ separation performance (FIG. 11A). Specifically, PBI, with tight chain packing derived from π - π stacking and hydrogen bonding, is carbonized at 500–600 °C (PBI T_c). Then, the films are exposed to 10 trimethylaluminum (TMA) and water vapor alternatively to atomically deposit AlO_x molecules within the membrane matrix (i.e., interior pore walls), narrowing micropores and enhancing size-sieving ability. The VPI-treated CMSs are named PBIT_c-t, where t represents the total exposure time of TMA vapor (40 - 100 s in one cycle). One single-cycle VPI 15 treatment narrows the micropores to sub-3.3 Å and remarkably increases H₂/CO₂ selectivity from 10 to 83. The PBIT_c-t films show stable separation properties when challenged with simulated syngas streams containing water vapor. The synergistic combination of lowtemperature carbonization and VPI provides a powerful and scalable approach to obtaining

20 [0147] Experimental. Materials. Celazole PBI powder and S10 PBI solution were purchased from PBI Performance Product Inc. (Charlotte, NC). N, N-dimethylformamide (DMF), dimethylacetamide (DMAc), and toluene were provided by Sigma-Aldrich Corporation (St. Louis, MO). Ceramic tubes were procured from by Media and Process Technology Inc. (Pittsburgh, PA). Gas cylinders of N2, H2, CO2, CH4, and C2H6 with ultrahigh purity were obtained from Airgas Inc. (Buffalo, NY).

desirable sub-nm pores from easily processable polymers for various industrial separations.

[0148] Preparation of PBI films, CMS films, VPI-treated films, and membranes. The PBI films were fabricated using a solution-cast method. Briefly, commercial m-PBI powders were added in DMF and dissolved under 160 °C overnight. The obtained solution was filtered through a 1-μm glass fiber filter and then cast into a glass petri dish. The solution was dried at 60 °C with a N₂ flow overnight. The obtained film was then dried under vacuum at 200 °C for 48 h. The film has a uniform thickness of ~ 50 μm. To prepare PBI T_c films, the as-prepared PBI films were sandwiched between two ceramic plates and carbonized in a tube furnace (MTI Corporation, Richmond, CA) with a N₂ flow of 200 mL/min. The temperature was ramped up from ≈ 23 °C to the carbonization temperature (T_c) by 10 °C/min, and the films

15

20

25

30

were soaked at T_c for 2 h. Finally, the furnace was naturally cooled down to ≈ 23 °C with the N₂ flow. To prepare CMS TFC membranes, ceramic tubes with an outer diameter of ~5 mm and an average surface pore size of 10 nm were first cut into ~ 5 cm long. Second, the commercial S10 PBI solution was diluted into 2 wt% by DMAc and toluene (50:50 by mass), and the solution was used to dip-coat the ceramic tube for 3 s before at 60 °C with a N2 flow for 6 h. The dip-coating process was repeated based on the design. Third, the tube was heated under a vacuum at 200 °C for 48 hours. Finally, the tubular membrane was carbonized at 550 °C using the same ramping process above to obtain the CMS TFC membrane module. VPI was conducted at 85 °C, maintaining a base chamber pressure of 0.2 Torr. Each AlO_x infiltration cycle for the VPI treatment comprised four sequential steps: First, the chamber was isolated, and TMA was introduced for 50 ms (ms = millisecond(s)) to achieve a TMA vapor pressure of ~1 Torr, PBI was exposed to TMA for certain period. Second, the chamber was purged with nitrogen gas at a flow rate of 100 sccm for 100 s, followed by evacuation to the base vacuum over 30 s. Third, water vapor, as the coreactant, was injected for 50 ms to reach a vapor pressure of ~1 Torr, Then PBI was exposed to the water vapor for a specified period. Fourth, the chamber was purged again with nitrogen at 100 sccm for 100 s, then pumped to base vacuum for 30 s. After completing the VPI cycles, the CMS TFC membrane was coated with a protective layer of polydimethylsiloxane (PDMS) to mitigate any defects. [0149] Characterization. WAXD patterns were obtained using a Rigaku Ultima IV X-ray diffractometer with Cu Kα x-ray source. A Renishaw inVia Raman Microscope (Renishaw plc, UK) was employed to obtain Raman spectra of the PBI600-t samples. The bulk density of the films was calculated based on the corresponding mass and volume. The skeletal density of the films was measured using a Micromeritics Accu-Pyc II 1340 Gas Pycnometer (Micromeritics Instrument Corporation, Norcross, GA). Mechanical properties of the PBIT_c-t samples were investigated using static tensile loading on a dynamic mechanical analyzer (DMA) (Q800 TA Instrument). Three areas of each sample were measured, and a loading rate of 0.1 N/min was applied to the areas (15 mm × 3 mm) until fracture occurred. Young's modulus was calculated from the slope of the elastic regime of the stress-strain curve, while tensile toughness was measured by computing the area underneath the entire stress-strain curve. X-ray photoelectron spectroscopy (XPS) probe (Physical Electronics Inc., Chanhassen, MN, USA) equipped with a monochromated Al kα radiation source. Each XPS spectrum was collected over a sample area of 100 µm in diameter, and 3 sample areas were examined for each specimen. XPS spectra were calibrated by setting adventitious C 1s binding energy at 284.8 eV. Atomic concentrations were calculated using CasaXPS package and manufacturer-

provided sensitivity factors. N₂ adsorption and desorption isotherms were collected at 77 K using a Quantachrome Autosorb-iQ3-MP/Kr BET Surface Analyzer. The powdered films were outgassed at 120 °C for 12 hours under a vacuum before each measurement. 67 adsorption and 40 desorption points were collected. Surface areas of samples were determined via BET method by fitting gas adsorption points between the pressure range 0.05-0.3 bar. NLDFT model was used to obtain the pore size distribution from gas adsorption isotherms. A scanning transmission electron microscope (STEM) (FEI Talos F200X; 200 kV; equipped with the EDS elemental mapping capability) and a focused ion beam SEM (FIB-SEM, Carl Zeiss Auriga CrossBeam, Germany) were used to characterize the morphologies 10 of the samples. For CMS films, pure-gas permeability was determined using a constantvolume and variable-pressure system. Pure-gas sorption was determined using a gravimetric sorption analyzer (IGA 001, Hiden Isochema, UK). Mixed-gas H₂/CO₂ separation performance was demonstrated on a constant-pressure and variable-volume apparatus. During the test, N₂ was employed as the sweep gas on the permeate side. Water vapor concentration 15 at the feed side was controlled by adjusting the temperature of the water bubbler, where the H₂:CO₂ mixture passed through before entering the cell. For the CMS tubular membranes, pure-gas permeance was determined using a custom-made constant-pressure and variablevolume cell in an oven.

[0150] Results and Discussion. The 100-s VPI has a negligible effect on the bulk carbon structures of PBI600 (FIGS. 16A and 16B), consistent with the Raman spectra, where the ratio of disordered carbon peak (I_D) to highly oriented graphitic carbon peak (I_G) fluctuates at 0.68 - 0.70 as the TMA exposure time increases to 100 seconds (FIG. 17A). Additionally, no significant changes were observed on the surface or cross-section of the films after the VPI treatment from the SEM images (FIGS. 18A-18D).

25 [0151] To better illustrate the structure change by VPI, a PBI600 sample was treated by three cycles with 100 seconds of TMA exposure for each cycle. The obtained sample (PBI600-100×3C) shows high Al/C and Al/N ratios of 4.9 and 0.38, respectively, indicating the accumulation of AlO_x on the surface (Table 7). The 3-cycle VPI retains an intact carbon structure in the bulk region of the film, i.e., the cross-sectional area ~ 40 nm below the VPI-treated surface (FIG. 11B).

[0152] FIG. 11C illustrates that AlO_x is confined to a thin, crystalline layer of 5 nm on the treated surface with a distinct presence in the subsurface region. Moreover, the cross-sectional EDS mappings demonstrate that Al and O elements are mainly located on the surface and 40-nm beneath the surface (FIGS. 11D, 19A, and 19B), confirming the TMA

15

30

infiltration, as neither element is presented in PBI T_c . On the other hand, the bulk film displays sparse Al element (FIG. 11E), indicating limited penetration of TMA vapor into the film and contrasting with other VPI-treated porous materials, where AlO_x is dispersed throughout the entire film. This discrepancy is attributed to the ultramicropores in PBI T_c , and the deposited TMA blocks the micropores and limits its further diffusion in the CMS.

[0153] FIG. 12A shows the Al 2p peak at 75 eV of the X-ray photoelectron spectroscopy (XPS) spectra for PBI600-t samples, which also exhibit characteristic peaks of C 1s (285 eV) and N 1s (399 eV), as well as O 1s (532 eV) because of water molecules adsorbed on the surface (FIG. 17B, 17C, and Table 7). The VPI treatment increases the Al peak. For example, the 100-s treatment increases the Al/C molar ratio from 0 to 0.051 and the Al/N ratio from 0 to 0.32 (FIG. 12B), confirming the infiltration of the AlO_x into the PBI600. In contrast, the STEM-EDS mapping (FIGS. 19C-19F) of the bulk films of PBI600-t (t = 10s - 100s) do not show visible changes in the Al element due to its low content.

[0154] FIG. 12C presents the effect of T_c and 100-s VPI treatment on the tensile stress-strain curves for PBI500 and PBI550. PBI550 exhibits higher strength than PBI500 because of the more rigid carbon structures caused by higher T_c . The VPI treatment decreases the fracture strains and increases Young's modulus (Table 8), further validating the TMA infiltration. For example, the VPI treatment of PBI550 increases Young's modulus from 21 to 38 MPa.

20 [0155] The PBI600-t samples exhibit a broad peak at ~22° in the wide-angle X-ray diffraction (WAXD) patterns (FIG. 17D and Table 9), corresponding to a d-spacing of 4.0 Å (FIG. 12D) calculated using Bragg's law, indicating that the VPI treatment has no discernible impact on the carbon stacking of PBI600. Moreover, there are no peaks corresponding to crystalline AlO_x because of the thin amorphous AlO_x layer on the interior surface and low

AlO_x content in the bulk. Similar trends are also observed in PBI550 films (FIG. 17E). However, the VPI increases *d*-spacings in both PBI and PBI500, indicating disturbed polymer chain packings. Additionally, *d*-spacing increases from PBI to PBI500 due to the mass loss and then decreases with increasing *T_c* due to carbon densification (FIG. 12D).

[0156] Both skeletal and bulk density of the PBI600 films were measured after the AlO_x infiltration. Skeletal density (ρ_s) of carbon strands remains constant at \approx 1.40 g/cm³, while bulk density (ρ_b) of the entire film increases from 1.148 g/cm³ for PBI600 to 1.170 g/cm³ for PBI600-100, leading to a slight decrease of porosity ($\varepsilon = 1 - \rho_b/\rho_s$) from 0.180 to 0.173 (FIG. 17F). This also validates that the AlO_x is deposited on the inner pore surface of the CMS, consistent with the TEM images.

15

20

25

30

[0157] FIG. 12E shows that the pore volume and surface area decrease with increasing TMA exposure time (FIG. 20). Moreover, the pore volume and surface area of PBI T_c are much lower than those of the CMS materials derived from PIM-1, cellulose, and polyimides due to the lower free volume in PBI derived from hydrogen bonding. FIG. 12F shows the PBI600 has a wide size distribution from 10 to 100 Å, which gradually shrinks to 10 - 40 Å after the VPI process with 100-s TMA exposure, consistent with the decreased porosity and pore volume.

[0158] FIG. 13A presents pure-gas H₂/CO₂ separation properties of PBI600-*t* at 100 °C. While the 40-s TMA exposure has a negligible impact on gas permeability, the 100-s TMA exposure dramatically decreases gas permeability, consistent with the decreased porosity and pore volume. For instance, the 100-s TMA exposure decreases CO₂ permeability from 89 to 1.5 Barrer and substantially increases H₂/CO₂ selectivity from 6.0 to 34. The same behaviors are observed for PBI500-*t* and PBI550-*t* (FIG. 13B and Table 10). Particularly, high H₂/CO₂ selectivity up to 83 can be obtained with 100-s TMA exposure time (FIG. 13C), indicating the molecular size cut-off of 3.3 Å formed by the AlO_x deposition on the inner pores. FIGS. 13B and 13C also show the effect of the *T_c* on H₂/CO₂ separation properties. Increasing *T_c* from 500 to 600 °C increases gas permeability and decreases H₂/CO₂ selectivity for both PBI*T_c* and PBI*T_c*-100 samples because of the increased porosity. Interestingly, PBI500-100 shows much lower H₂ permeability but much higher H₂/CO₂ selectivity than PBI-100, presumably because of the larger pore sizes and more infiltration of AlO_x in PBI500-100.

[0159] FIG. 13F benchmarks the PBI T_c -t in Robeson's upper bound plot at 100 °C. The carbonization of PBI dramatically increases H₂ permeability without significantly decreasing H₂/CO₂ selectivity before T_c reaches 600 °C. The AlO_x infiltration tremendously increases H₂/CO₂ selectivity, leading to superior H₂/CO₂ separation properties far surpassing the upper bound.

[0160] PBI550-100 exhibits the best combination of H₂ permeability (19 Barrer) and H₂/CO₂ selectivity (61) at 100 °C, and it is further evaluated using gas mixtures at various temperatures and humidity levels. FIG. 14A illustrates that H₂ permeability at 100 °C slightly decreases with increasing CO₂ partial pressure, decreasing mixed-gas H₂/CO₂ selectivity.

This phenomenon is commonly observed in CMS and other porous materials due to competitive CO₂ sorption.

[0161] FIG. 14B depicts that mixed-gas H₂ and CO₂ permeability increase with increasing temperature, which can be described using the Arrhenius equation (Equation 2):

15

20

25

30

$$P_A = P_{0,A} \exp(-E_{P,A}/RT) \tag{2}$$

where $P_{0,A}$ and $E_{P,A}$ are the pre-exponential factor and activation energy of the permeation, respectively. R is the gas constant, and T is the testing temperature. PBI550-100 exhibits similar $E_{P,A}$ values for H₂ (25 kJ/mol) and CO₂ (26 kJ/mol), and consequently, mixed-gas H₂/CO₂ selectivity barely changes within 70 – 200 °C.

[0162] Typical biomass-derived syngas may contain 50 – 60% H₂ and 50 – 40% CO₂ saturated by water vapor. In this study, PBI550-100 was challenged with an H₂/CO₂ mixture (50/50) at 150 °C and various water vapor contents for 100 hours. As shown in FIG. 14C, increasing water vapor content slightly decreases H₂ permeability and H₂/CO₂ selectivity because of water vapor sorption within the internal pores, blocking H₂ permeation. Nevertheless, PBI550-100 maintains stable separation performance, irrespective of water vapor levels. Notably, both H₂ permeability and H₂/CO₂ selectivity completely recover upon reverting to the dry condition, reflecting the excellent stability of these VPI-engineered CMS materials against hydrothermal conditions and physical aging.

[0163] FIGS. 14D and 18E compare H₂/CO₂ separation characteristics of two representative materials (PBI500-100 and PBI550-100) with other leading CMS and ALD-engineered materials reported in the recent decade. Among the CMS materials with $T_c < 700$ °C, the PBI T_c -t materials exhibit the highest H₂/CO₂ selectivity (FIG. 14D). Particularly, the PBI550-100 exhibits one of the best combinations of H₂ permeability and H₂/CO₂ selectivity. Elevating T_c tends to densify carbon structures and generate smaller pores in CMS materials, increasing H₂/CO₂ selectivity. For instance, increasing T_c from 625 to 925 °C on Torlon CMS increased H₂/CO₂ selectivity from 4.9 to 57, though higher T_c (\geq 700 °C) causes brittleness, making them difficult to fabricate at a large scale. Nonetheless, PBI550-100 remains highly competitive with the leading CMS materials at $T_c \geq$ 700 °C and other ALD-engineered materials (FIG. 14E).

[0164] To demonstrate the potential of the PBI T_c -t materials for industrial separations, PBI550-100 was fabricated into thin-film composite (TFC) membranes by coating a PBI solution on ceramic tubular substrates via a dip-coating method and then following the same carbonization protocol and VPI process (FIG. 15A). The ceramic tube has a length of ~ 5 cm and an outer diameter of ~ 0.5 cm, leading to an effective membrane area of ~ 8 cm². The CMS layer has a uniform thickness of ≈ 1.4 μ m, and it is overcoated with polydimethylsiloxane (PDMS) to seal any defects (FIGS. 15B, 21A, and 21B).

15

20

[0165] PBI550-100 TFC membrane was tested with pure gas at 100 - 180 °C and 5 bar. It shows H₂/CO₂ selectivity of 25 at 150 °C, much higher than that (7.8) of the PBI550 membrane (Table 13), validating the VPI process on enhancing the size-sieving ability. Increasing the testing temperature increases gas permeance (FIG. 15C), which can be described using the Arrhenius equation. The $E_{P,A}$ value for H₂ permeation is 43 kJ/mol, much higher than that (28 kJ/mol) for CO₂. Therefore, H₂/CO₂ selectivity increases from 16 to 31 as the temperature increases from 100 to 180 °C. The PBI550-100 membrane shows H₂/CO₂ separation performance comparable to other leading CMS membranes (FIG. 15D).

[0166] This disclosure developed a new class of CMS membranes by synergistically combining low-temperature carbonization and subsequent VPI nanoengineering to maximize strong size-sieving abilities and good mechanical properties and processability. By controlling the VPI time, the CMS micropores can be precisely tailored to sub-3.3 Å for efficient H_2/CO_2 separation. The 100-s VPI treatment remarkably increases H_2/CO_2 selectivity of the PBI500 from 9.6 to 83, surpassing the upper bound and leading CMS materials with $T_c < 700$ °C. TFC membranes were successfully prepared and exhibit H_2/CO_2 separation properties superior to leading membranes, demonstrating their potential for H_2 purification and carbon capture to enable biomass conversion to green H_2 . This study unveils a facile and scalable way to fine-tune micropores, which may be used to engineer emerging porous materials to obtain desirable sub-nm pores and nanopores for practical molecular separations and other energy applications involved with molecular diffusion, such as adsorption, catalysts, and energy storage.

[0167] Table 7. Elemental compositions and their molar ratios on the surfaces of PBI600 and VPI-treated PBI600 analyzed using XPS.

Samples	Elemental composition (mol%)				Element molar ratio (mol/mol)	
	C	N	O	Al	Al/N	Al/C
PBI600	64	13	23	0	0	0
PBI600- 40	59	8.8	31	1.4	0.16	0.024
PBI600- 70	48	7.3	43	2.1	0.29	0.045
PBI600- 100	45	7.0	46	2.3	0.32	0.051
PBI600- 100×3C	18	1.4	74	6.8	4.9	0.38

25 [0168] Table 8. Young's modulus, tensile strength, fracture strain, and toughness of PBI CMS and VPI-treated samples.

Samples	Young's modulus (MPa)	Tensile strength (MPa)	Failure strain (%)	Toughness (MJ/m³)
PBI500	23	110	5.9	350
PBI500- 100	34	84	3.0	130
PBI550	21	33	1.7	17
PBI550- 100	38	15	0.45	2.9

[0169] Table 9. Skeletal and bulk densities, porosity, *d*-spacing, pore volume, and surface area of all samples.

Samples	Skeletal density (g/cm ³)	Bulk density (g/cm³)	Porosity	d-spacing (Å)	Pore volume (cm ³ /g) [‡]	Surface area (cm²/g) [‡]
PBI600	1.400 ± 0.010	1.090 ± 0.054	0.175 ±0.010	4.0	0.019	10
PBI600-40	1.394 ± 0.009	1.150 ± 0.020	0.175 ± 0.010	4.0	0.015	8.6
PBI600-70	1.393 ± 0.009	1.160 ± 0.017	0.167 ± 0.040	4.0	0.012	5.7
PBI600-100	1.415 ± 0.040	1.200 ± 0.078	0.152 ± 0.040	4.0	0.0070	4.1

Note: [‡]values are obtained from N₂ adsorption at – 196 °C; ^{**}N/A means data is not available.

[0170] Table 10. Pure-gas permeability and H₂/CO₂ selectivity of AlO_x-infiltrated PBI and PBI CMS films at 100 °C.

Camenlas	TMA exposure	H ₂ permeability	CO ₂ permeability	H ₂ /CO ₂
Samples	time (s)	(Barrer)	(Barrer)	selectivity
	0	9.0	0.82	11
PBI	40	12	1.3	9.2
	100	13	1.3	10
	0	27	2.8	9.6
DD1500	40	18	1.6	11
PBI500	70	4.2	0.085	49
	100	2.5	≤ 0.030	≥ 83
	0	190	19	10
PBI550	40	130	12	11
P D 1330	70	83	2.6	32
	100	19	0.31	61
	0	360	89	4.0
	40	330	85	3.9
PBI600	70	240	38	6.3
	100	50	1.5	33
	100×3 C	0.69		

[0171] Table 11. Parameters of the dual-mode sorption model for CO₂ and C₂H₆ sorption in PBI600 and PBI600-100 at 100 °C. The units for k_D , b, and C'_H are cm³(STP) cm⁻³·atm⁻¹, atm⁻¹, and cm³(STP) cm⁻³, respectively.

Comples		CO_2			C_2H_6	
Samples	k_D	b	C'_H	k_D	b	C_H'
PBI600	0.91	0.41	31	0.56	0.47	25
PBI600-100	1.2	0.38	27	0.30	0.39	22

5 **[0172]** Table 12. H₂/CO₂ separation properties in selected membrane materials for comparison. Mixed gas contains 50% CO₂ and 50% H₂.

Materials			Mixed- or pure- gas	Temp.	H ₂ perm. (Barrer)	H ₂ /CO ₂ selectivity
	1	PBI500-100	Pure	100	2.5	83
CMS in this study	2		Pure	100	19	61
	3	PBI550-100	Mixed	200	80	44
CMS materials (T _c < 700 °C)	4	PBI-PPA600	Mixed	150	120	32
	5	PBI600	Pure	90	300	9
	6	Cellophane600	Pure	30	39	59
	7	Torlon675	Pure	35	1030	4.9
	8	MTI aramide675	Pure	35	630	5.3
	9	Cellulose600	Pure	25	121	28.9
	10	Metal oxide-PFA525	Pure	100	15	9.8
	11	Matrimid500	Pure	150	50.7	7.2
	12	PPG-Cellulose550	Pure	25	544	11.6
CMS materials $(T_c \ge 700 $ °C)	13	Polyimide700	Pure	200	660	24
	14	Cellulose700	Mixed	90	225	31
	15	PBI900	Mixed	100	36	53
	16	Torlon925	Mixed	35	16	57
	17	MTI aramide925	Mixed	35	3.5	156
	18	CANAL-TB900	Mixed	100	8.2	1 <i>7</i> 4
	19	PABZ-6FDA850	Pure	35	190	13
	20	Polyester800	Pure	150	230	8.4
ALD- engineered membranes	21	Pd/Al ₂ O ₃	Pure	188	694	13
	22	PBI/Al ₂ O ₃	Mixed	200	110	20
	23	ZIF-8	Mixed	100	3400	7.8
	24	$PIM-1/Al_2O_3$	Pure	35	2492	4.0
	25	SSZ-13	Pure	200	128	4.1

[0173] Table 13. Pure-gas H₂/CO₂ separation performance of CMS TFC membranes at 150 °C.

Membranes	Pressure (bar)	H ₂ permeance (GPU)	CO ₂ permeance (GPU)	H ₂ /CO ₂ selectivity
PBI550	3.0	140	18	7.8
FBI 330	5.0	140	18	7.8
PBI550-100	3.0	32	1.3	25
PB1330-100	5.0	33	1.3	25

15

20

[0174] Table 14. Pure-gas H₂/CO₂ separation performance of CMS TFC membranes in FIG. 14D.

CMS membrar	100	Materials	Temp.	H ₂ permeance	H ₂ /CO ₂
Civis memoranes		Matchais	(°C)	(GPU)	selectivity
This study 1		PBI550-100	180	66	31
	2	Torlon675	35	20.3	4.9
CMS TFC	3	MTI aramide675	35	16	5.3
membranes	4	Cellulose550	130	467	11.1
$(T_c < 700 \text{ °C})$	5	Metal oxide- PFA525	25	99	11.4
	6	Matrimid500	150	507	7.2
	7	Polyimide700	200	3300	24
CMS materials	8	Torlon925	35	0.65	94
	9	MTI aramide925	35	0.23	366
$(T_c \ge 700 \text{ °C})$	10	Cellulose850	130	148	84
	11	Polyester800	150	1850	8.4

EXAMPLE 5

5 **[0175]** The following is an example of polymer-based membranes of the present disclosure, methods of making same, and uses thereof.

[0176] This example describes atomically fine-tuning 6FDA-DAM-derived carbon molecular sieve (CMS) membranes for propylene/propane (C₃H₆/C₃H₈) separation.

[0177] A commercial polyimide, 6FDA-DAM, was carbonized at 500 °C, and then treated using vapor-phase infiltration for C₃H₆/C₃H₈ separation. The treated 6FDA-DAM-derived CMS, named as 6FDA-DAM500-*x*, where 500 and x represent carbonization temperature and VPI cycles (2-10 cycles), respectively. Compared to the pristine 6FDA-DAM500, the 6FDA-DAM500-*x* films exhibited much higher C₃H₆/C₃H₈ selectivity, indicating the versatility of VPI treatment on enhancing size-sieving ability of CMS materials.

[0178] Preparation of 6FDA-DAM films, CMS films, and VPI-treated films. The 6FDA-DAM films were fabricated using a solution-cast method. Briefly, commercial 6FDA-DAM (M.W,: 215K) powders were added in DMF and dissolved for 1 hour. The obtained solution was filtered through a 1- μ m glass fiber filter and then cast into a glass petri dish. The solution was dried at 60 °C with a N₂ flow overnight. The obtained film was then dried under vacuum at 150 °C for 48 h. The film has a uniform thickness of ~ 50 μ m. To prepare 6FDA-DAM500 films, the as-prepared 6FDA-DAM films were sandwiched between two ceramic plates and carbonized in a tube furnace (MTI Corporation, Richmond, CA) with a N₂ flow of 200 mL/min. The temperature was ramped up following the procedures below:

10

15

25

- 1. From 23 °C to 250 °C by 10 °C/min;
- 2. From 250 °C to 485 °C by 3.85 °C/min;
- 3. From 485 °C to 500 °C by 0.25 °C/min;
- 4. soak at 500 °C for 2 hours
- 5. naturally cooled down ≈ 23 °C with the N₂ flow.

[0179] VPI was conducted at 85 °C, maintaining a base chamber pressure of 0.2 Torr. Each AlOx infiltration cycle for the VPI treatment comprised four sequential steps: First, the chamber was isolated, and TMA was introduced for 50 ms to achieve a TMA vapor pressure of ~1 Torr, PBI was exposed to TMA for 100 s. Second, the chamber was purged with nitrogen gas at a flow rate of 100 sccm for 100 s, followed by evacuation to the base vacuum over 30 s. Third, water vapor, as the coreactant, was injected for 50 ms to reach a vapor pressure of ~1 Torr, Then PBI was exposed to the water vapor for a specified period. Fourth, the chamber was purged again with nitrogen at 100 sccm for 100 s, then pumped to base vacuum for 30 s.

- [0180] Characterization. WAXD patterns were obtained using a Rigaku Ultima IV X-ray diffractometer with Cu Kα x-ray source. A Renishaw inVia Raman Microscope (Renishaw plc, UK) was employed to obtain Raman spectra of the 6FDA-DAM500 samples. The bulk density of the films was calculated based on the corresponding mass and volume. The skeletal density of the films was measured using a Micromeritics Accu-Pyc II 1340 Gas
- 20 Pycnometer (Micromeritics Instrument Corporation, Norcross, GA). For CMS films, pure-gas permeability was determined using a constant-volume and variable-pressure system.
 - [0181] FIG. 22A shows that all 6FDA-DAM500 films exhibit a broad peak at ~12° in the wide-angle X-ray diffraction (WAXD) patterns, corresponding to a d-spacing of 7.4 Å calculated using Bragg's law, indicating that the VPI treatment has no discernible impact on the carbon stacking of 6FDA-DAM500. On Raman spectra of those samples (FIG. 22B), the ratios of disordered carbon peak (I_D) to highly oriented graphitic carbon peak (I_G) are same at 0.68, reflecting that VPI has a negligible effect on the bulk carbon structures of 6FDA-DAM500. FIG. 22C shows C_3H_6/C_3H_8 selectivity increases up to 110 when the VPI cycles increases to 10, though C_3H_6 permeability decreases.

30 EXAMPLE 6

[0182] The following is an example of polymer-based membranes of the present disclosure, methods of making same, and uses thereof.

15

20

25

30

separation properties enabled by Few-Cycle Atomic Layer Deposition. Oxygen plasma treatment of polysiloxane composite is a rapid (e.g., less than 3 minutes) approach to convert the polymer skin layer into polyorganosilica material with desirable H2/CO2 separation properties. However, the POSi membranes are unstable in hydrothermal condition, where simultaneous hydrolysis and condensation reaction of siloxane linkages leads to POSi network rearrangement. Atomic layer deposition of aluminum oxide was used to induce Al-O-Si covalent linkage, tightening the POSi porous structure and stabilizing siloxane linkage against hydrothermal condition. FIG. 23A presents the schematic of the chemical structure of polysiloxane, POSi, and POSi-AlOx, where the oxygen plasma treatment enables the conversion of rubbery polysiloxane into porous silica-like POSi structure with prominent hydroxyl groups(-OH). These -OH groups are desirable for the deposition of aluminum oxides, tightening the POSi structure for precise H2/CO2 separation.

[0184] FIG. 23A presents the schematic of the chemical structure of polysiloxane, POSi, and POSi-AlOx, where the oxygen plasma treatment enables the conversion of rubbery polysiloxane into porous silica-like POSi structure with prominent hydroxyl groups(-OH). These -OH groups are desirable for the deposition of aluminum oxides, tightening the POSi structure for precise H₂/CO₂ separation.

[0185] Experimental. Materials. Porous Polysulfone (PSF) support with a molecular weight cut-off of 20 kDa was purchased from Solecta, Inc. (Oceanside, CA). Wacker Dehesive 944 (vinyl-functionalized PDMS in toluene), Cross-linker V 24 (polymethylhydrosiloxane or PMHS), and Catalyst OL (1 mass% Platinum in PDMS) were kindly provided by Wacker Chemical Corporation (Ann Arbor, MI). Isopropanol (IPA), isooctane, and hexane were provided by Fisher Scientific (Hampton, NH). Ultrahigh purity (> 99.999%) gas cylinders of H₂, CO₂, and N₂ were supplied from Airgas USA (Buffalo, NY). Fabrication of POSi membranes. First, the PSF support was pretreated with water, [0186]IPA, and isooctane (1 day in each solvent) to remove pore preservations, then dried in a fume hood overnight. Second, ~0.83 mass% poly(DMS-co-MHS) solution in hexane was prepared by mixing PDMS, PMHS, and OL at a mass ratio of 63:23:14 and was mixed for 3 hours at room temperature before being used as a coating solution. Third, the polysiloxane solution was coated onto treated PSF support using dip-coater (MTI Corporation, Richmond, CA) with a soaking time of 5 s (s = second(s)) and a drawing speed of 5 cm/min (min = minute(s)). The liquid film was rapidly dried using a heat gun to avoid pore penetration. Oxygen plasma treatment of polysiloxane TFC membranes was conducted using ICP-RIE

15

20

25

30

plasma chamber Phantom III (Trion Technology, Inc., Clearwater, FL). The treatment condition is set at an ICP power of 200W, RIE power of 20W, chamber pressure of 100 mTorr, exposure time of 120s, and oxygen flowrate of 20 sccm.

[0187] Atomic layer deposition of aluminum oxide on POSi membrane. ALD was conducted in Cambridge Nanotech Savannah S100 system at 80°C under N₂ environment at ~100 mTorr. Trimethylaluminum (TMA) was used as an organometallic precursor, while water was used as an oxidant. A cycle of ALD treatment consists of 15 ms injection of TMA, followed by 30s N₂ purging, then 15 ms injection of water followed by 60 s N₂ purging. The ALD on POSi was performed for 1, 3, 5 and 7 cycles immediately after the oxygen plasma treatment. The ALD-treated POSi is named POSi-xC, where x denotes the number of ALD cycles (i.e, POSi-3C denotes POSi membrane with 3 cycles of ALD).

[0188] Characterization. The cross-sectional image of the membrane was captured using focused ion beam scanning electron microscope (FIB-SEM) (Carl Zeiss Auriga CrossBeam, Germany). AFM was conducted using Bruker Dimension Icon with ScanAsyst[®].

[0189] Pure-gas permeance of POSi membranes was determined at 150 °C with the feed pressure between 40-120 psig (pounds per square inch gauge) using a constant-volume and variable-pressure apparatus. Mixed-gas transport properties were determined via a variable-volume and constant-pressure apparatus at 60 psig and 150 °C, where the feed gas concentration is controlled by mass-flow-controller (Sierra Instrument, CA). The total feed flow rate is kept at 200 cm³(STP) min⁻¹ (sccm (standard cubic centimeter per minute)) to achieve a stage-cut of less than 2%. Water vapor was introduced by passing the feed gas through a bubbler at 23°C to attain water vapor content of 0.52 mol%. The permeate side was swept with 2 - 10 sccm of nitrogen gas which was analyzed using a Micro GC 3000 gas analyzer (Inficon Inc., East Syracuse, NY).

[0190] Result and Discussion. FIGS. 23B and 23C present the SEM cross-sectional images of POSi membranes before and after 3-cycle of ALD treatments, respectively. The combined thickness of the selective layer was roughly 140 nm, where distinction between polysiloxane, POSi and AlOx layers is non-trivial. This can be attributed to the ultrathin effective thickness of plasma treatment and nano-scale deposition of aluminum oxide (Al₂O₃ thickness of roughly 2.4Å for deposition at 80°C on silicon wafer). The ALD treatment of POSi membranes shows neglectable surficial morphology changes as presented by the SEM surface of POSi-3C (FIG. 23D) and surface roughness values of POSi membranes at different deposition cycles (FIG. 23E).

[0191] FIG. 24A presents the gas transport properties of POSi membranes with different number of ALD cycles at 150°C and 60 psig. Increasing the ALD cycles from POSi-0C to POSi-3C decreases the H₂ permeance decreases from 580 GPU to 290 GPU. On the other hand, the gas permeance of CO₂. N₂ and CH₄ decreases much more rapidly with increasing ALD cycle. For example, the POSi-0C exhibits the CO₂, N₂ and CH₄ permeance of 24, 2.7 and 2.9 GPU, respectively, while the POSi-3C exhibits gas permeance of 0.78, 0.21 and 0.39 GPU, respectively. These results indicate tightening of POSi nanoporous structure, enabling strong improvement in the H₂/gas selectivity (FIG. 24B). For instance, with 3 cycles of ALD treatment, the H₂/CO₂ selectivity increases from 25 to 380, and the H₂/CH₄ increases from 10 200 to 750. Interestingly, the CH₄ gas permeance is higher than that of N₂ gas at all cycles of ALD, which can be attributed to the nano-defect, inducing Knudsen permeation. FIG. 25A presents the temperature effect on the H₂/CO₂ gas transport properties [0192]of POSi-1C. Increasing the temperature between 75°C and 150°C, drastically increases the H₂ permeance from 70 GPU to 300 GPU, while the CO₂ permeance slightly increases from 3.1 15 GPU to 4.0 GPU. This leads to a strong improvement in H₂/CO₂ from 23 to 74. To elucidate the promising attributes of POSi-AlOx membrane for practical application, the membranes are challenged with simulated syngas conditions. FIG. 25B presents the H₂/CO₂ transport properties of POSi-3C at various gas mixtures. Increasing CO₂ partial pressure exhibits negligible changes in the gas permeance and H₂/CO₂ gas selectivity. 20 Specifically, the POSi-3C exhibits constant H₂ permeance of 200 GPU and H₂/CO₂ selectivity of 110 when increasing the CO₂ partial pressure from 1.9 to 6.5 atm, indicating resistance against CO₂ plasticization effect. FIG. 25C shows the long-term stability of POSi-3C at 150°C and the cycle of dry-wet conditions. The POSi-3C exhibits a stable H₂ permeance of 240 GPU with an H₂/CO₂ selectivity of 115 in dry gas for up to 58 hours. Introducing 0.52 mol% water decreases the H₂ permeance to 140 GPU while retaining the 25 H₂/CO₂ selectivity at 115 for 14 hours. The H₂ permeance does not recover upon switching back to dry feed, and the H₂/CO₂ remains constant at 115.

[0194] Although the present disclosure has been described with respect to one or more particular embodiment(s) and/or example(s), it will be understood that other embodiment(s) and/or example(s) of the present disclosure may be made without departing from the scope of the present disclosure.

CLAIMS:

1. A polymer-based membrane comprising:

optionally, a substrate;

- optionally, an interlayer disposed on the substrate; and
 - i) a polymer film comprising a plurality of polymer chains; and a metal oxide layer disposed on at least a portion or all of an exterior surface or surfaces of the polymer film, wherein at least a portion of the polymer chains are immobilized and/or crosslinked by metal oxide groups of the metal oxide film,

10 or

15

20

- ii) a carbonized polymer film comprising a plurality of micropores or a polyorganosilica film comprising a plurality of ultramicropores; and a plurality of a metal oxide domains disposed on at least a portion or all of an exterior surface or surfaces of at least a portion, substantially all, or all of the micropores or ultramicropores.
- 2. The polymer-based membrane of to claim 1, wherein the polymer film comprises polybenzimidazole, polyimides, polyamides, polysulfones, polycarbonates, cellulose acetates, Pebax polymers, PolyActive polymers, polyethers, structural analogs thereof, copolymers thereof, or any combination thereof.
- 3. The polymer-based membrane of claim 1, wherein the polymer film comprises one or more linear dimension(s) of about 10 nm to about 10,000 nm.
- 4. The polymer-based membrane of claim 1, wherein the metal oxide layer comprises one or more linear dimension(s) of about 10 nm to about 10,000 nm.
 - 5. The polymer-based membrane of claim 1, wherein the polymer-based membrane comprises a carbonized polymer film comprising a plurality of micropores, wherein at least a portion, substantially all, or all of the micropores comprise a size of about 2 nm to about 100 nm, or a polyorganosilica film comprising a plurality of ultramicropores, wherein at least a portion, substantially all, or all of the micropores comprise a size of about 0.3 nm to about 1 nm, and/or the porosity of the carbonized film or polyorganosilica film is about 1 volume

percent to about 20 volume percent (based on the total volume of the carbonized polymer film or polyorganosilica film).

- 6. The polymer-based membrane of claim 1, wherein the polymer film further comprises a plurality of nanoparticles.
- 7. The polymer-based membrane of claim 6, wherein at least a portion, substantially all, or all of the nanoparticles have a size of about 10 nm to about 100 nm and/or are present in the polymer film at about 0 to about 40 percent by weight (based on the total weight of the polymer film).
- 8. The polymer-based membrane of claim 1, wherein the metal oxide layer or metal oxide domains is/are chosen from AlOx layers or domains, SiOx layers or domains, TiOx layers or domains, ZnOx layers or domains, SnOx layers or domains, structural analogs thereof, and any combination thereof.
- 9. The polymer-based membrane of claim 1, wherein the polymer-based membrane exhibits one or more or all of the following:
- an H₂ permeability of about 1 to about 1000 Barrer;
- an H₂/CO₂ selectivity of about 10 to about 200;

10

- thermal stability to at least about 200 °C or about 300 °C.
- 10. A method of making a polymer-based membrane of claim 1, the method comprising forming a polymer film;
- optionally, drying the polymer film;
 optionally, at least partially, substantially, or completely carbonizing the polymer film
 optionally, plasma treating the polymer film; and
 - contacting the carbonized polymer film or plasma-treated polymer film with one or more vapor-phase metal oxide precursor(s) and, optionally, water vapor,
- optionally, repeating the contacting a desired number of times. wherein the polymer-based membrane is formed.
 - 11. The method of claim 10, the contacting is carried out sequentially.

- 12. The method of claim 10, wherein the contacting is repeated 1, 2, 3, 4, 5, 6, 7, 8, 9, 10, 11, 12, 13, 14, or 15 times.
- 13. The method of claim 10, wherein the vapor-phase metal oxide precursor(s) is/are chosen from vapor-phase AlOx precursors, vapor-phase SiOx precursors, vapor-phase TiOx precursors, vapor-phase ZnOx precursors, vapor-phase SnOx precursors, structural analogs thereof, and any combination thereof.
- 14. The method of claim 13, wherein the vapor-phase AlOx precursor(s) is/are chosen from trialkyl aluminum compounds, structural analogs thereof, and any combination thereof; and/or the vapor-phase SiOx precursor(s) is/are chosen from silicon tetrahalides, tris(dialkyl amino)silane compounds, structural analogs thereof, and any combination thereof; and/or the vapor-phase TiOx precursor(s) is/are chosen from titanium alkoxide compounds, titanium halide compounds, or any combination thereof; and/or the vapor-phase ZnOx precursor(s) is/are chosen from dialkyl zinc compounds, structural analogs thereof, and any combination thereof and/or the vapor-phase SnOx precursor(s) is/are chosen from stannic halide compounds, structural analogs thereof, and any combination thereof.
- 20 15. The method of claim 10, wherein the polymer film comprises a plurality of nanoparticles.
 - 16. A system comprising one or more polymer-based membrane(s) of claim 1.

- 17. The system of claim 16, wherein the polymer-based membrane(s) is/are disposed in a
 25 housing, the housing comprising one or more orafic(es) configured for introduction, control, or the like of gas(es) into the housing.
 - 18. The system of claim 16, the system wherein the system is configured for gas separation and/or gas enrichment.
 - 19. The system of claim 16, the system further comprising one or more components suitable for use in gas separation and/or gas enrichment.

20. A method of separating one or more gas(es) from a mixture comprising the one or more gas(es) and at least one other gas and/or enriching one or more gas(es) in a mixture comprising at least one other gas, the method comprising:

contacting the mixture or the like with one or more polymer-based membrane(s) of claim 1; and

optionally, repeating the contacting with contacted mixture or a portion thereof a desired number of times;

wherein one or more of the gas(es) in the mixture is separated from the mixture and/or enriched in the mixture.

10

15

- 21. The method of claim 20, wherein the mixture is an effluent from a fossil fuel power plant, an industrial gas effluent, or a mixture from syngas processing.
- 22. The method of claim 20, wherein the polymer-based membrane(s) is/are reused in a subsequent separation and/or enrichment.
 - 23. The method of claim 20, wherein the polymer-based membranes(s) is/are cleaned prior to use in each of the subsequent separation(s) and/or enrichment(s).

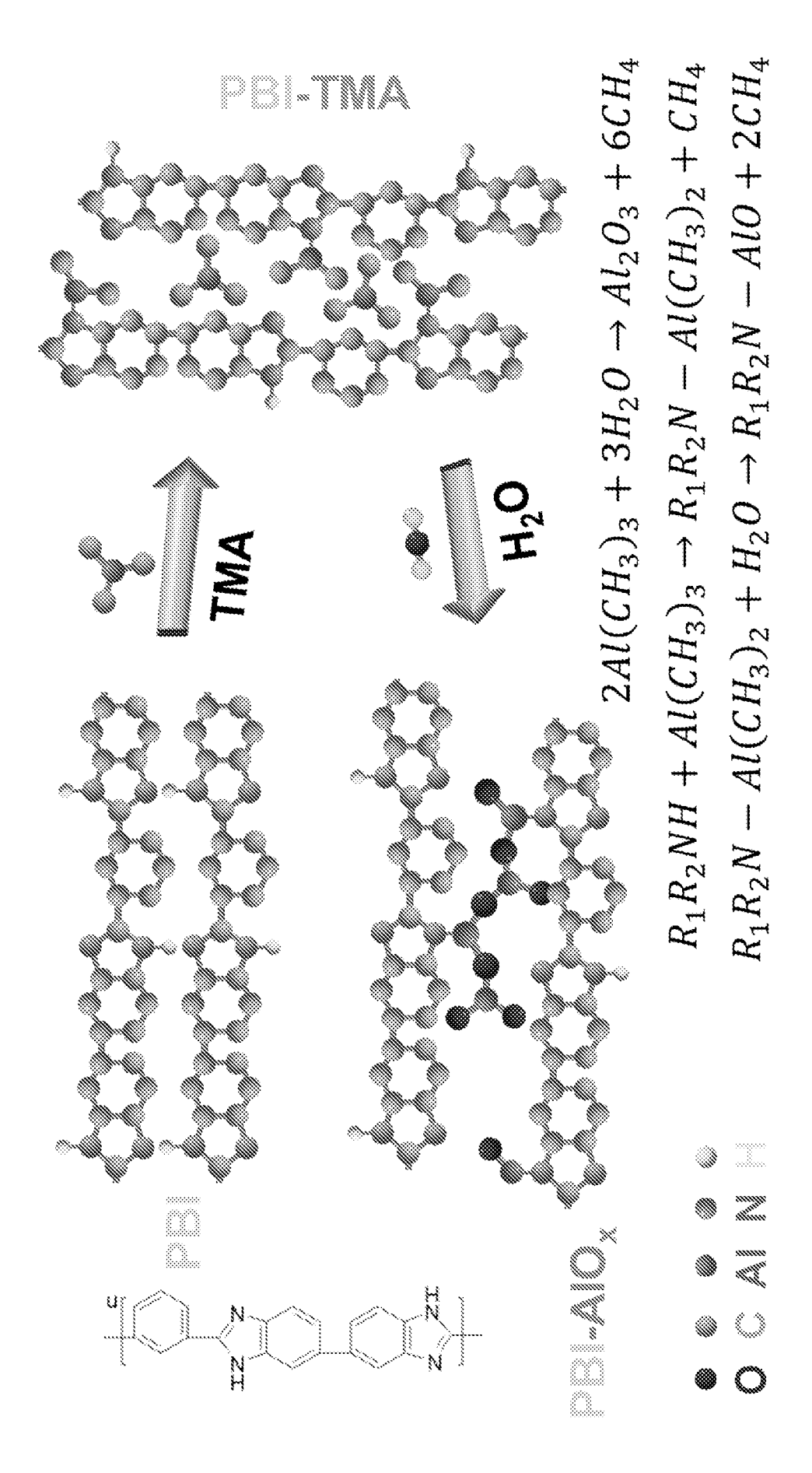


FIG. 1A

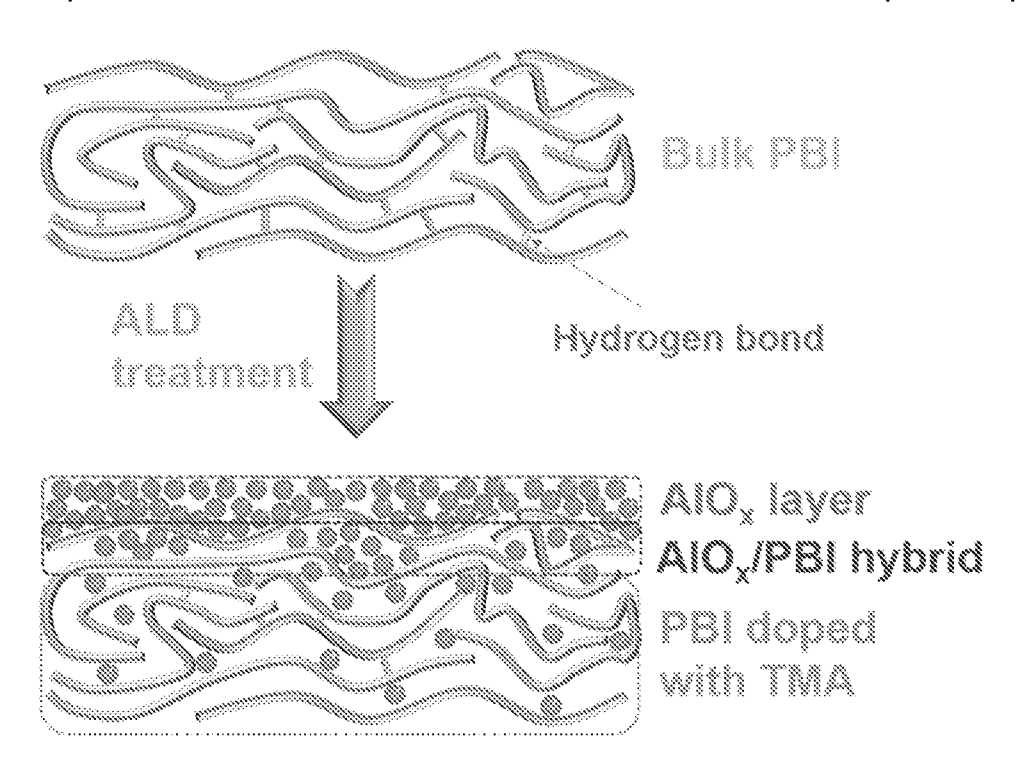


FIG. 1B

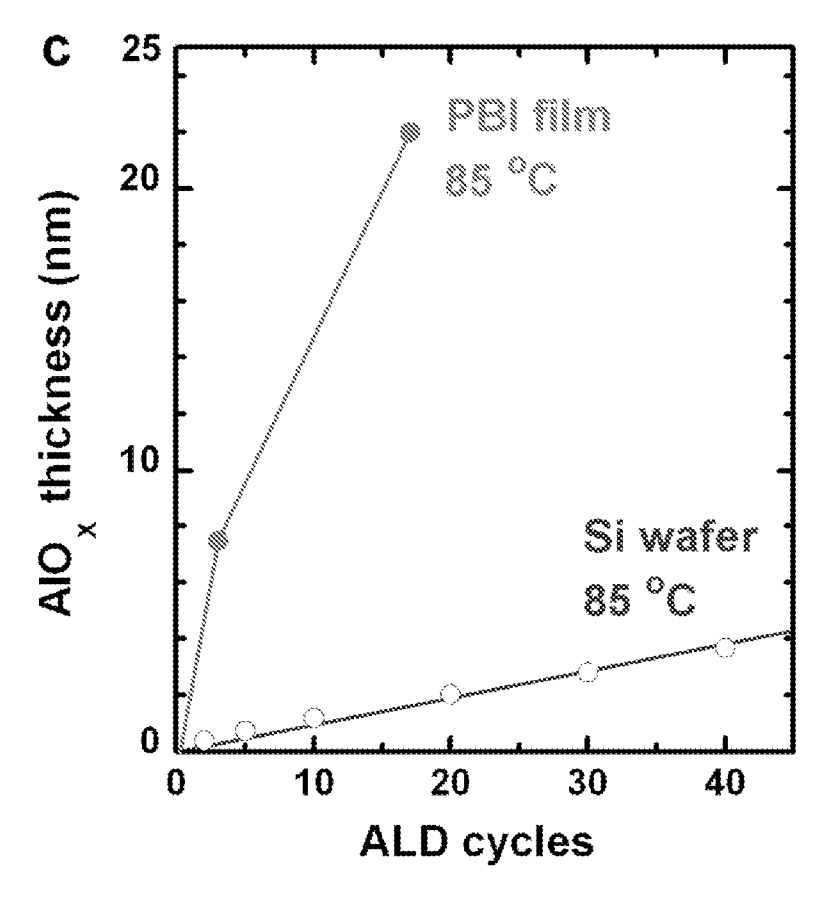


FIG. 1C

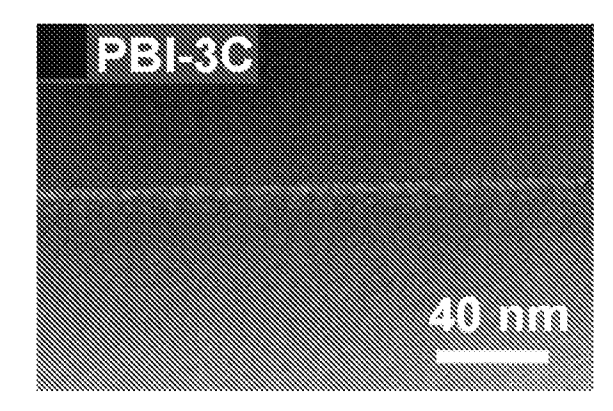


FIG. 1D

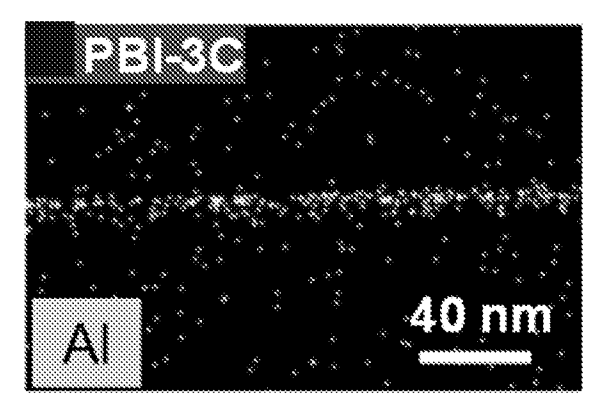


FIG. 1E

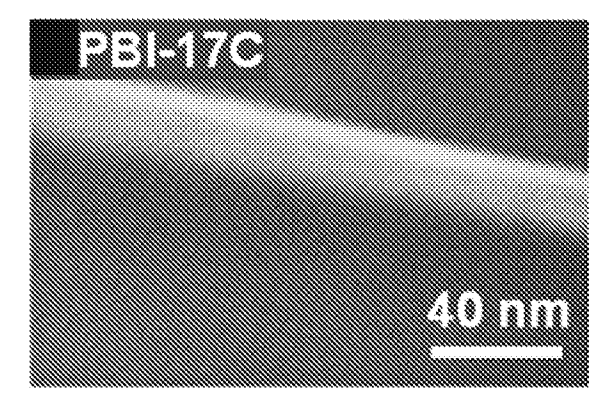


FIG. 1F

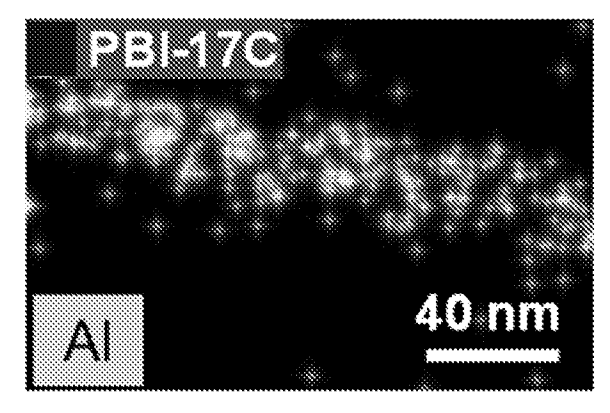


FIG. 1G

WO 2025/111491 PCT/US2024/056939

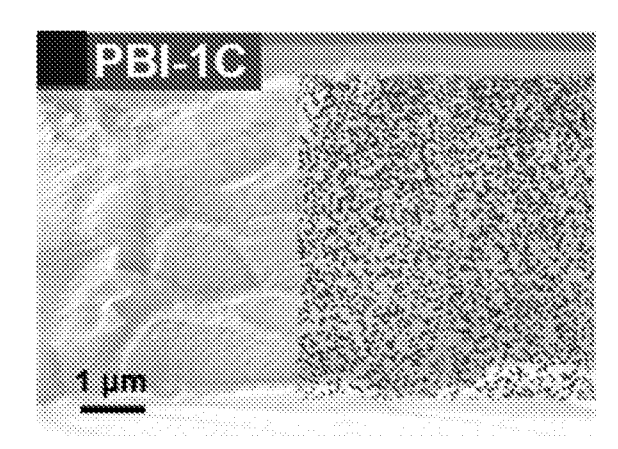


FIG. 1H

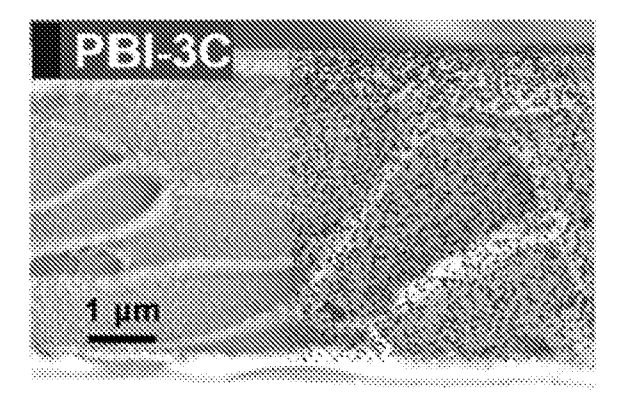


FIG. 11

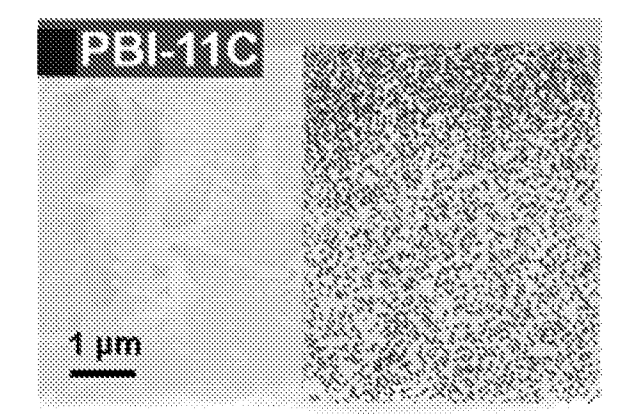


FIG. 1J

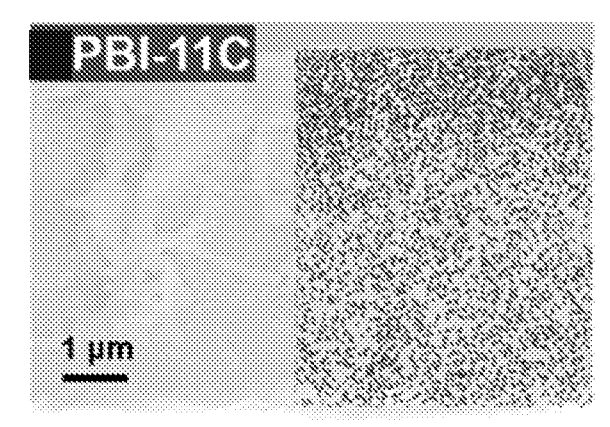
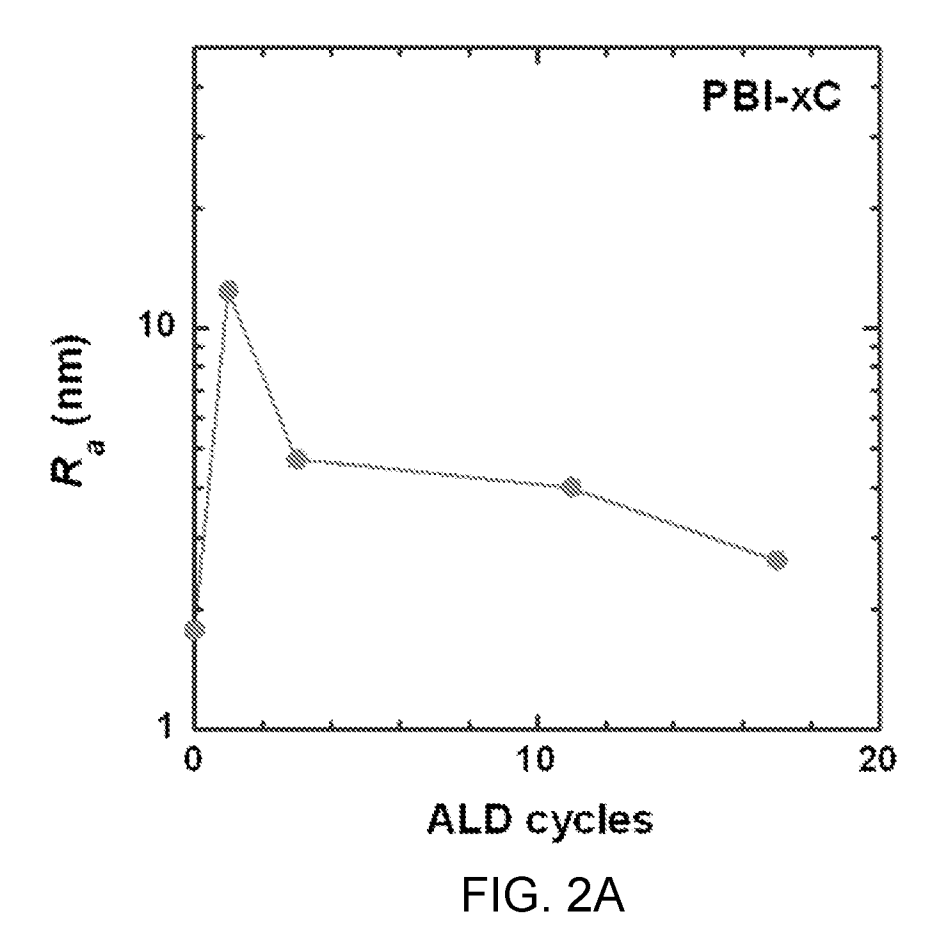
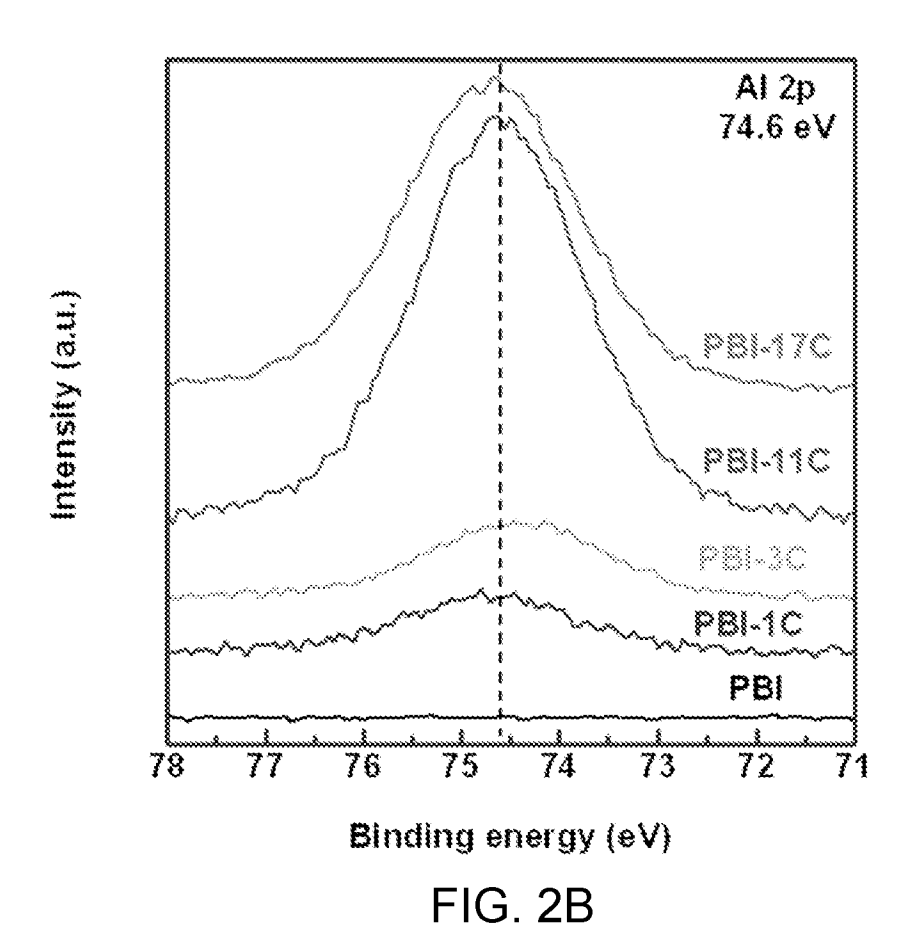
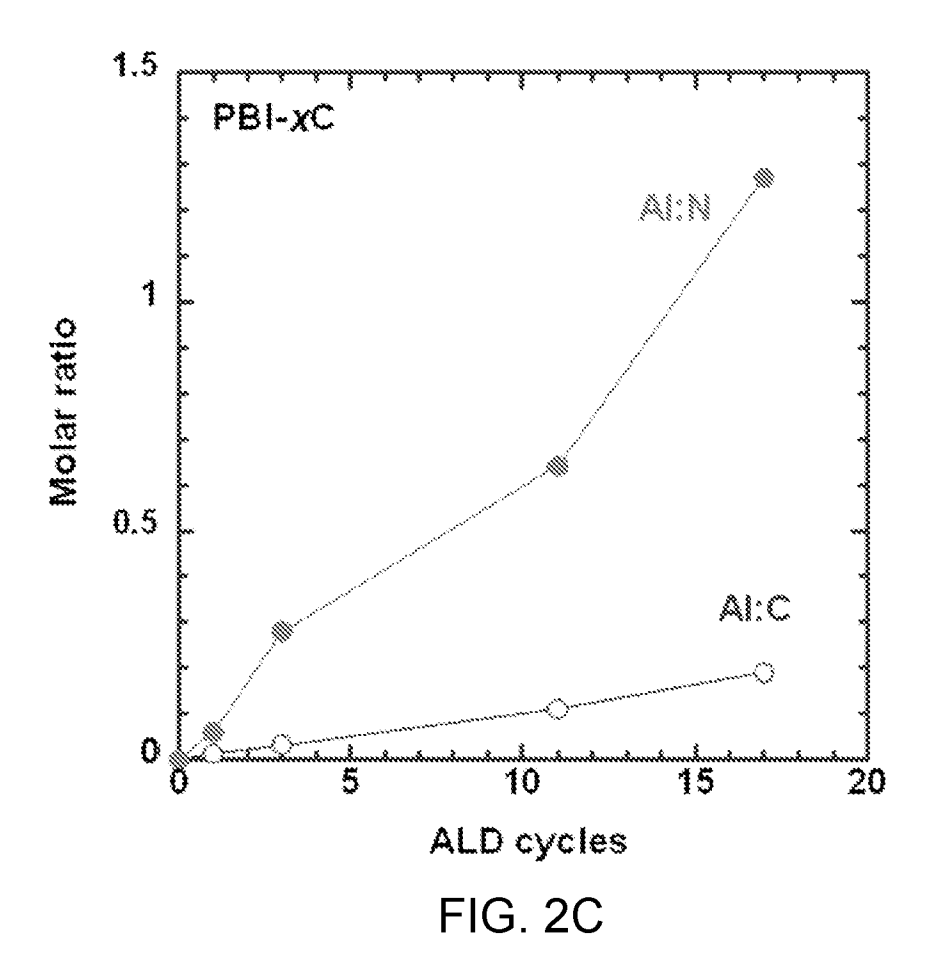
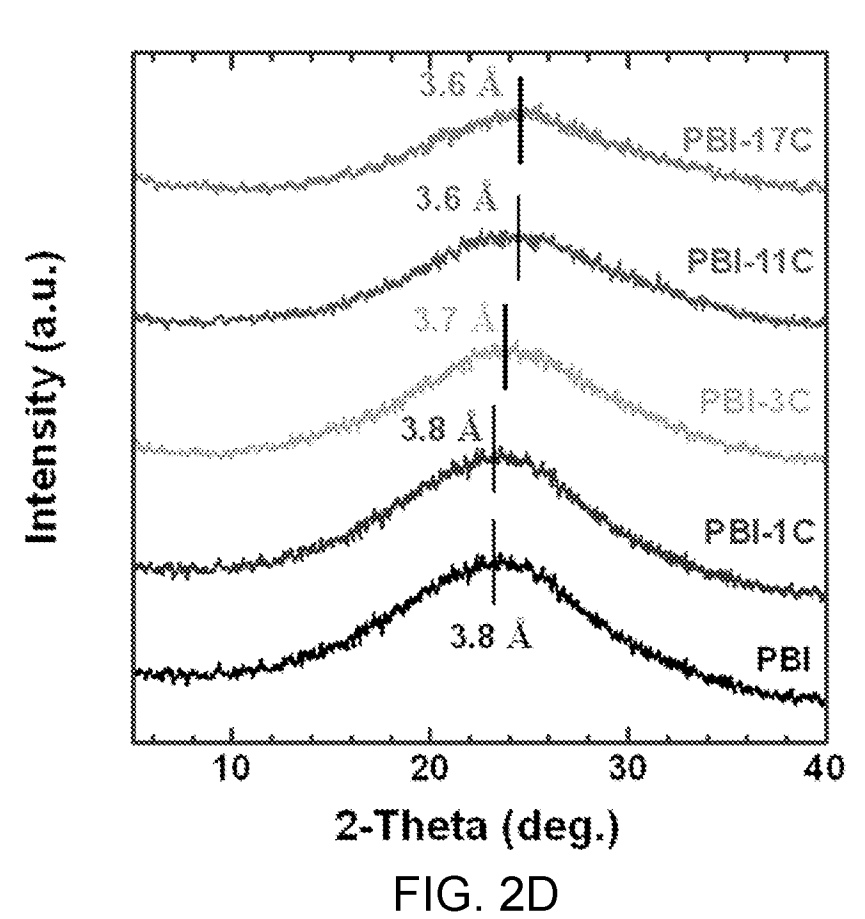


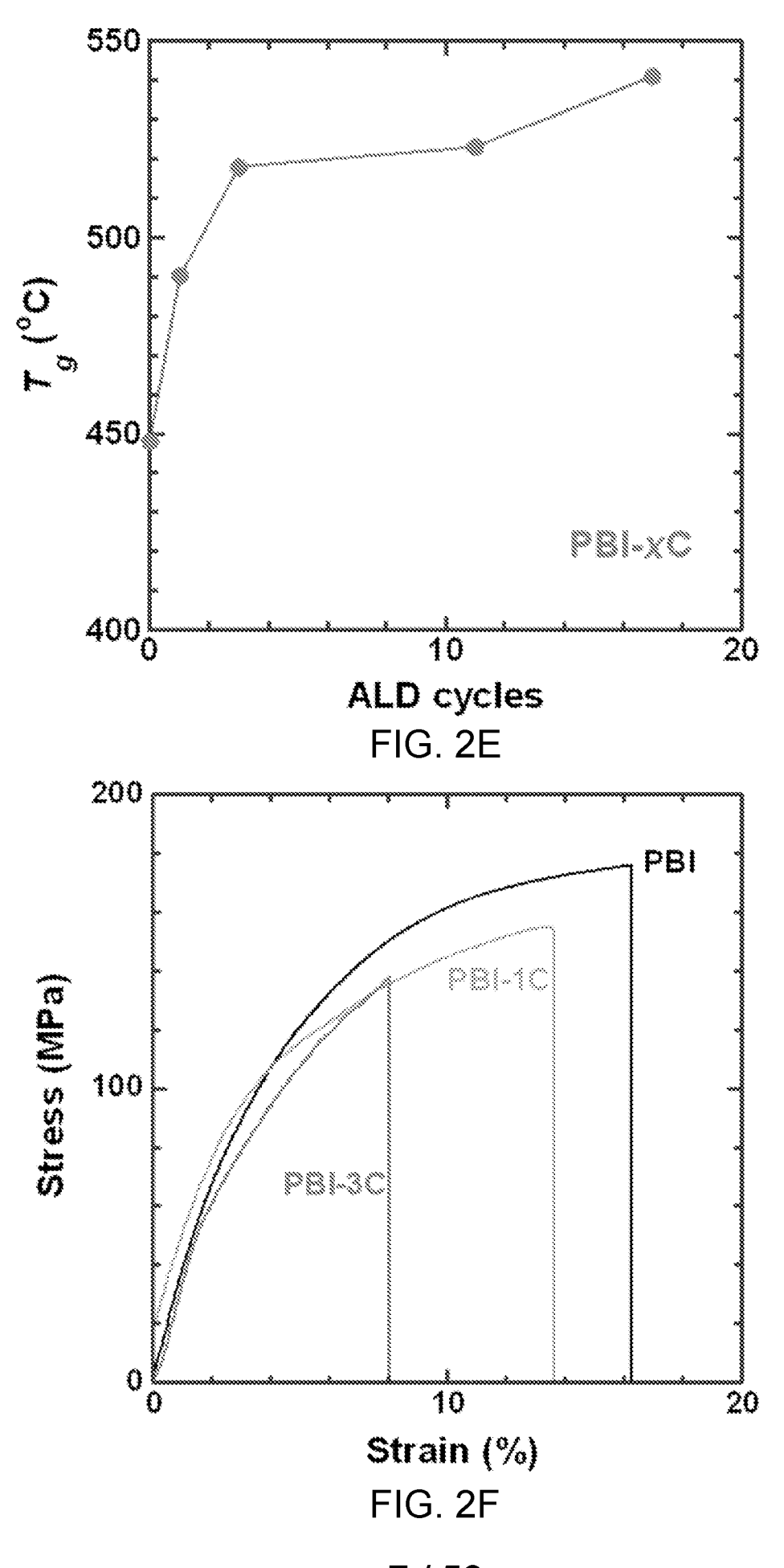
FIG. 1K











7 / 59

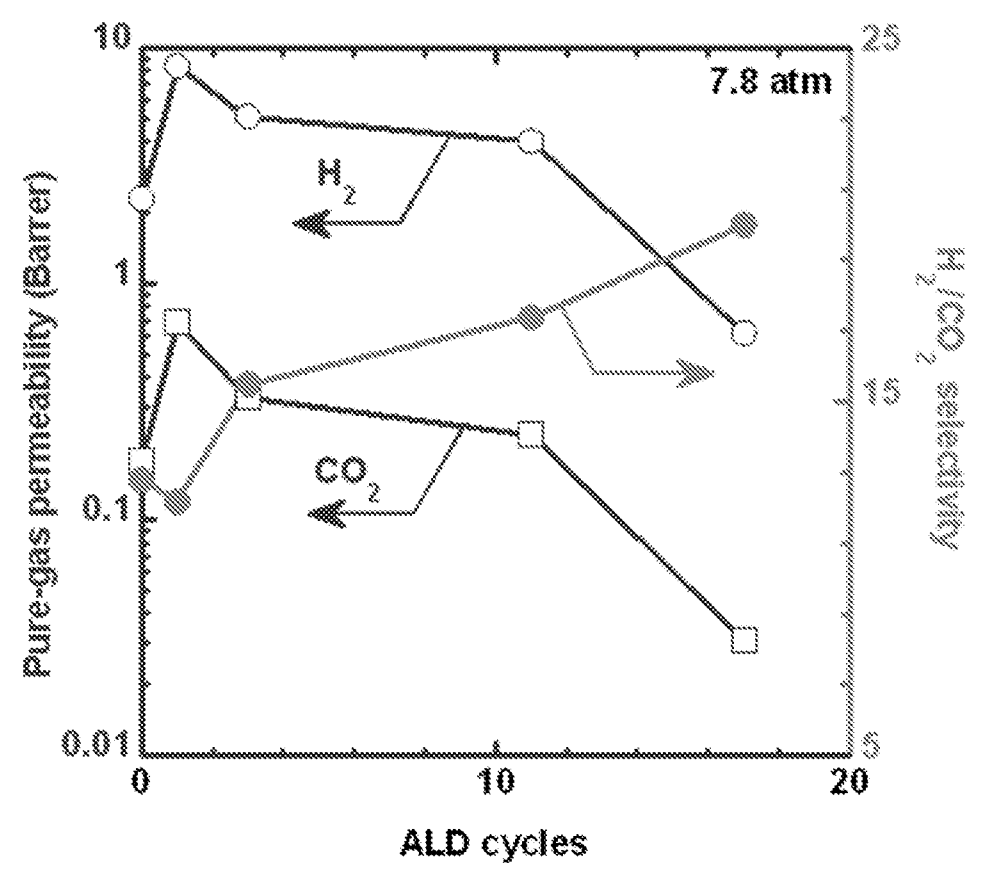


FIG. 3A

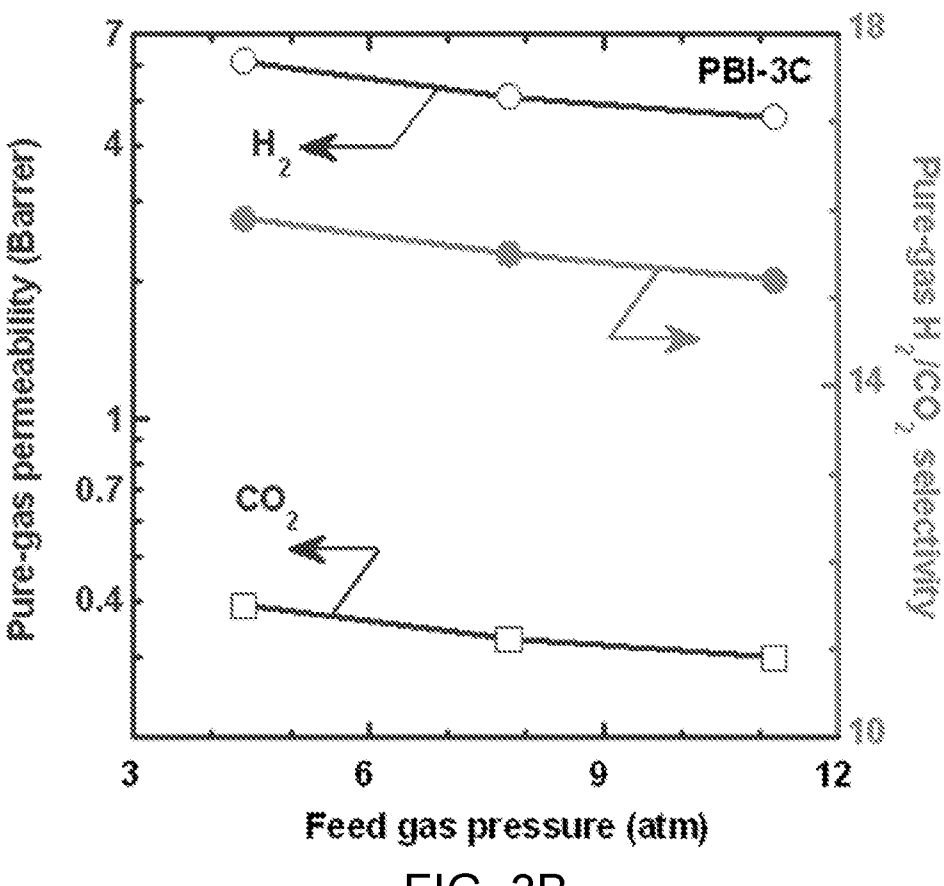
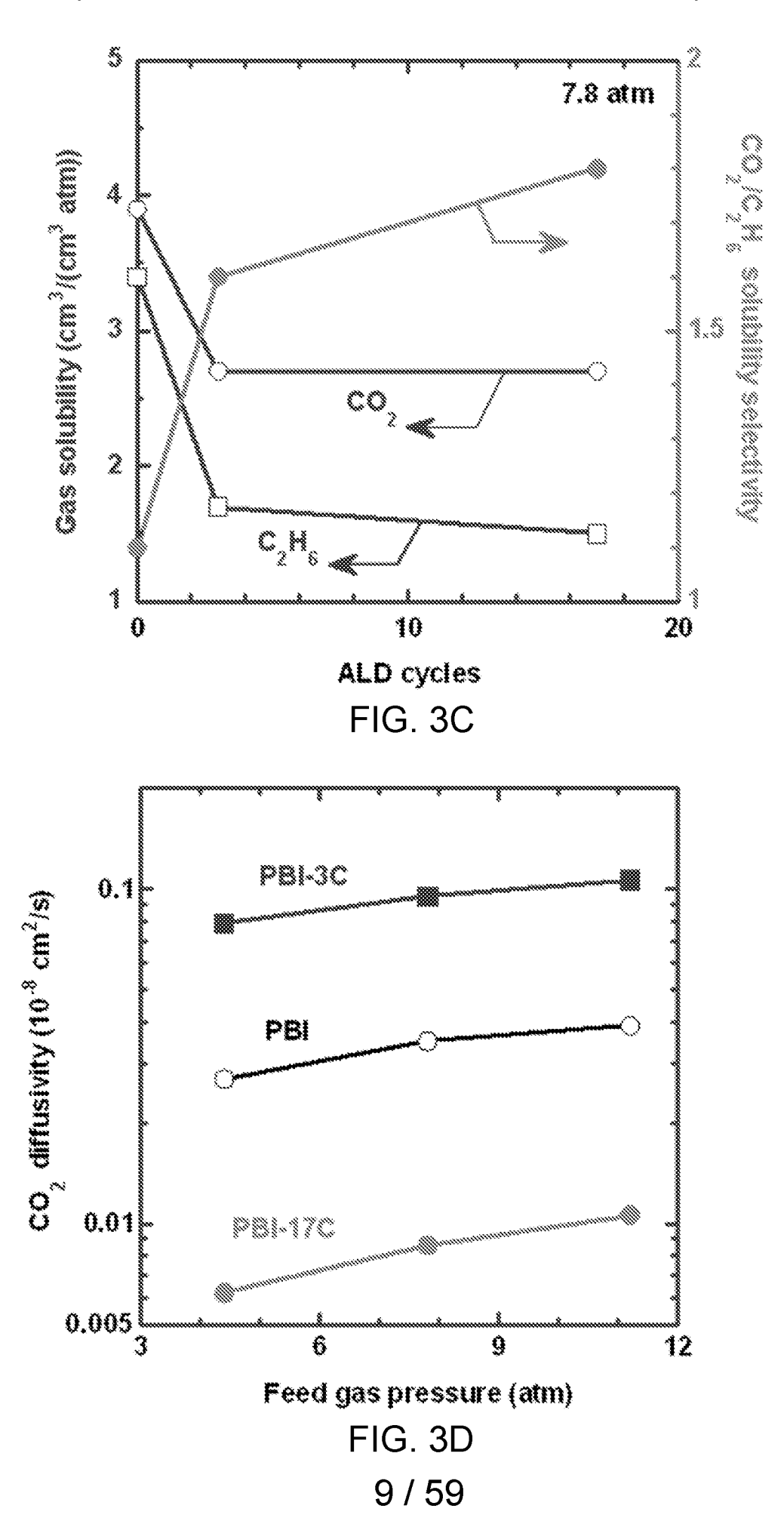
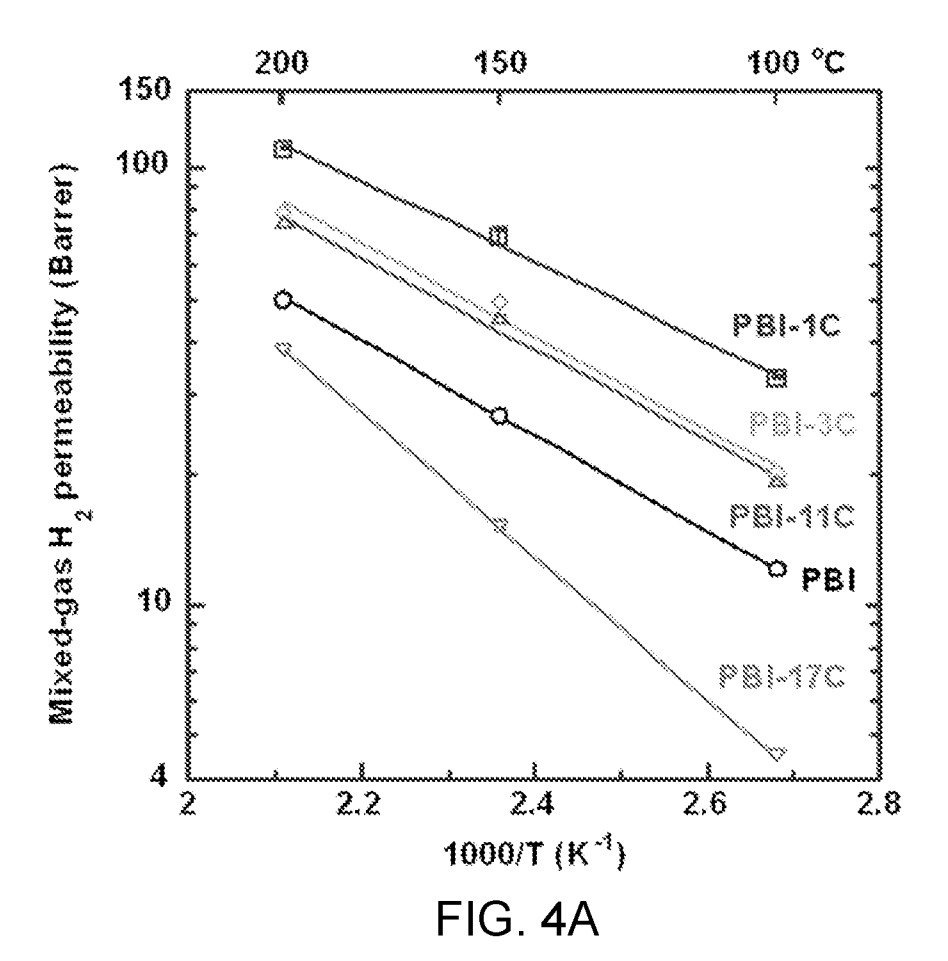
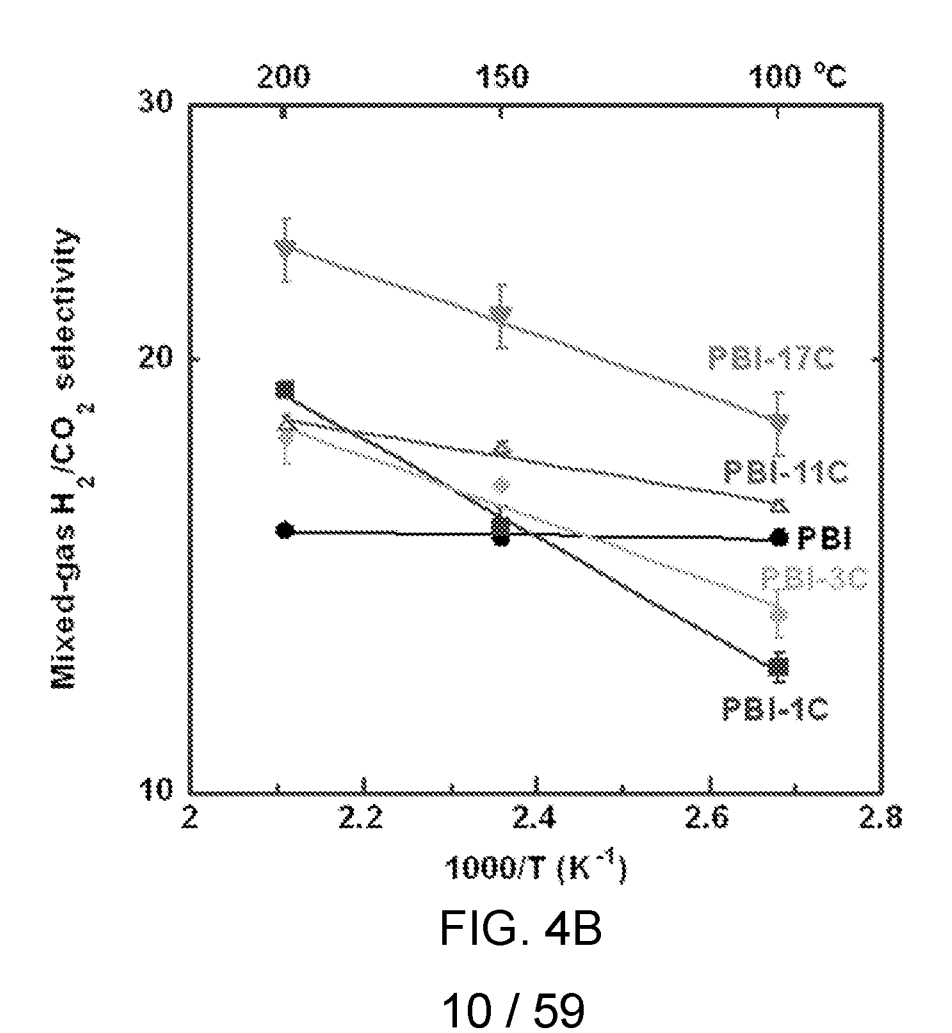


FIG. 3B 8 / 59







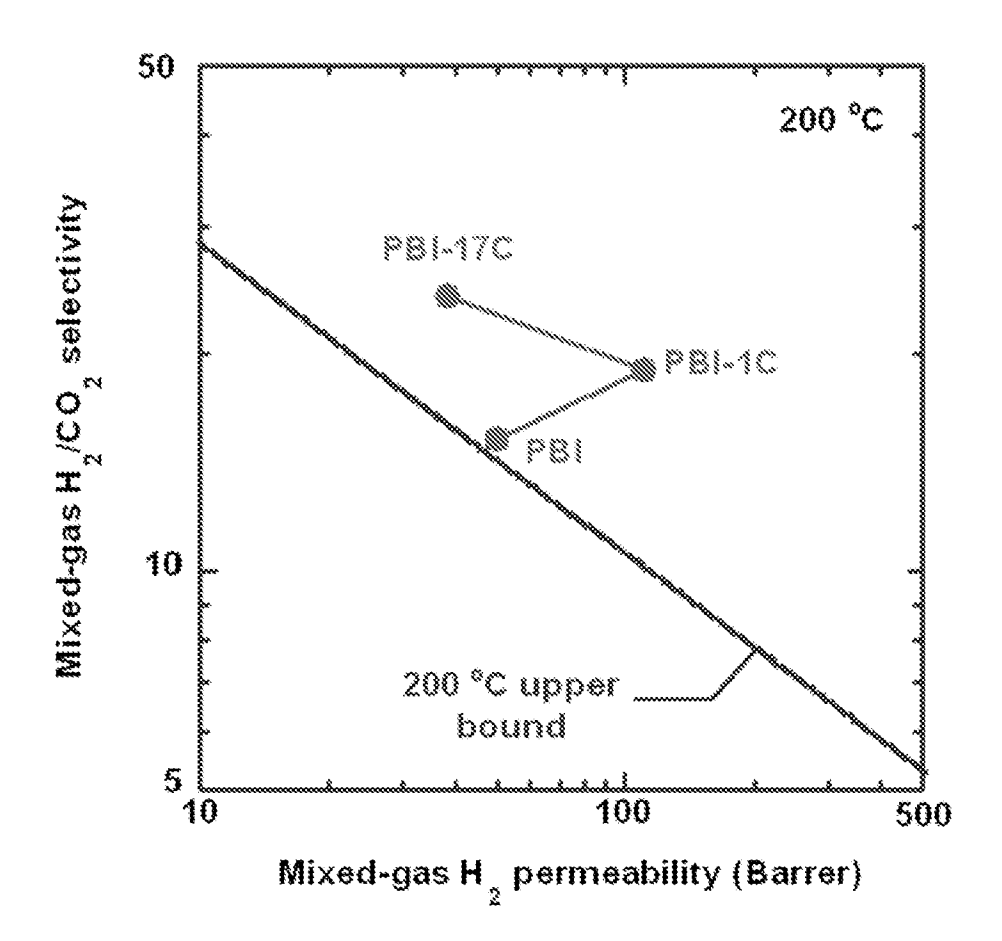
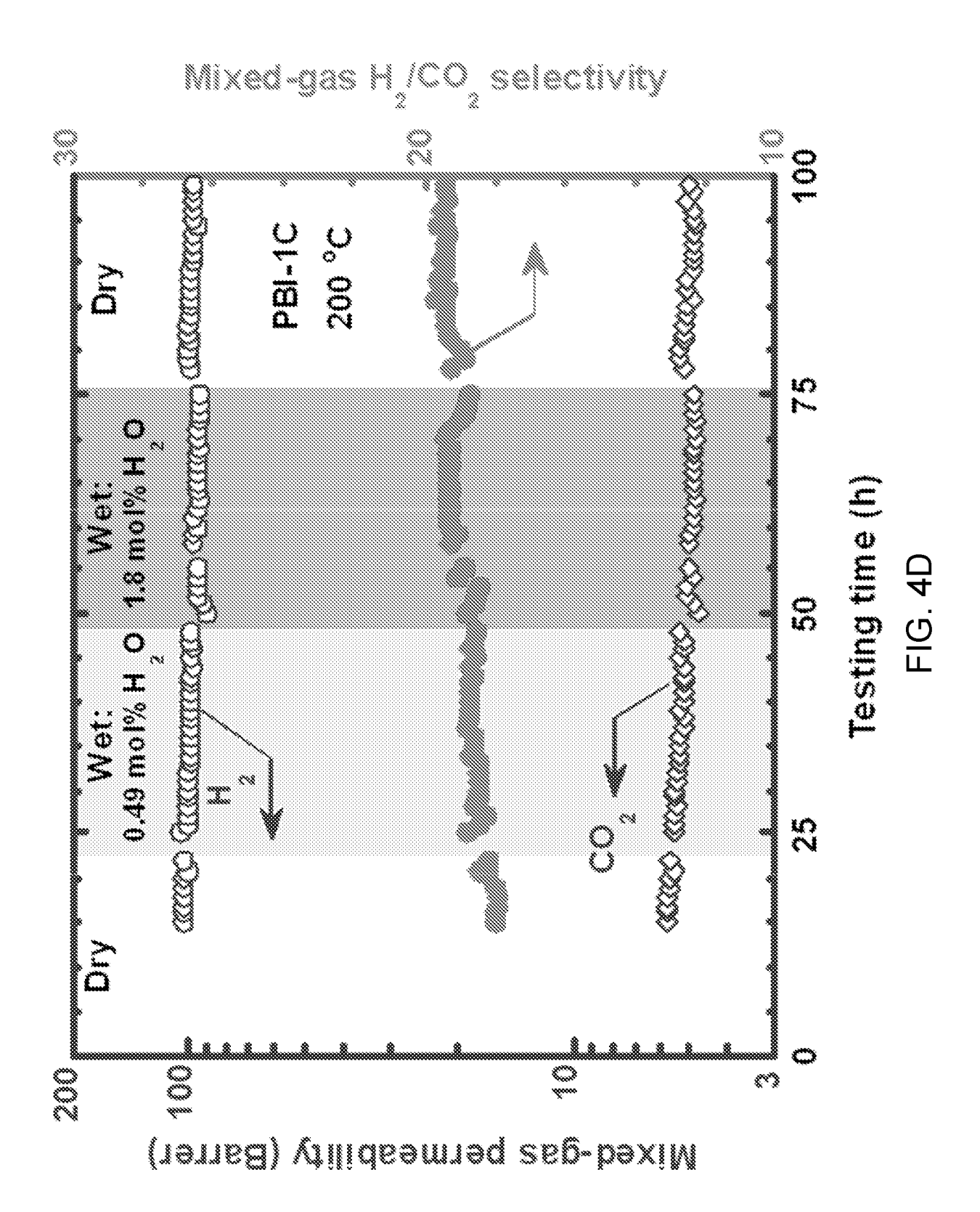
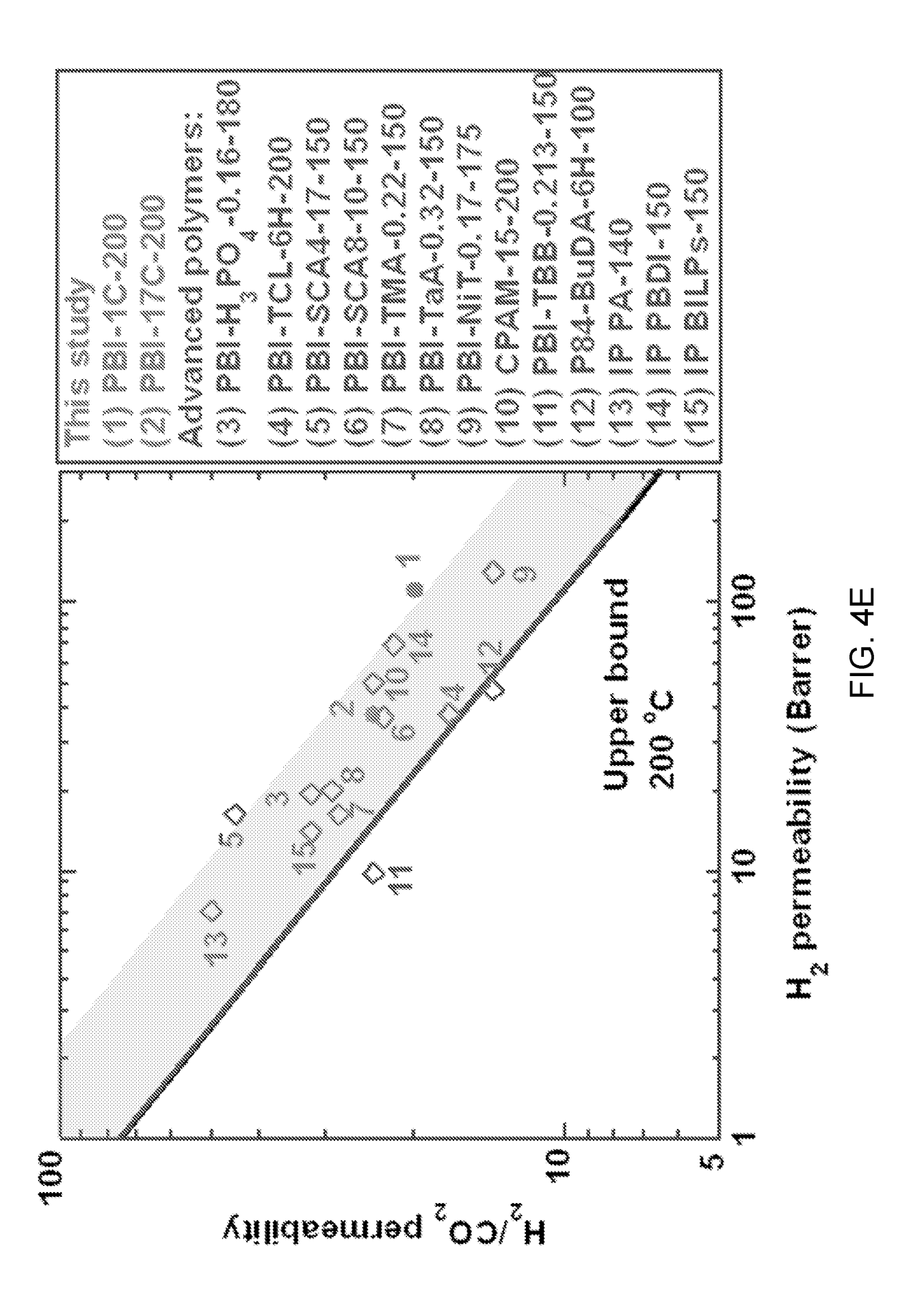


FIG. 4C



12 / 59



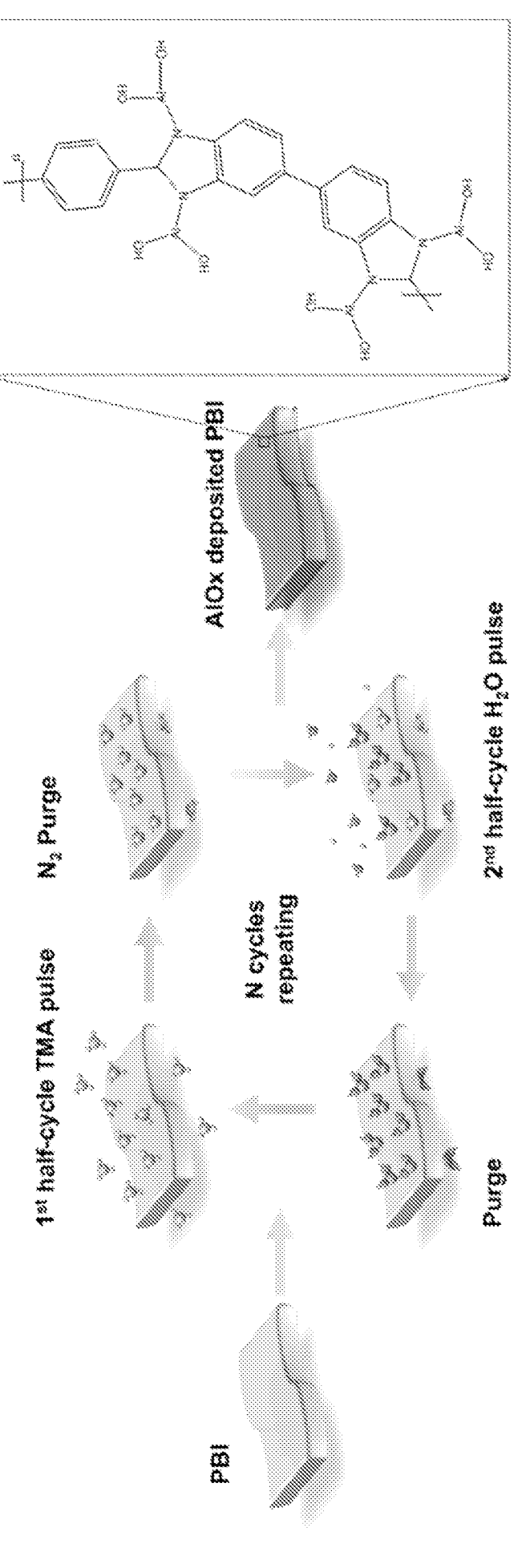


FIG. 5

PBI

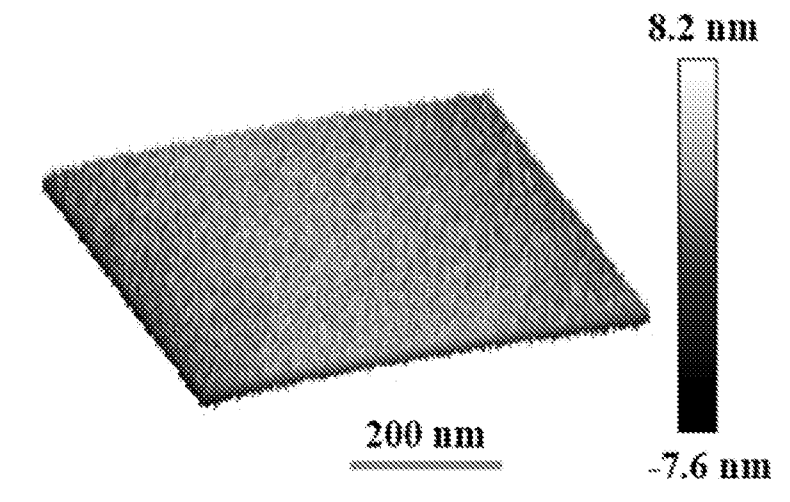


FIG. 6A

PBI-1C

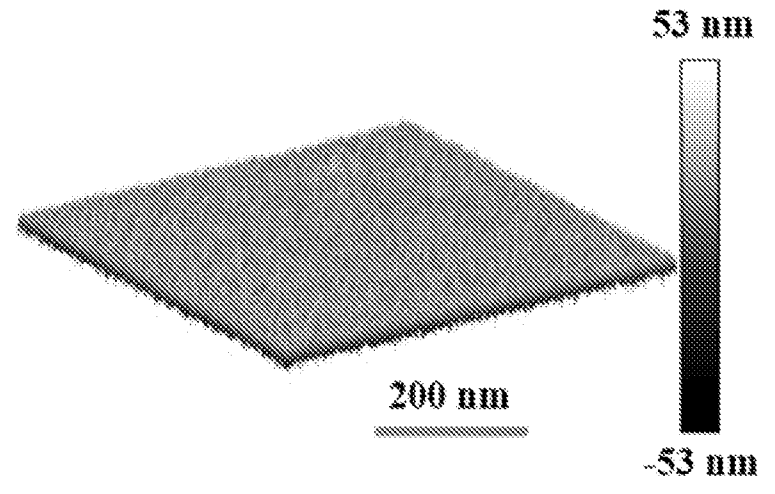


FIG. 6B

PBI-3C

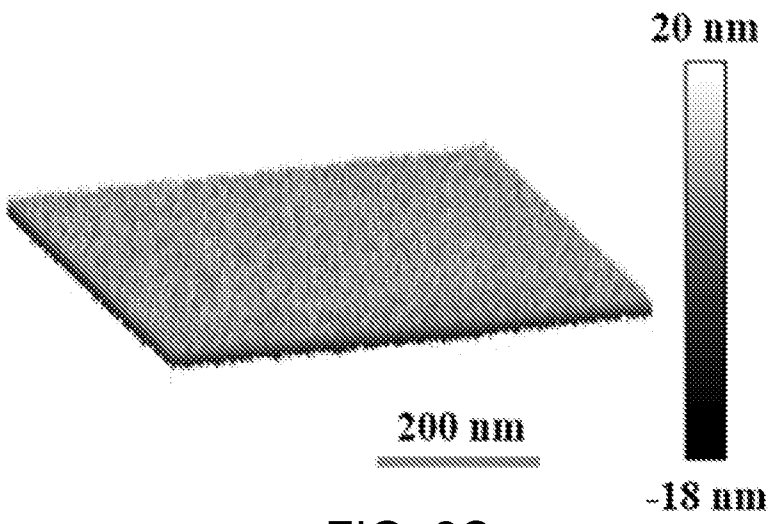


FIG. 6C

15 / 59

PBI-11C

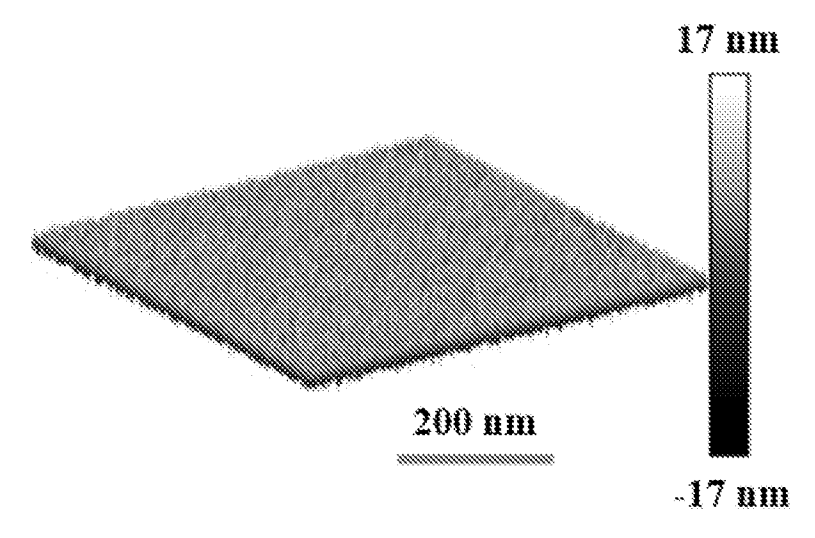


FIG. 6D

PBI-17C

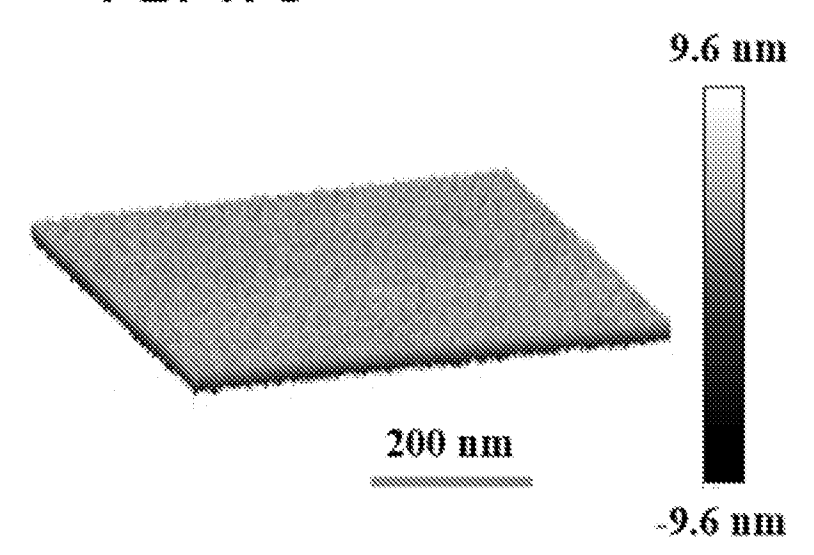
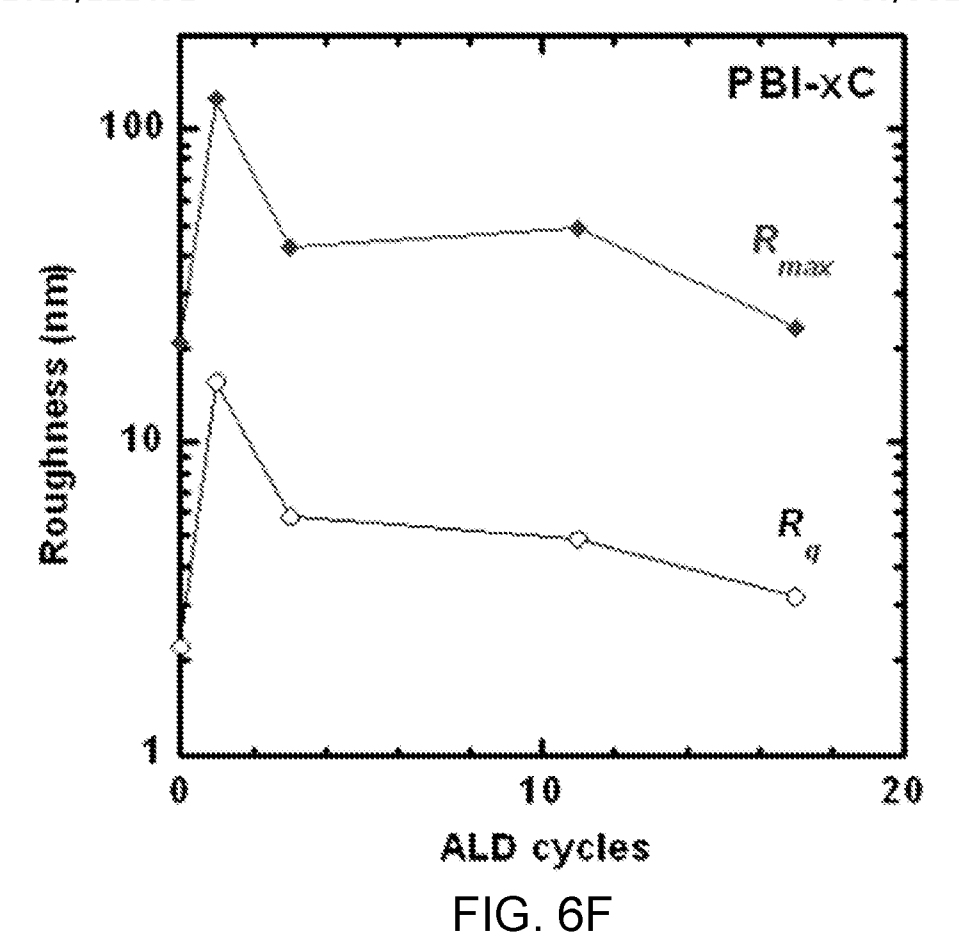


FIG. 6E



O 1s

PBI-17C

PBI-11C

PBI-11C

PBI-10

PBI-1

17 / 59

FIG. 7

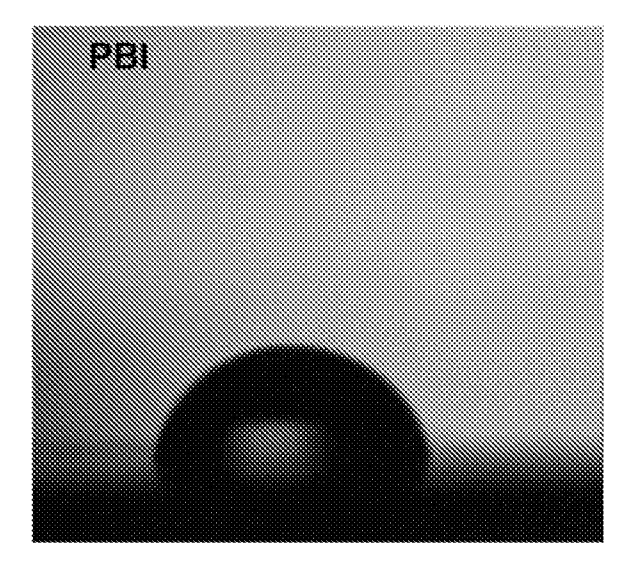


FIG. 8A

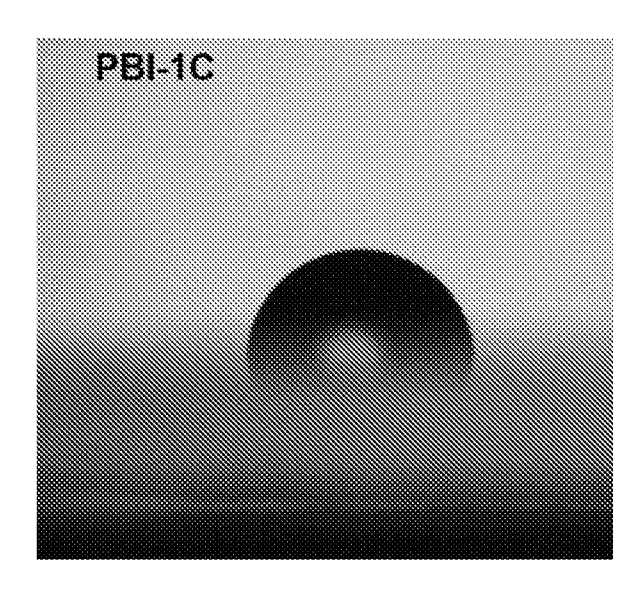


FIG. 8B

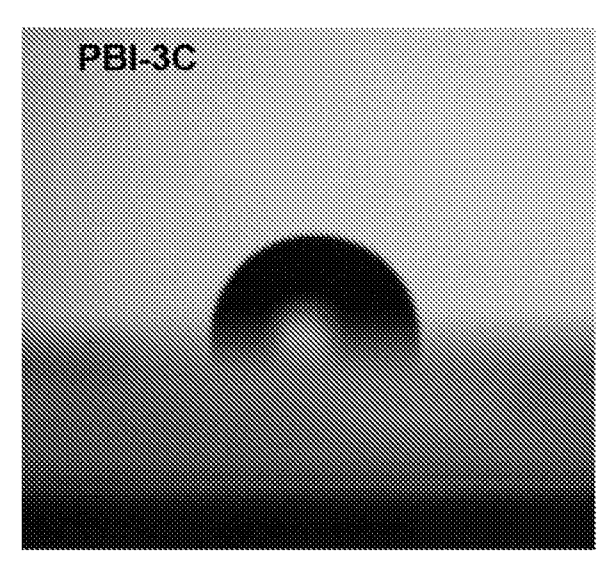


FIG. 8C

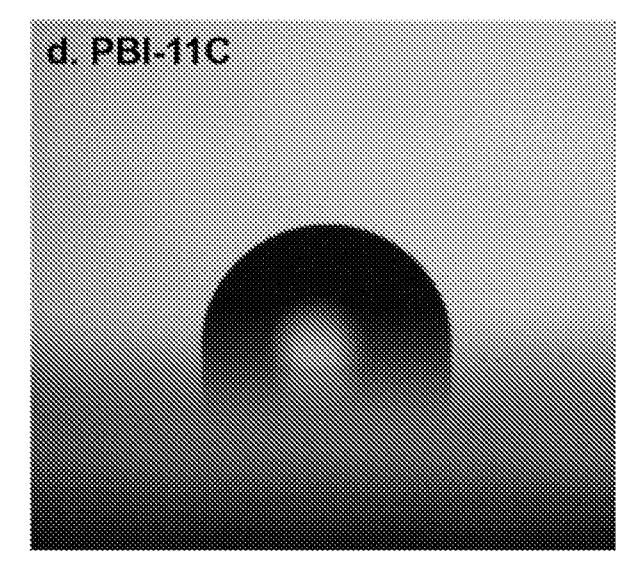
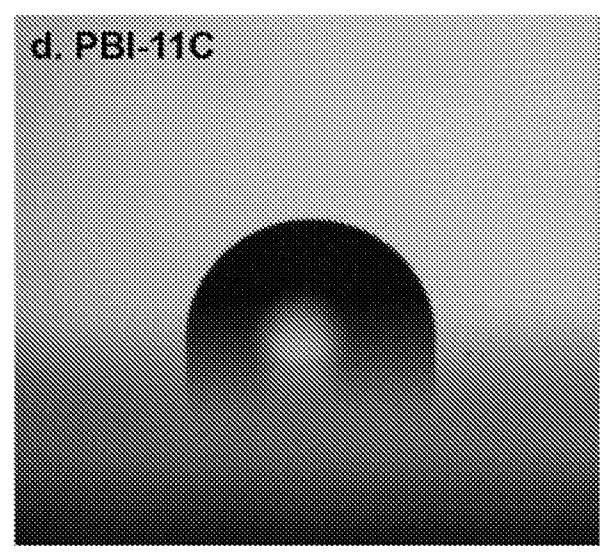
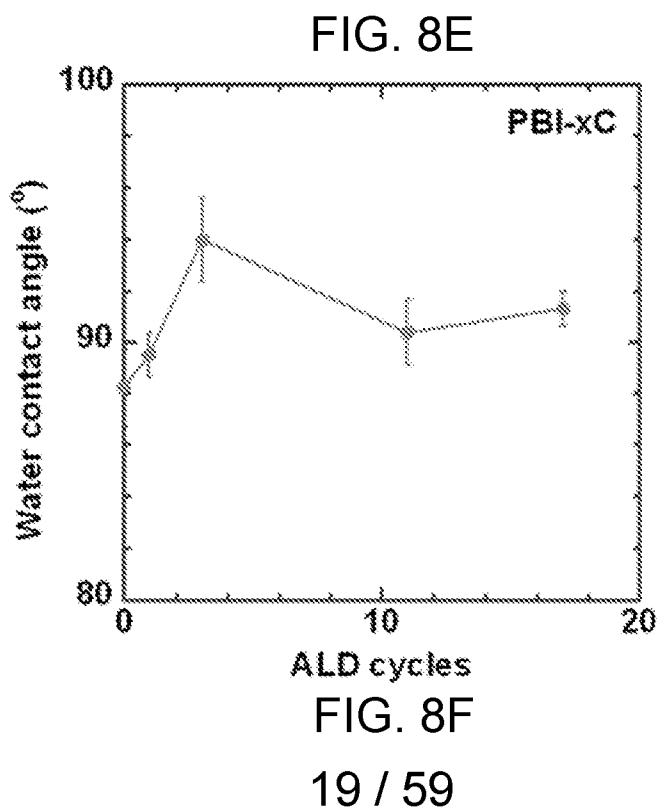


FIG. 8D





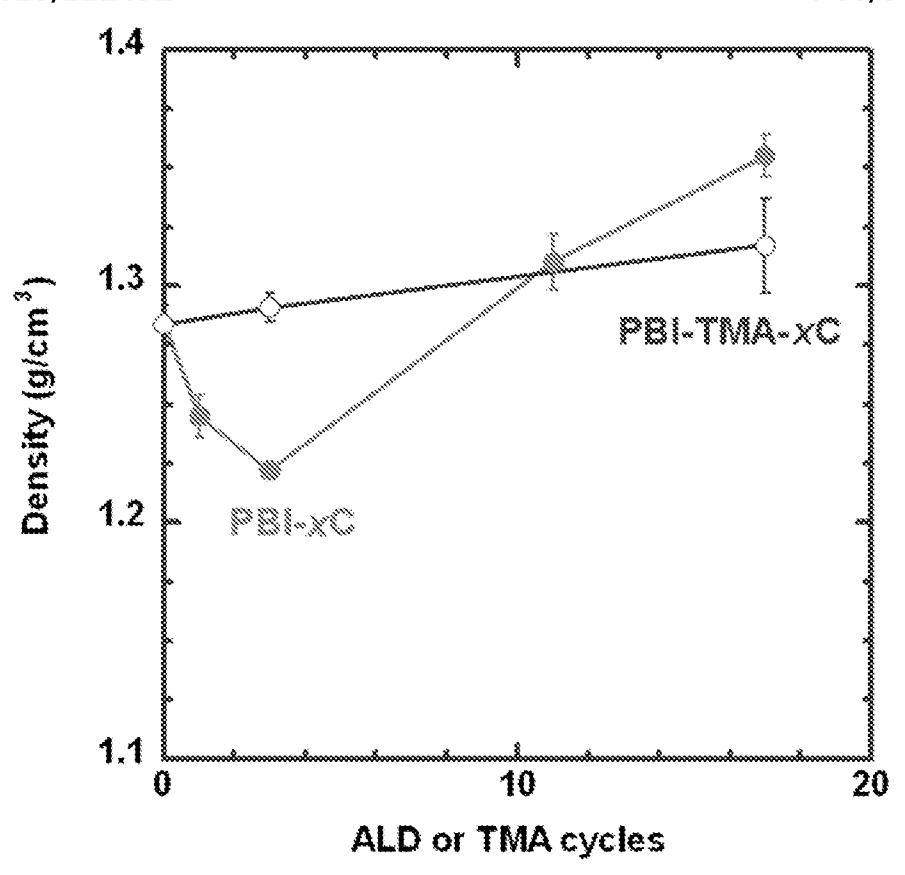


FIG. 9A

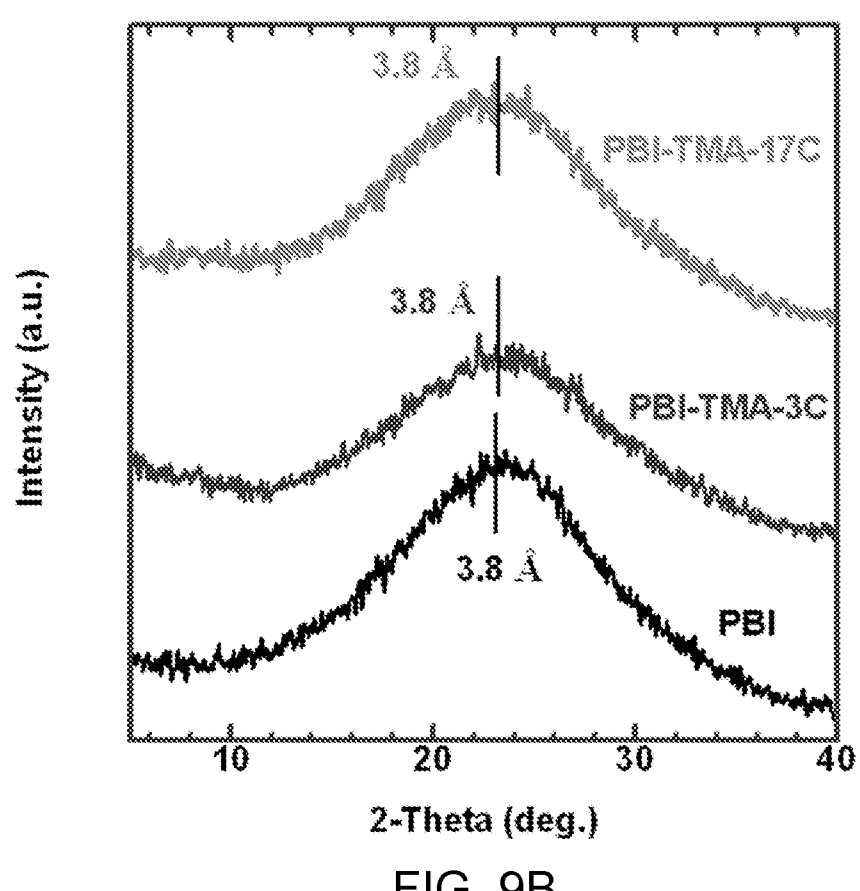
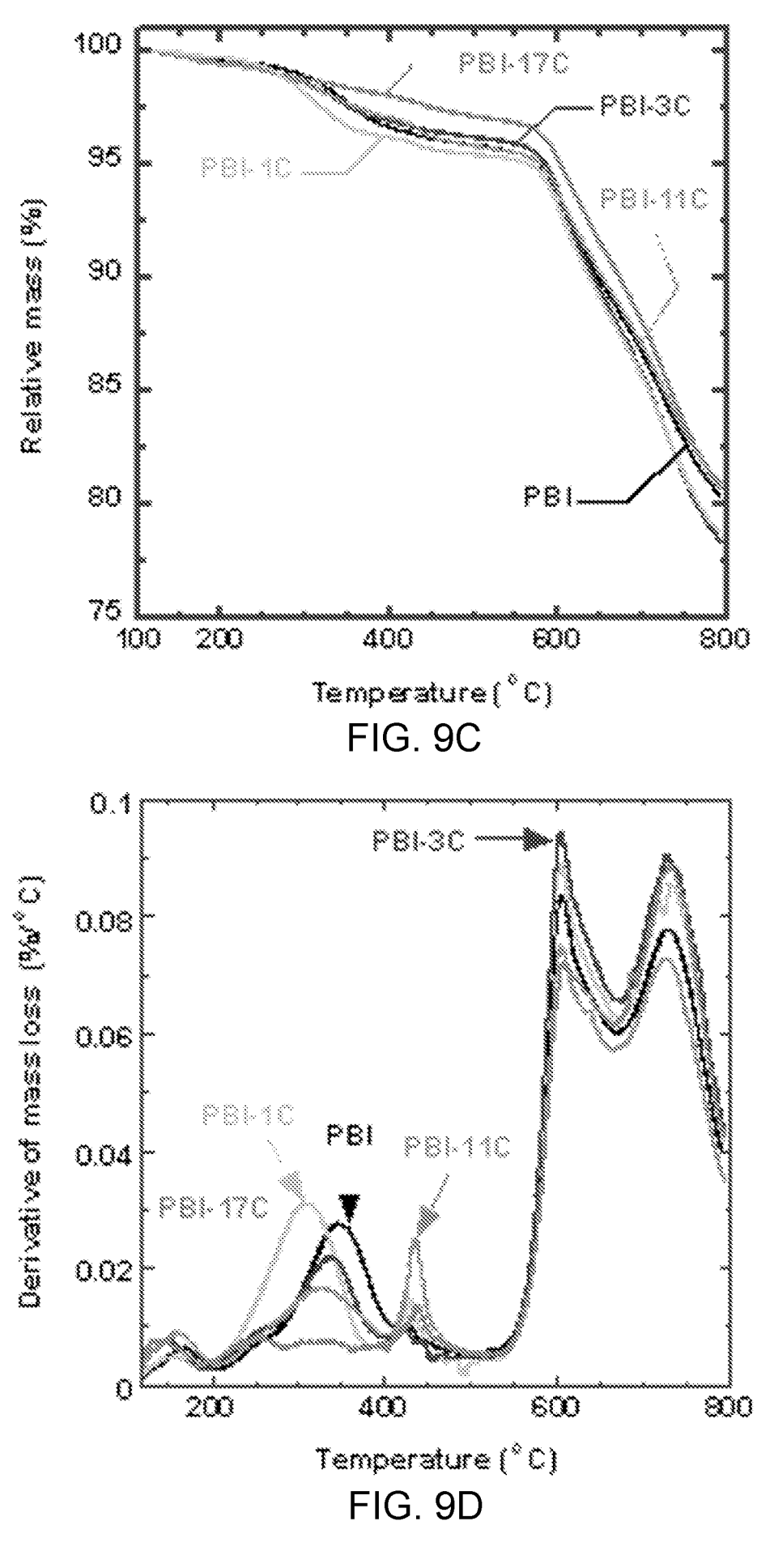
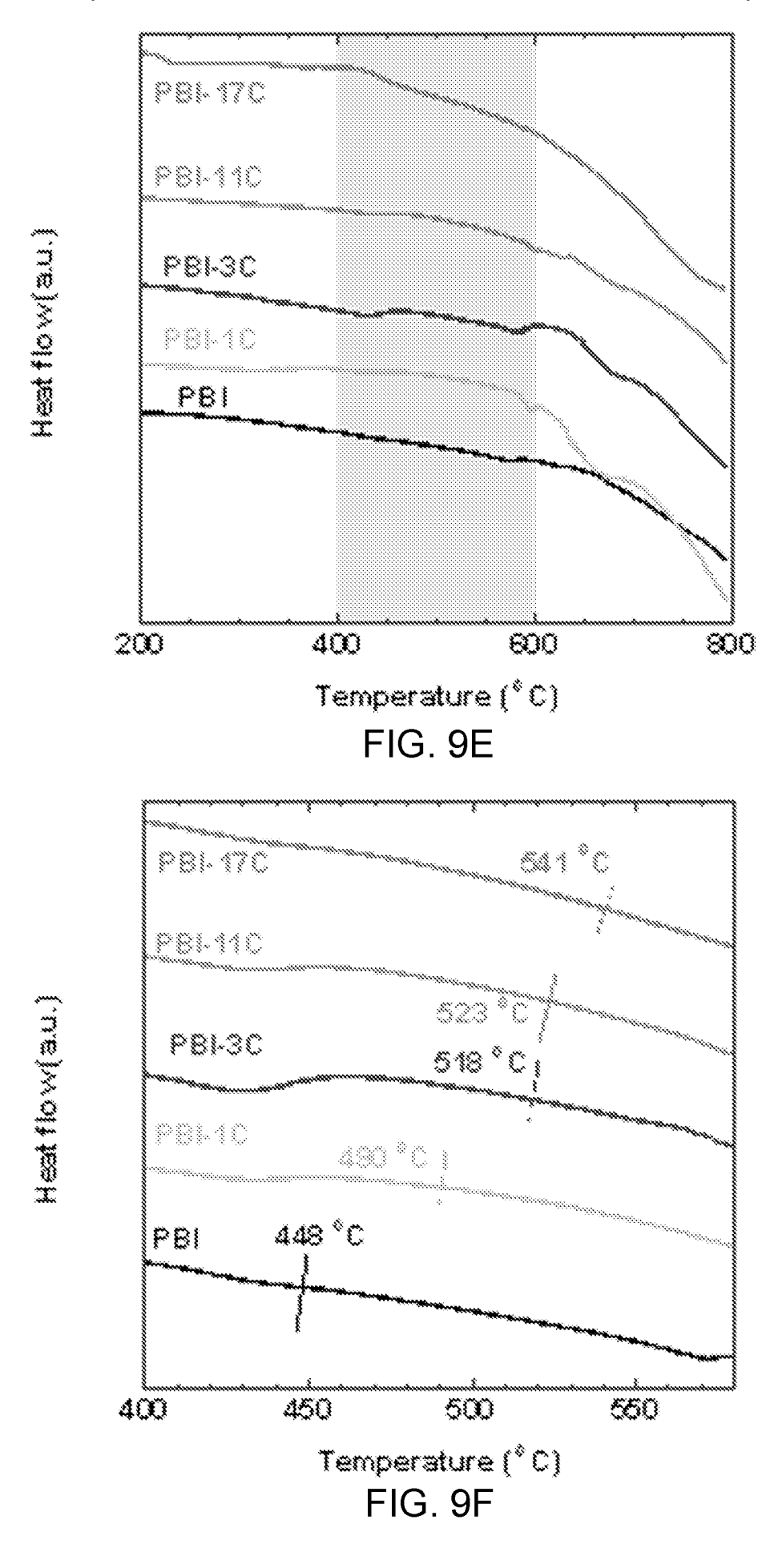


FIG. 9B

20 / 59



21 / 59



22 / 59

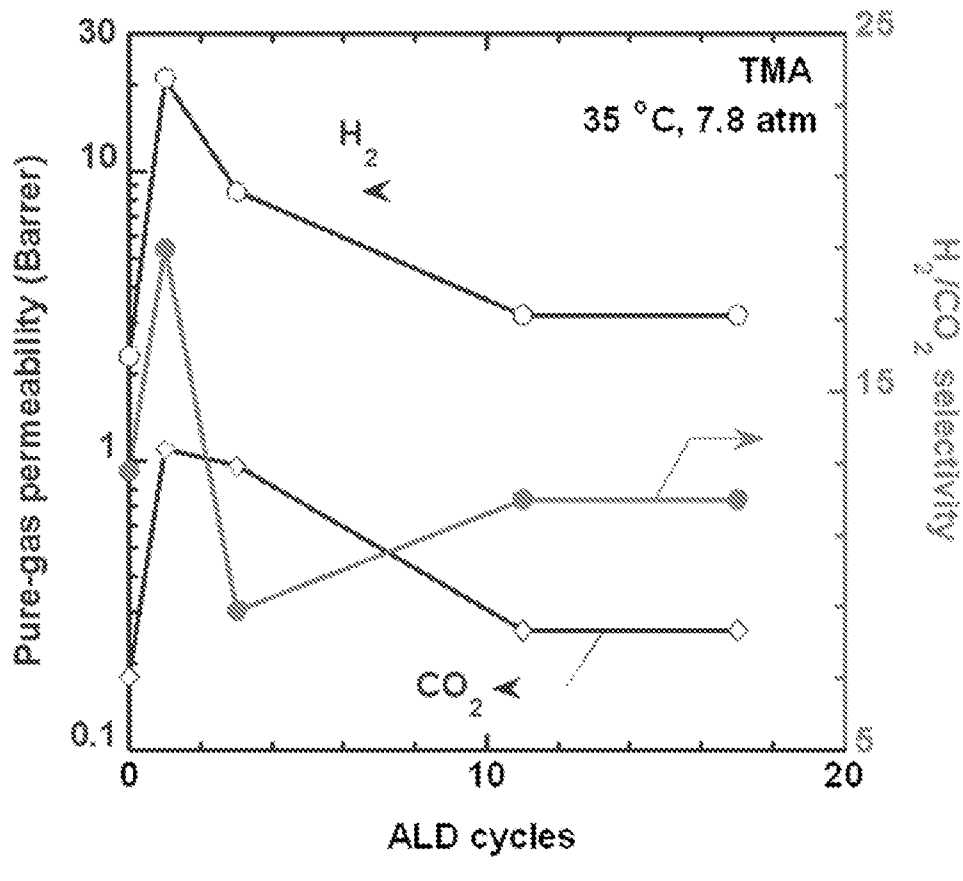
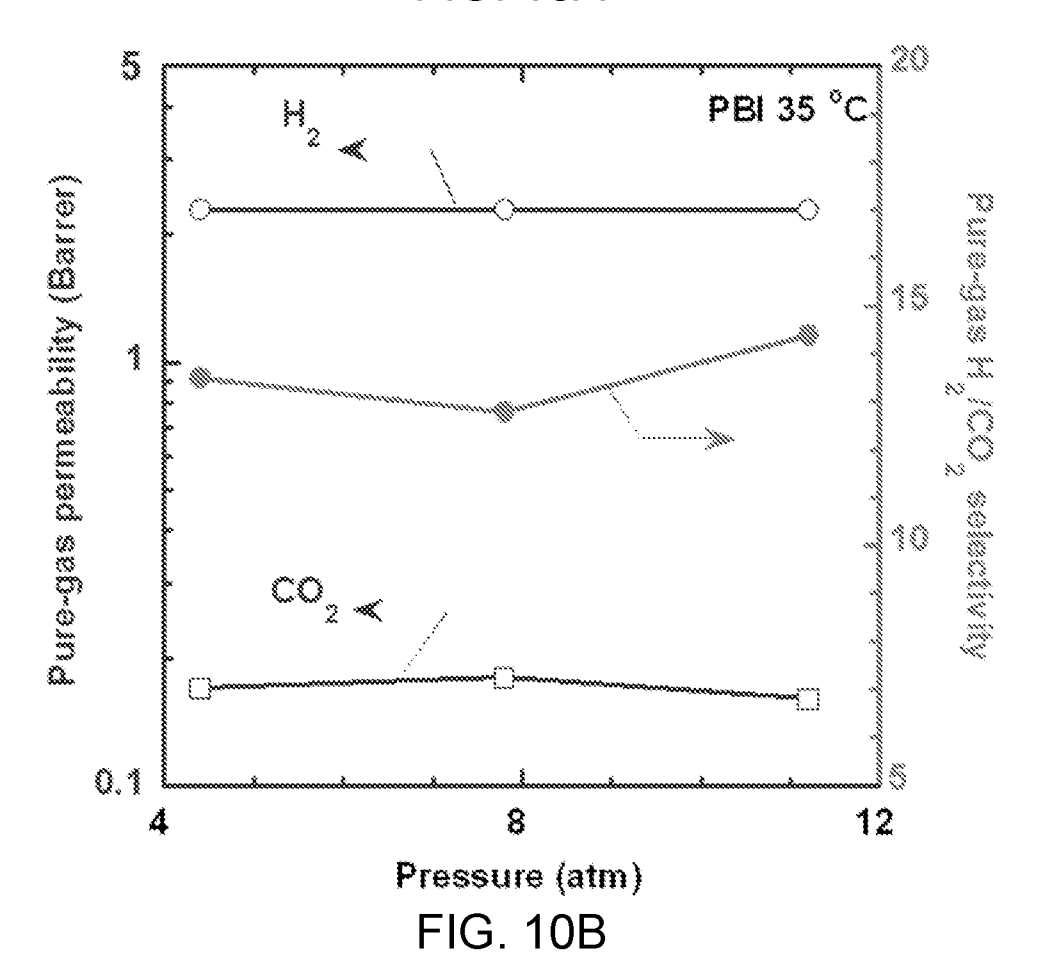
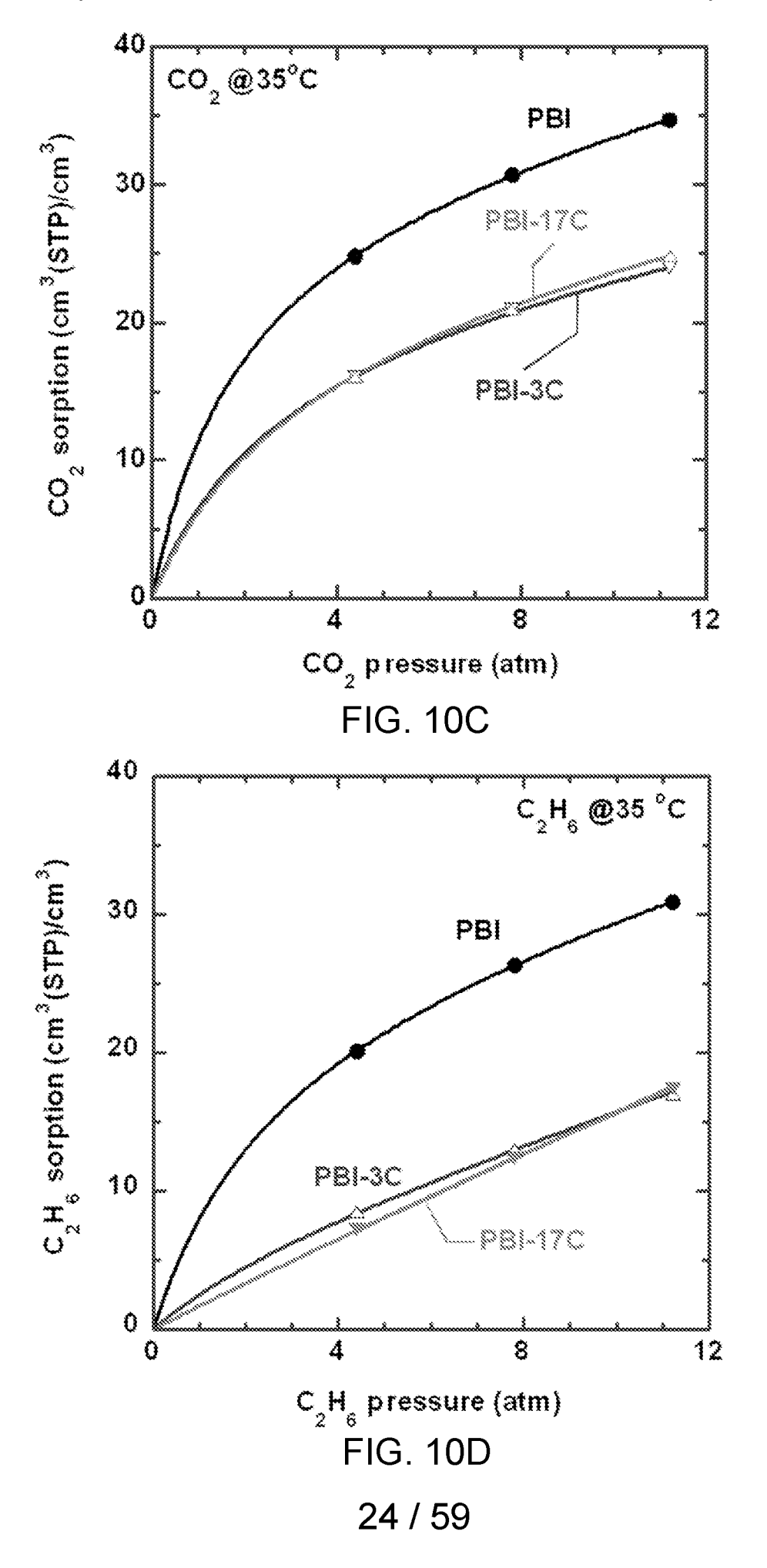


FIG. 10A



23 / 59



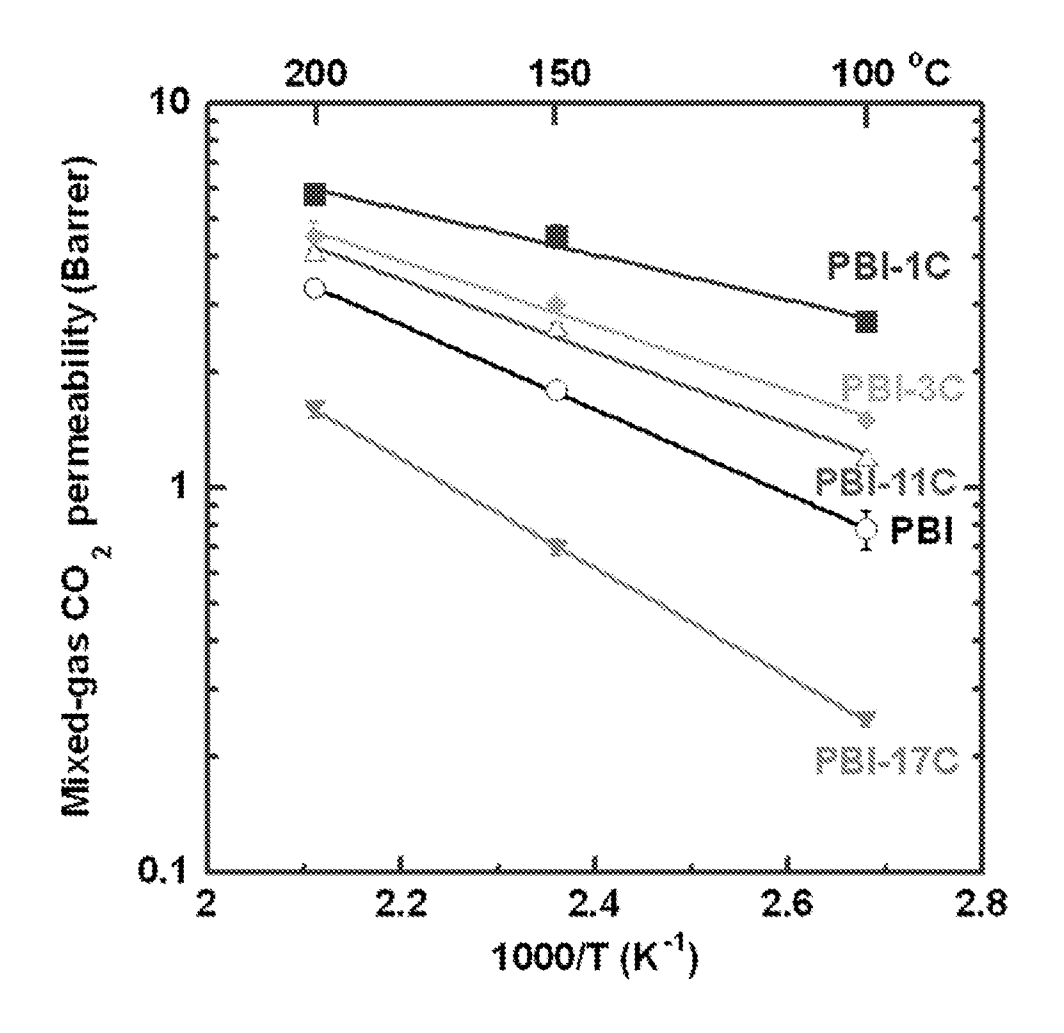


FIG. 10E

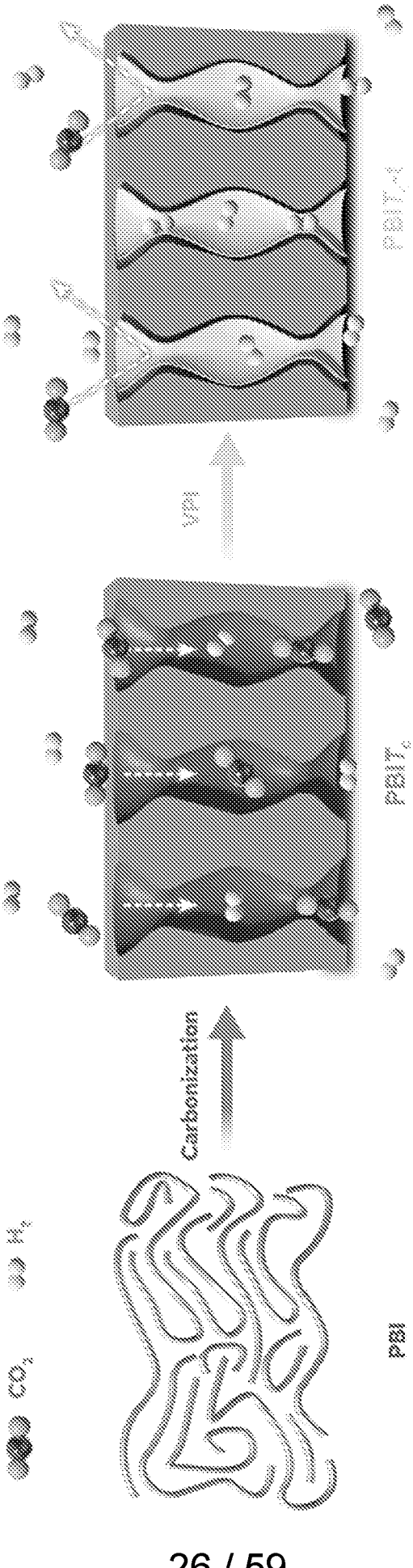


FIG. 11A

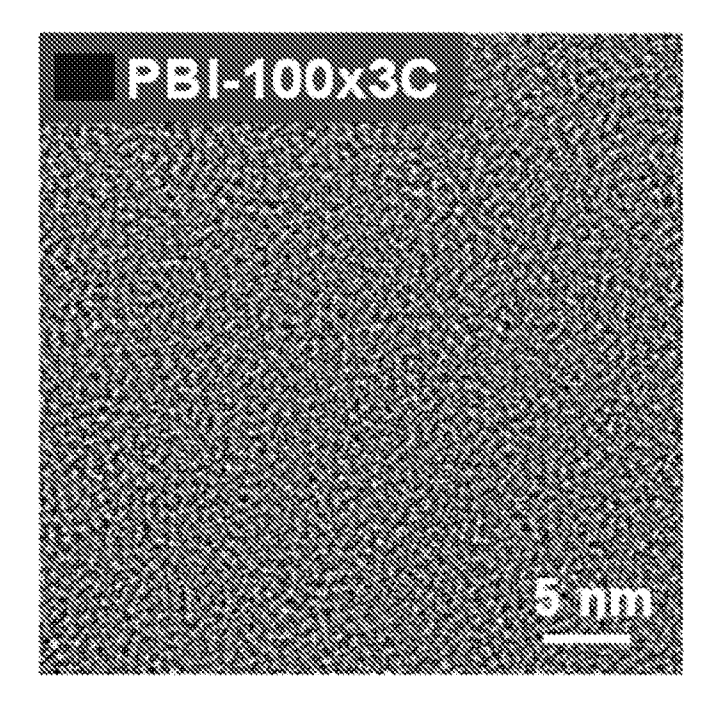


FIG. 11B

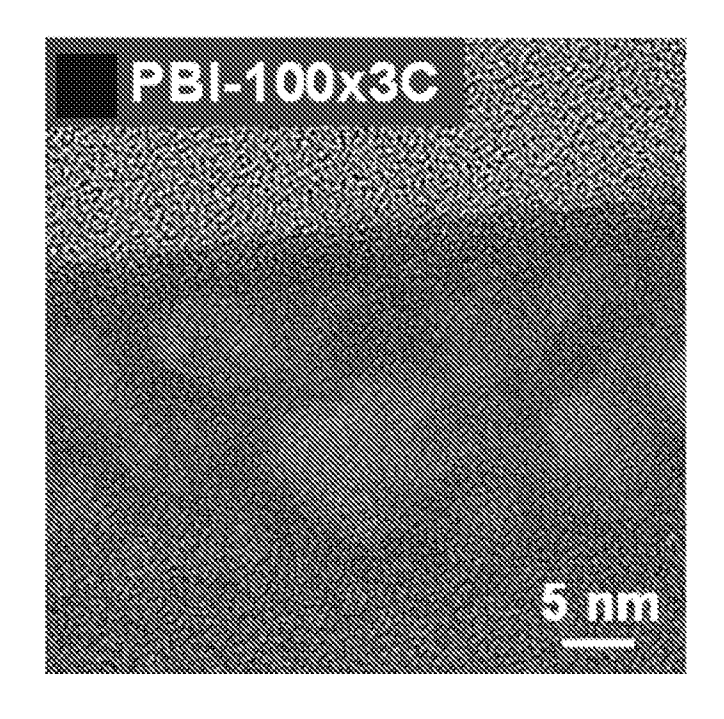


FIG. 11C

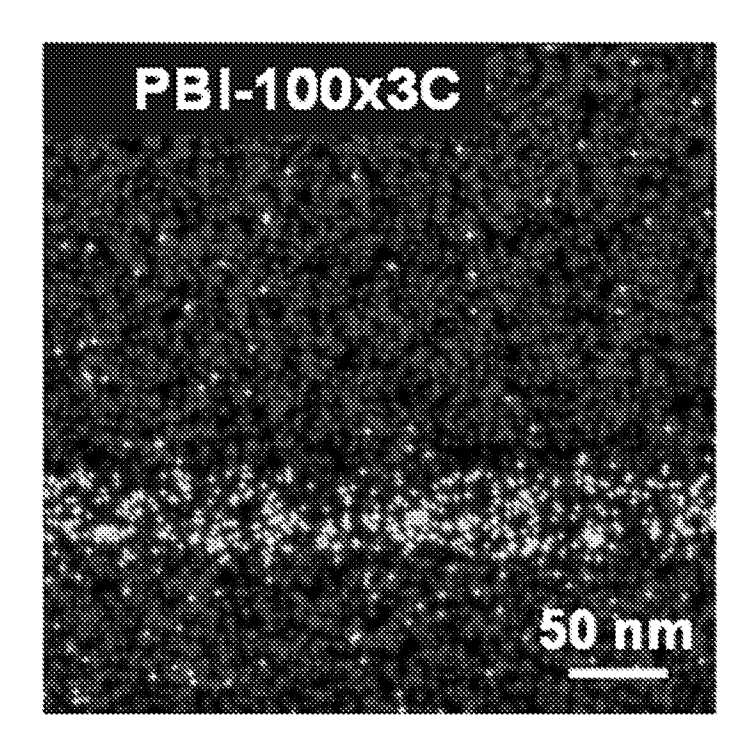


FIG. 11D

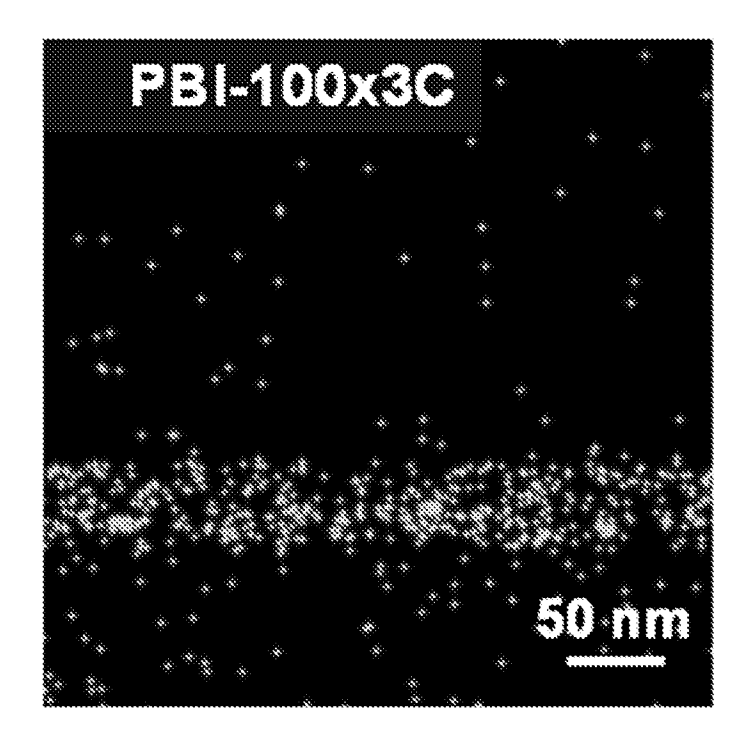
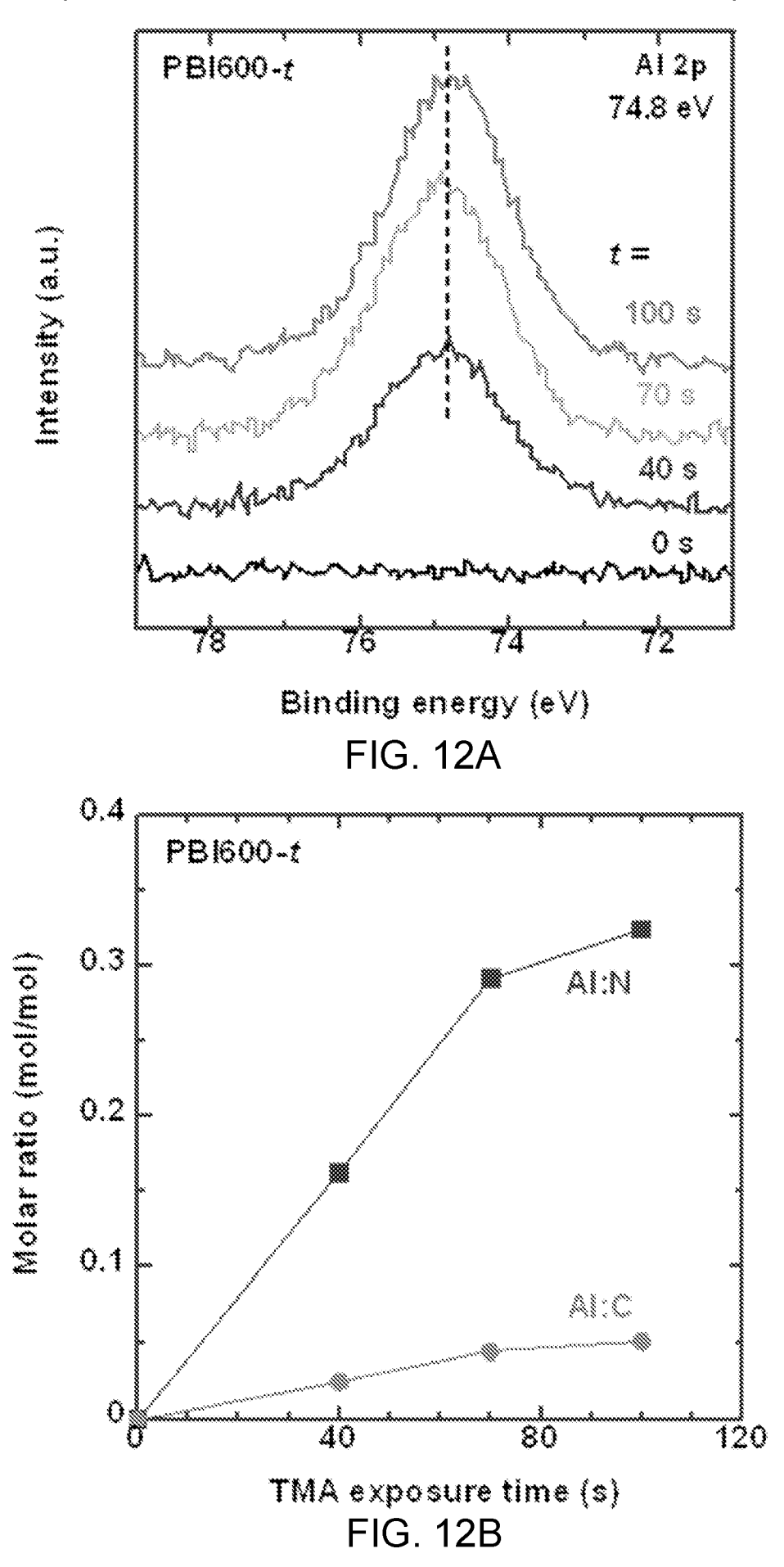
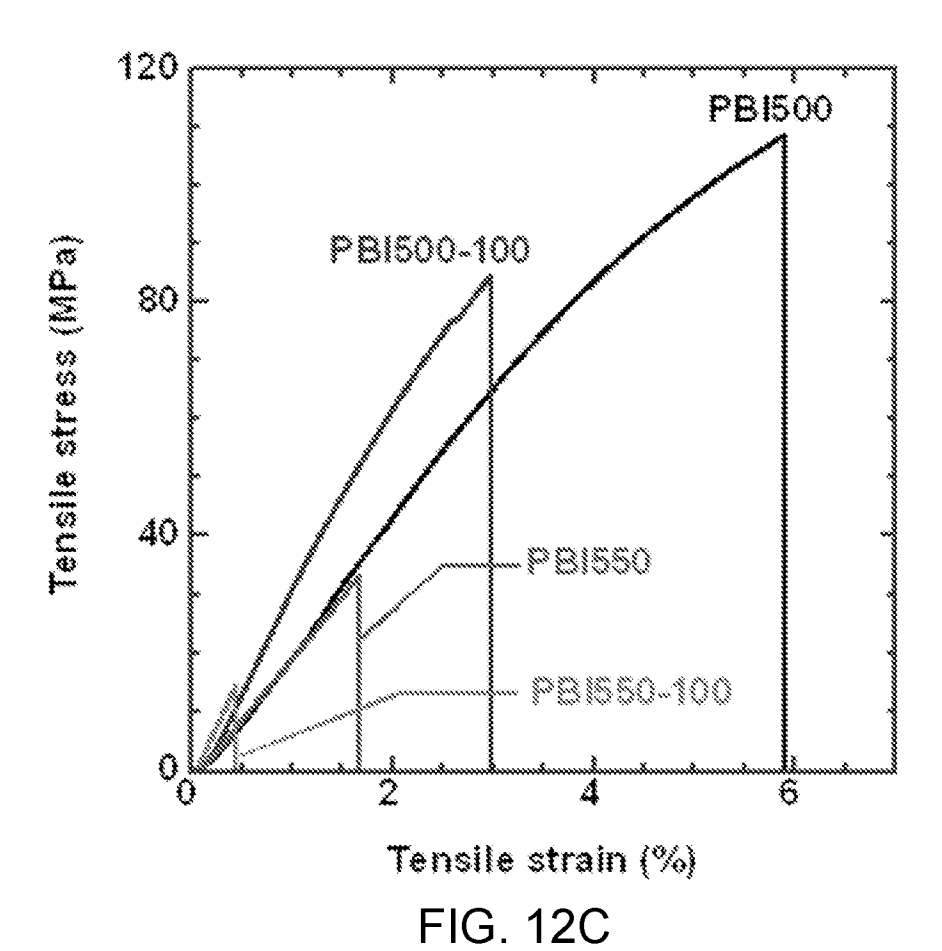
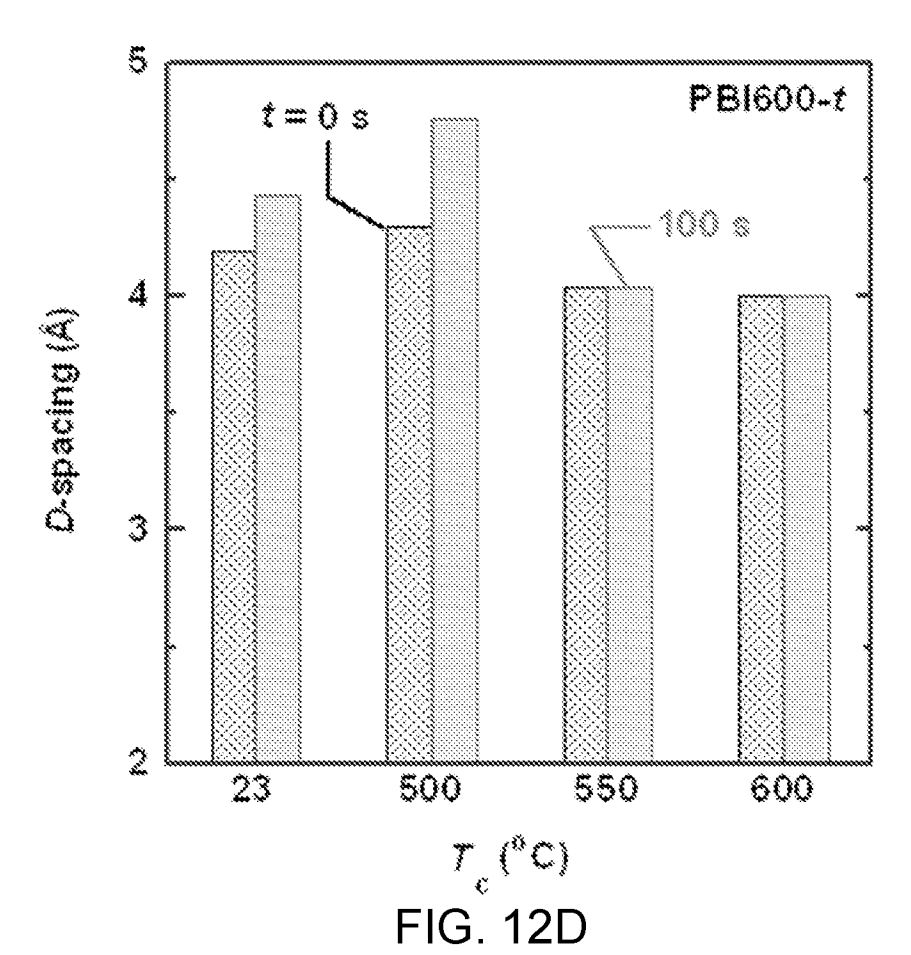
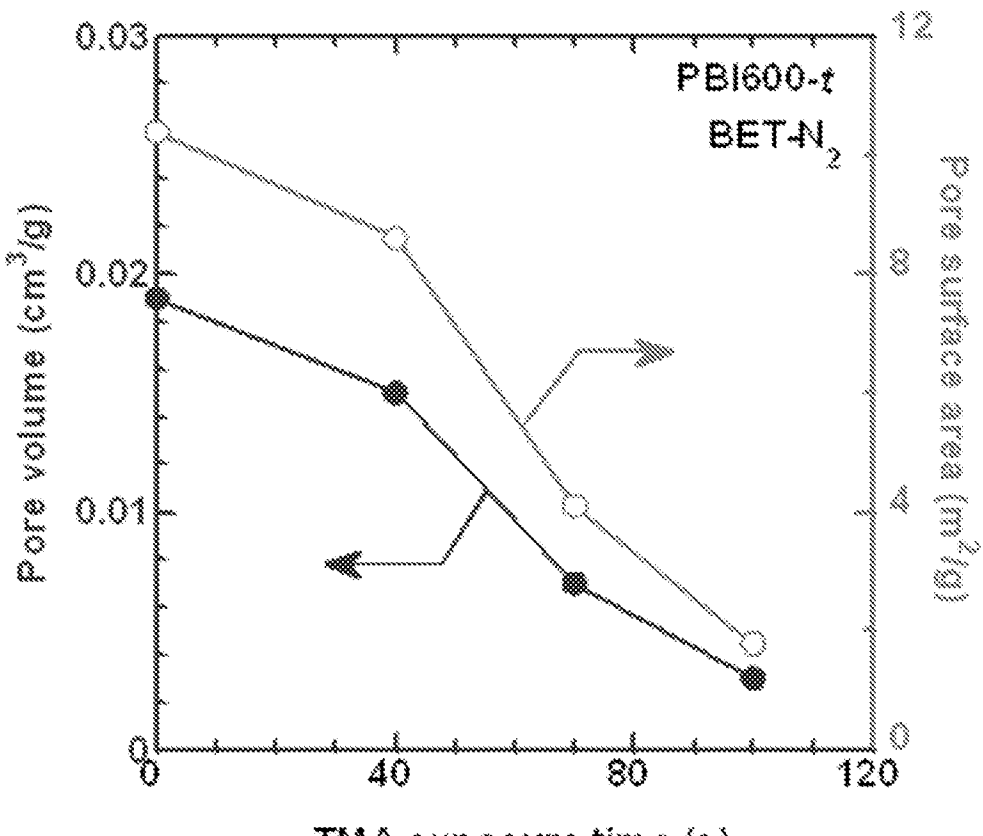


FIG. 11E



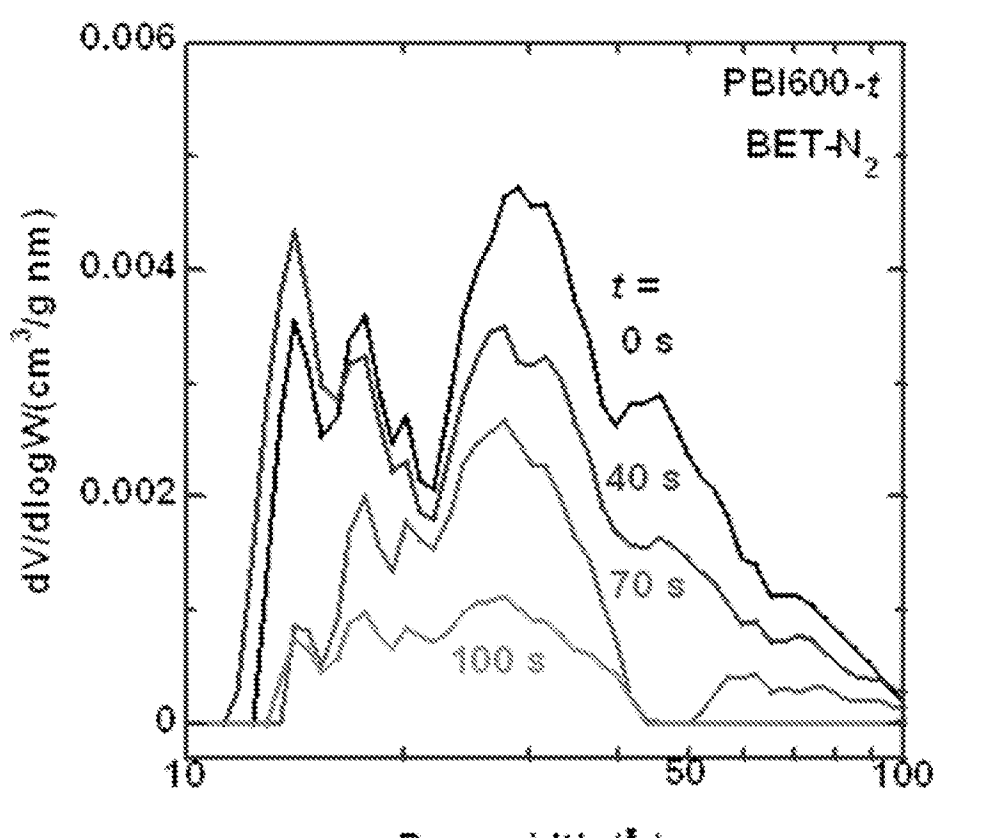




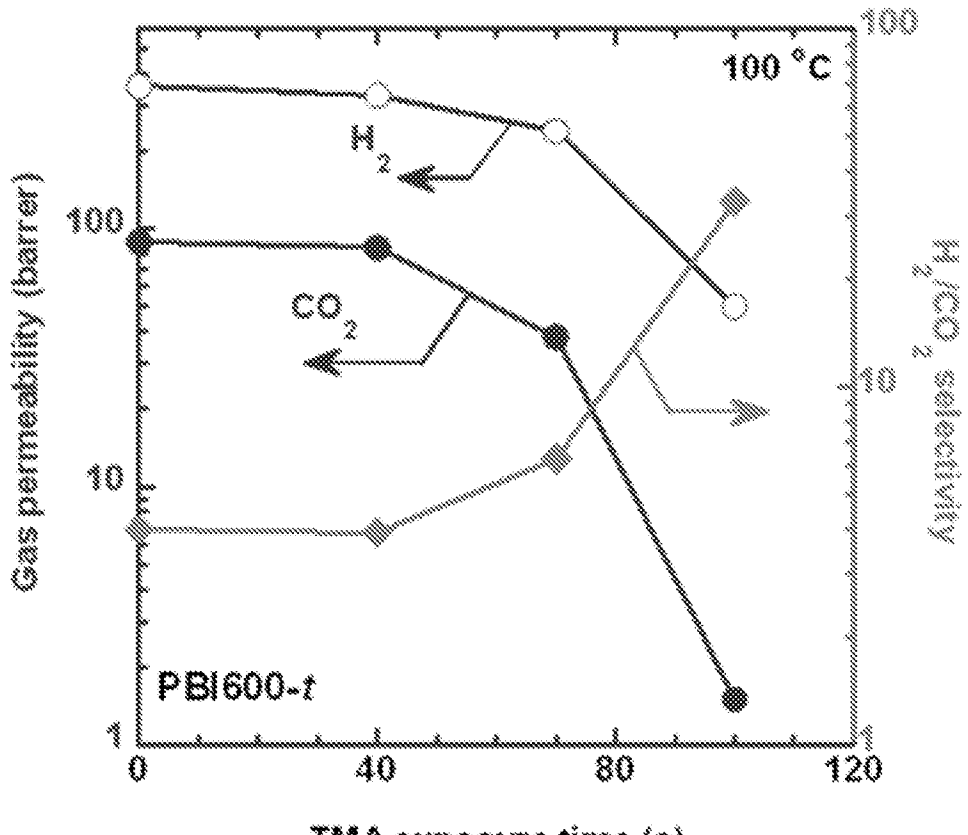


TMA exposure time (s)

FIG. 12E

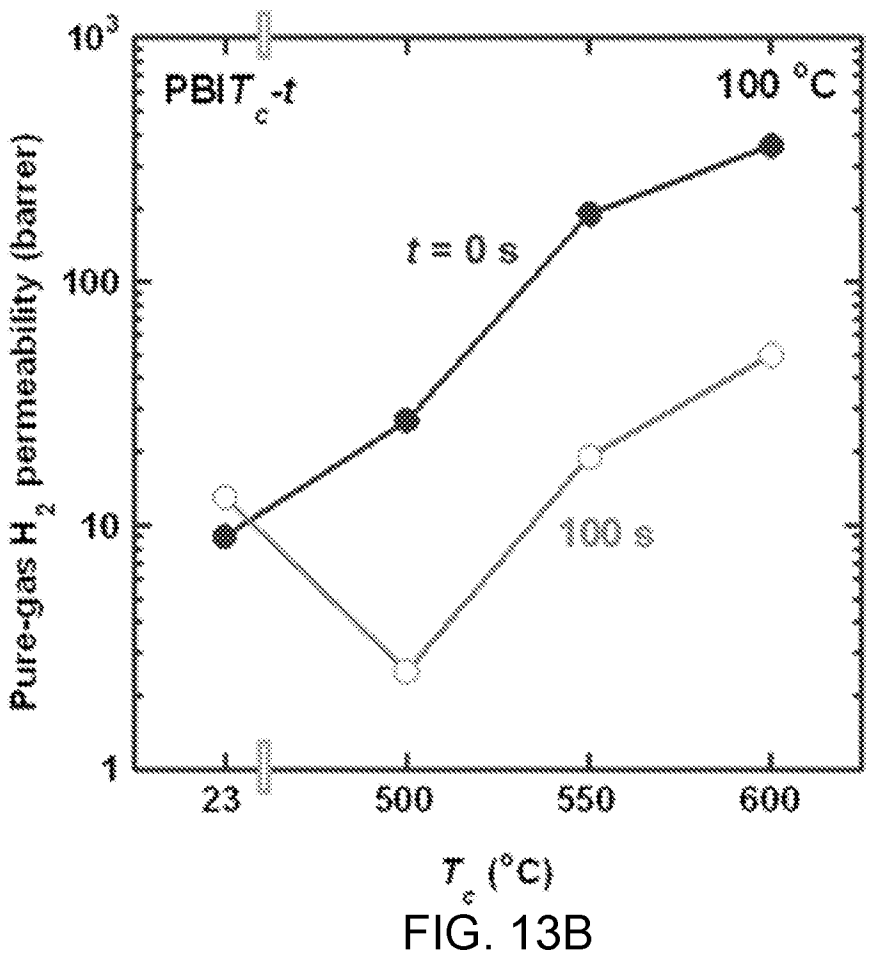


Pore width (*) FIG. 12F

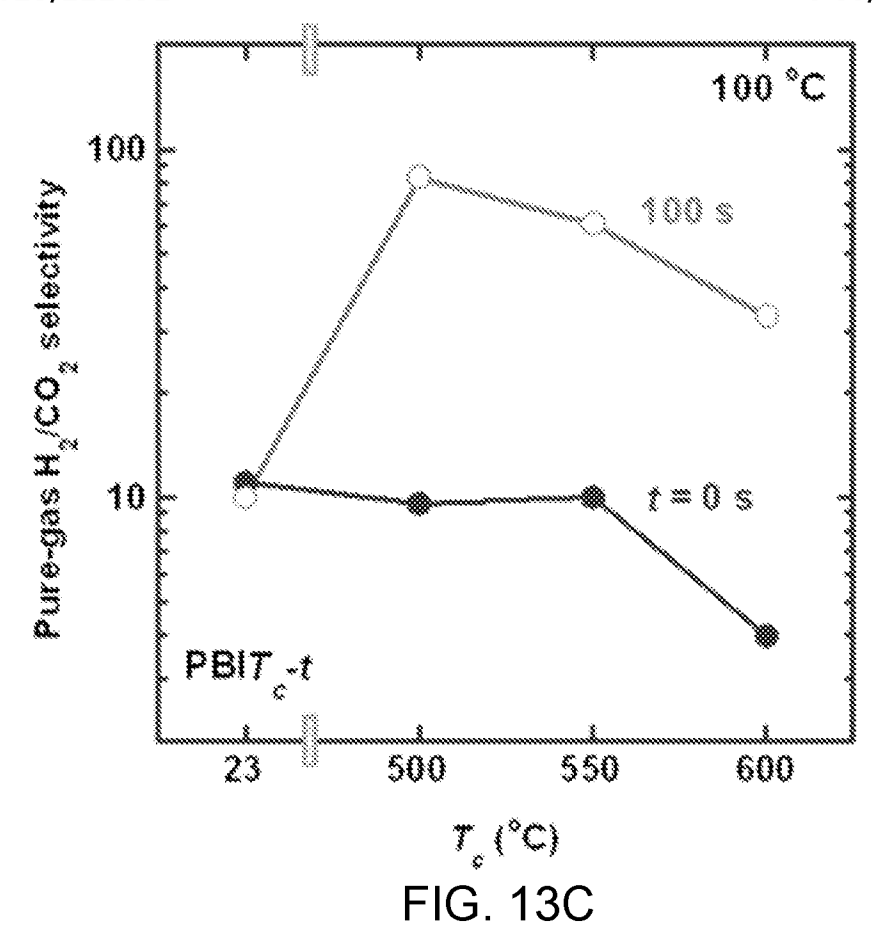


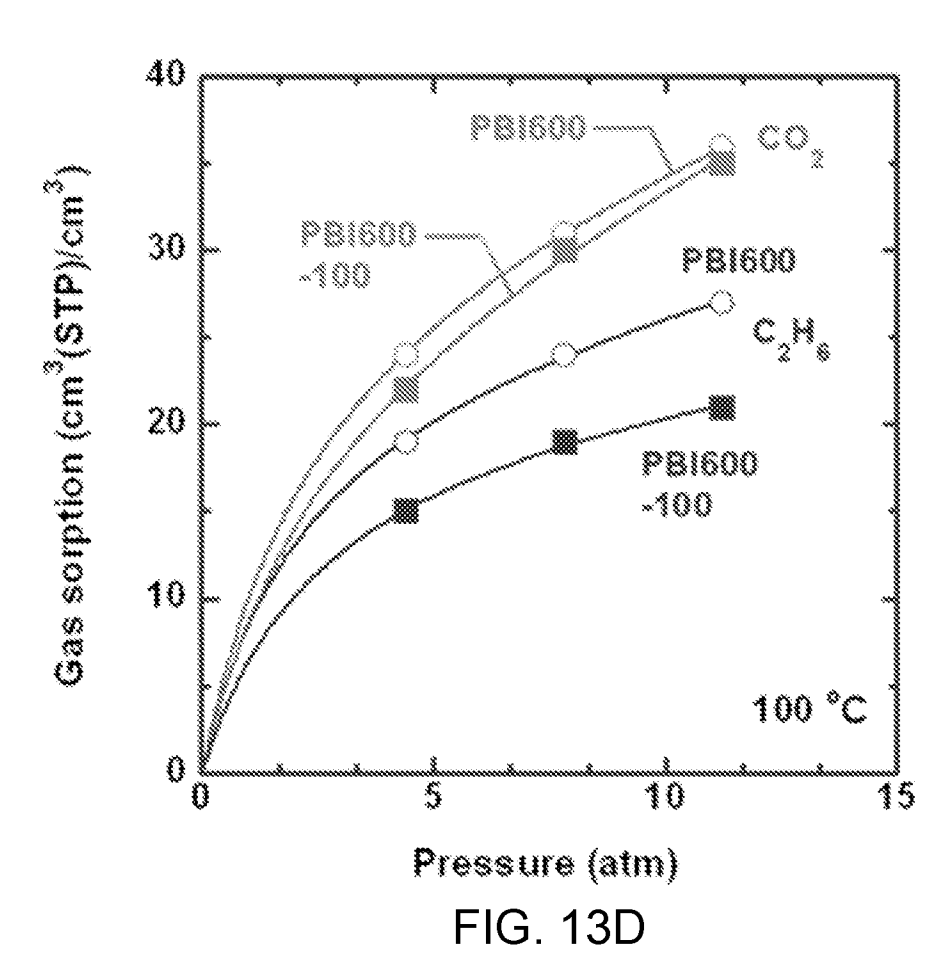
TMA exposure time (s)





32 / 59





33 / 59

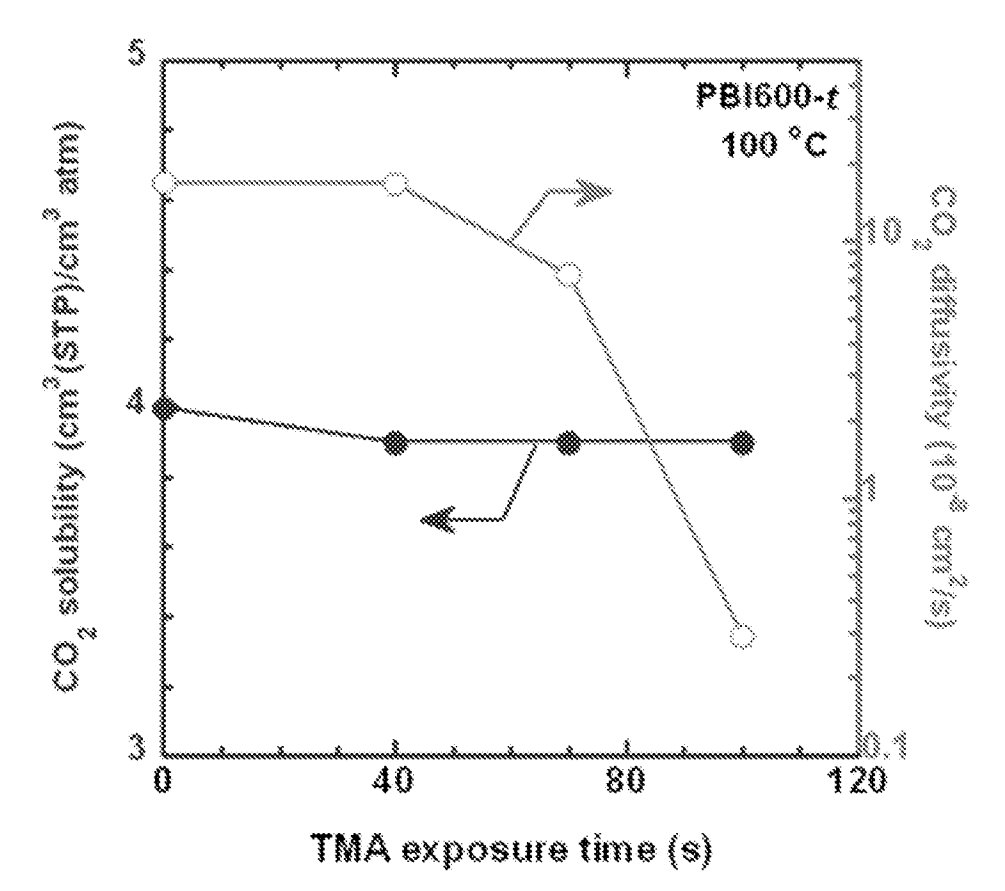
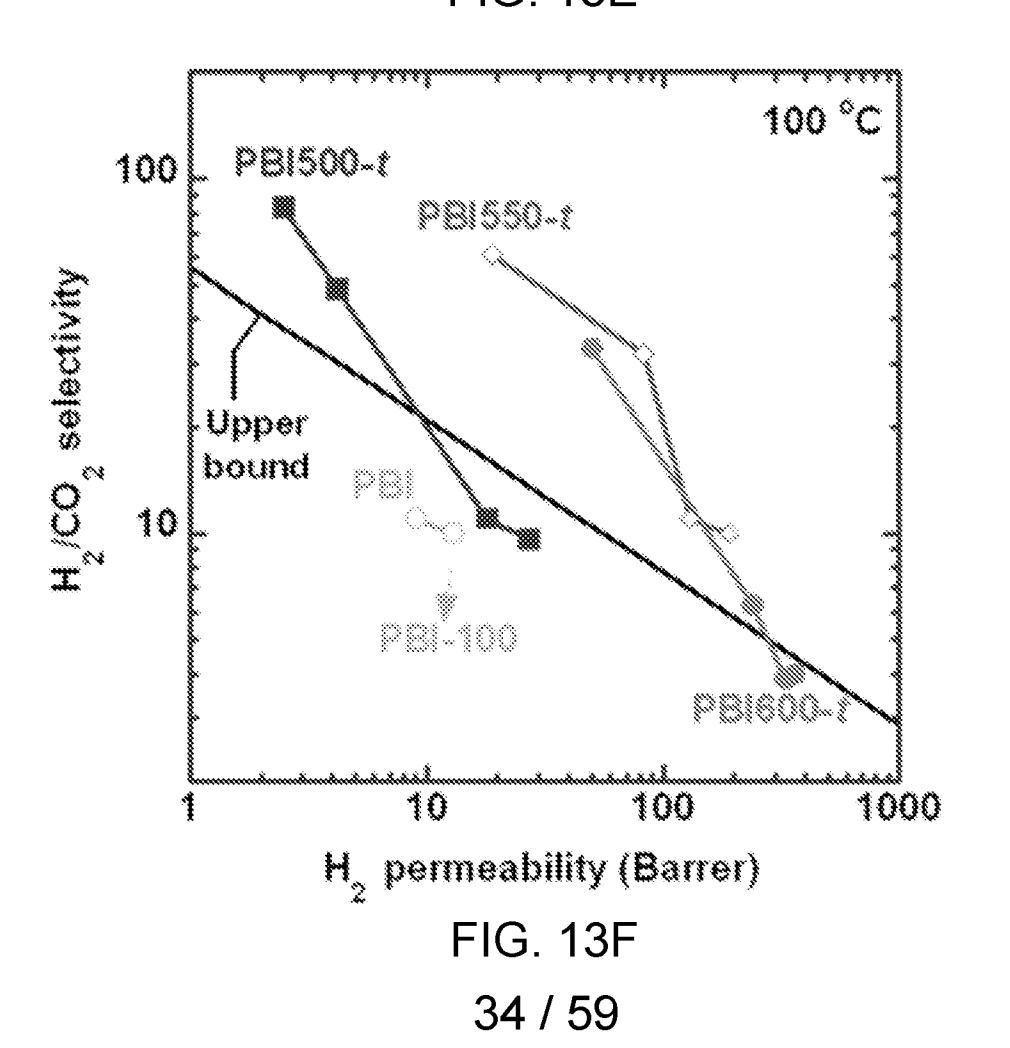


FIG. 13E



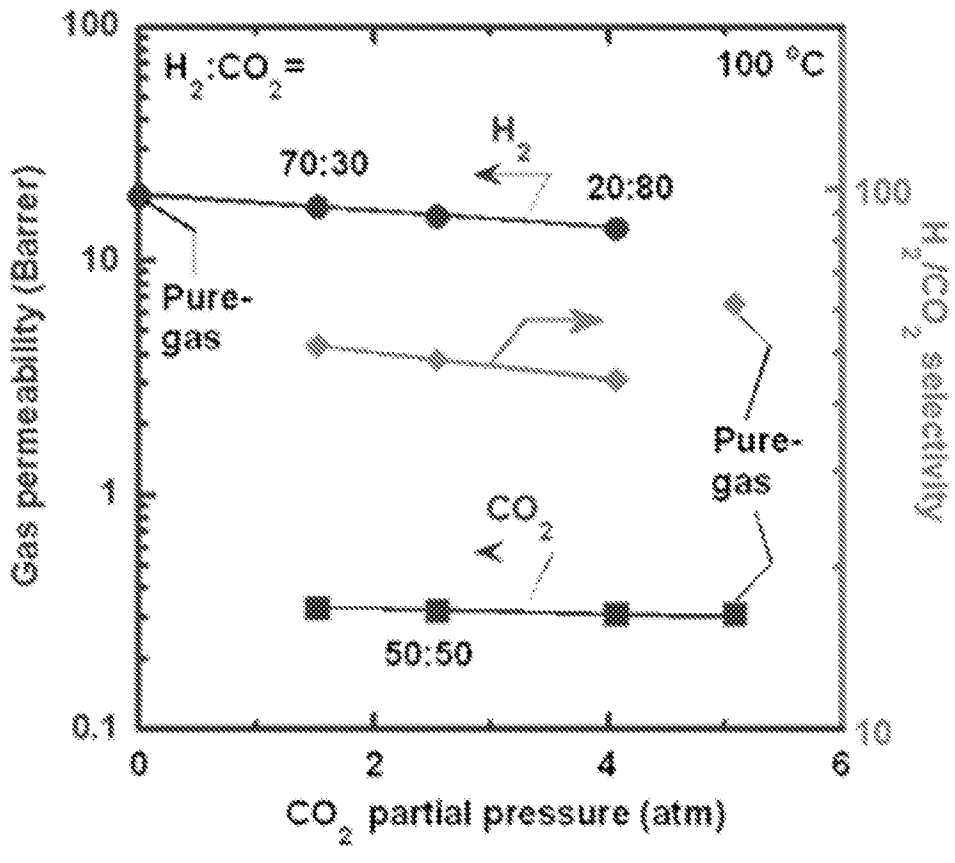
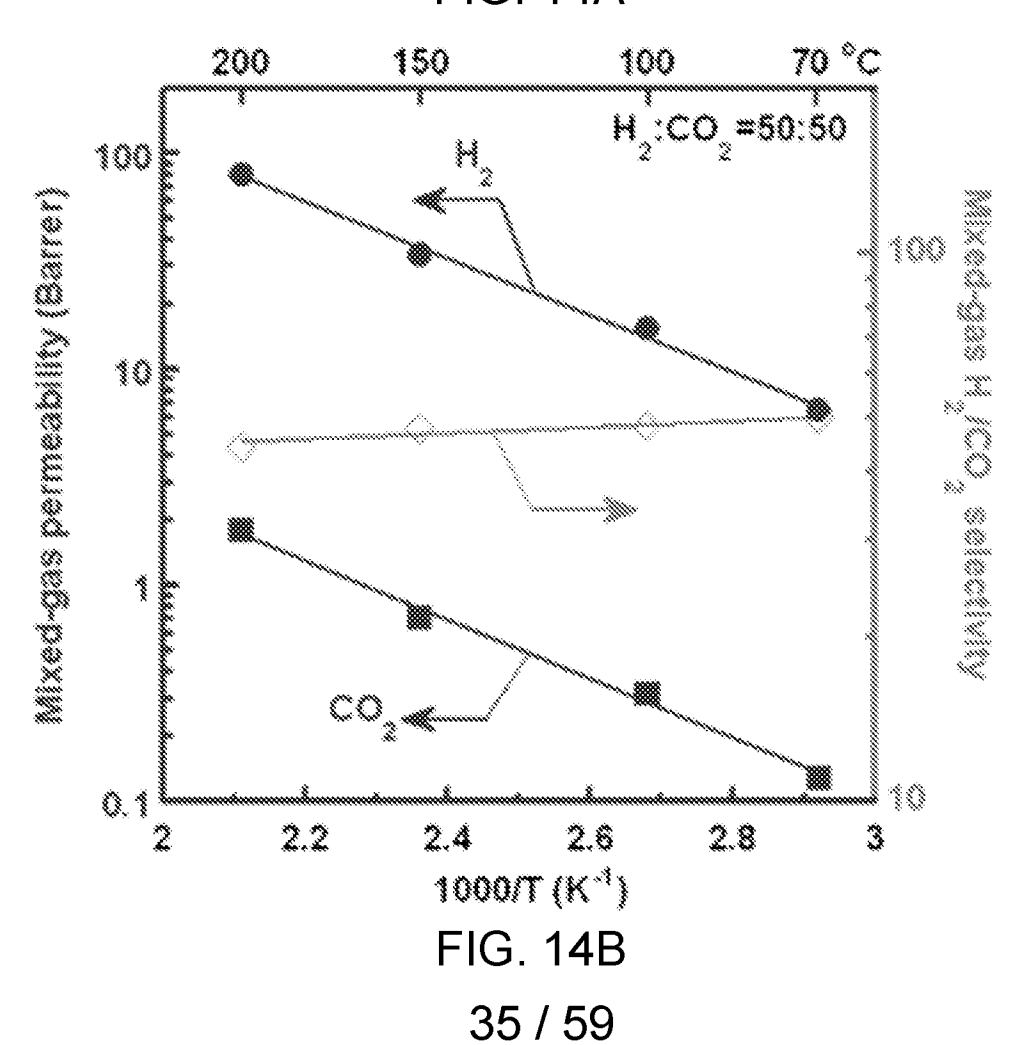


FIG. 14A



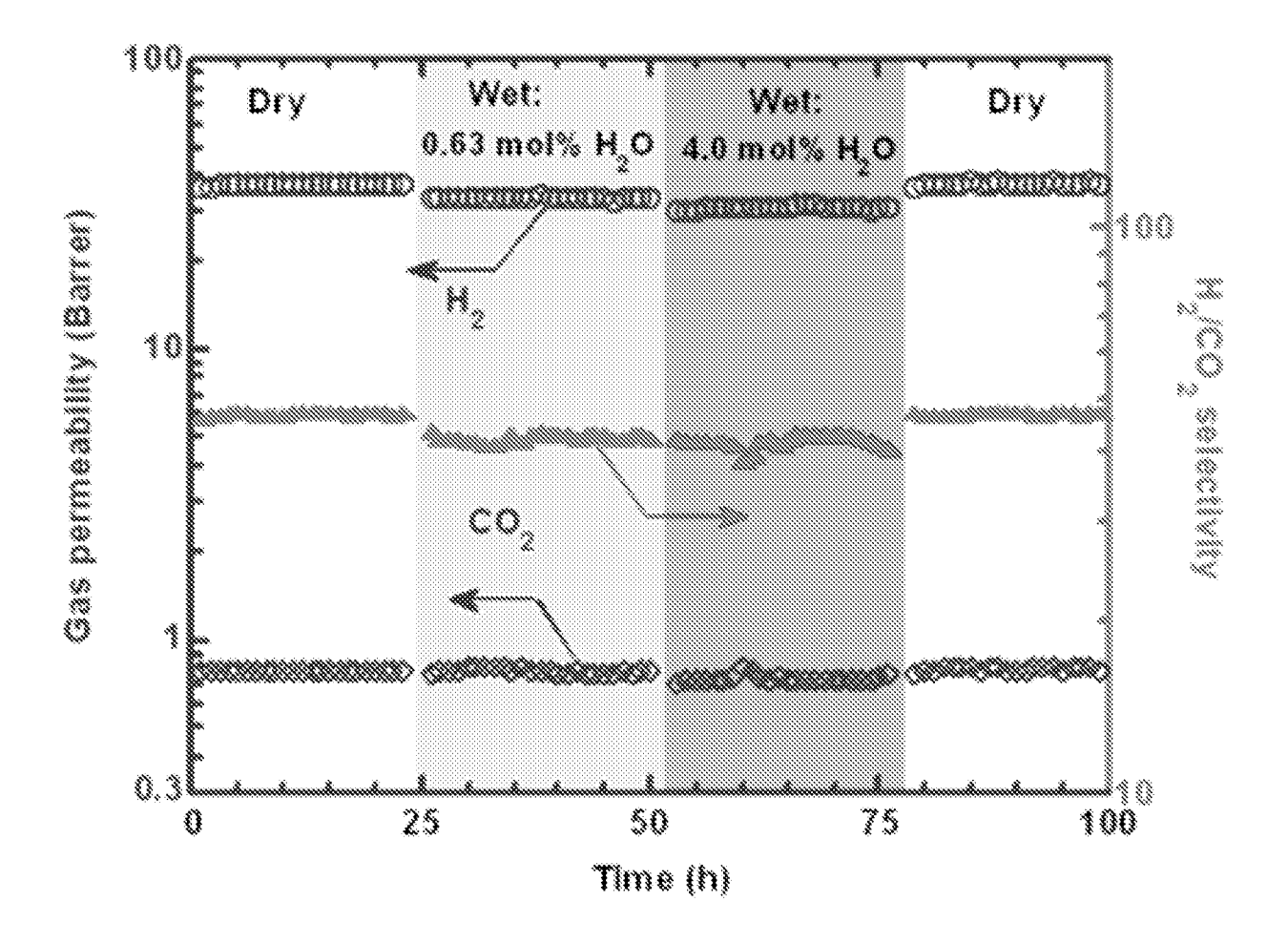
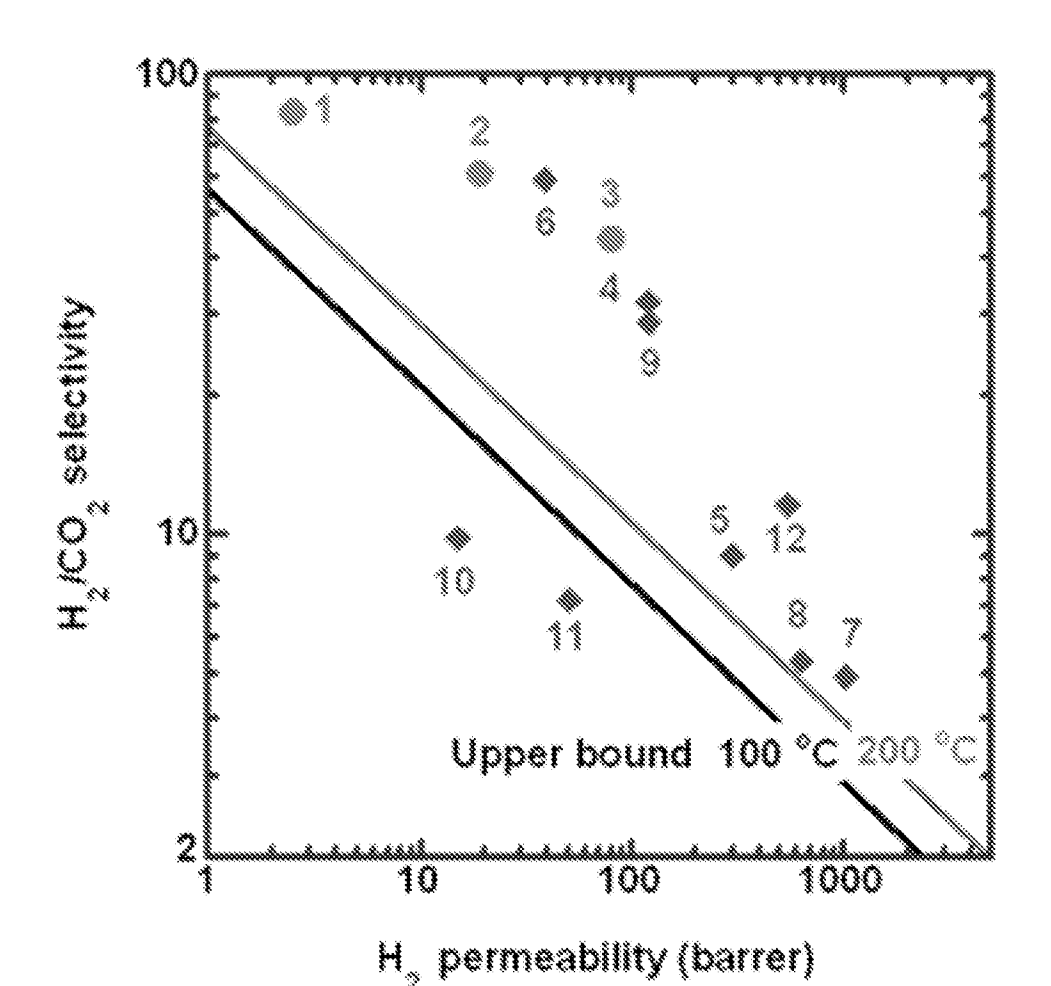


FIG. 14C



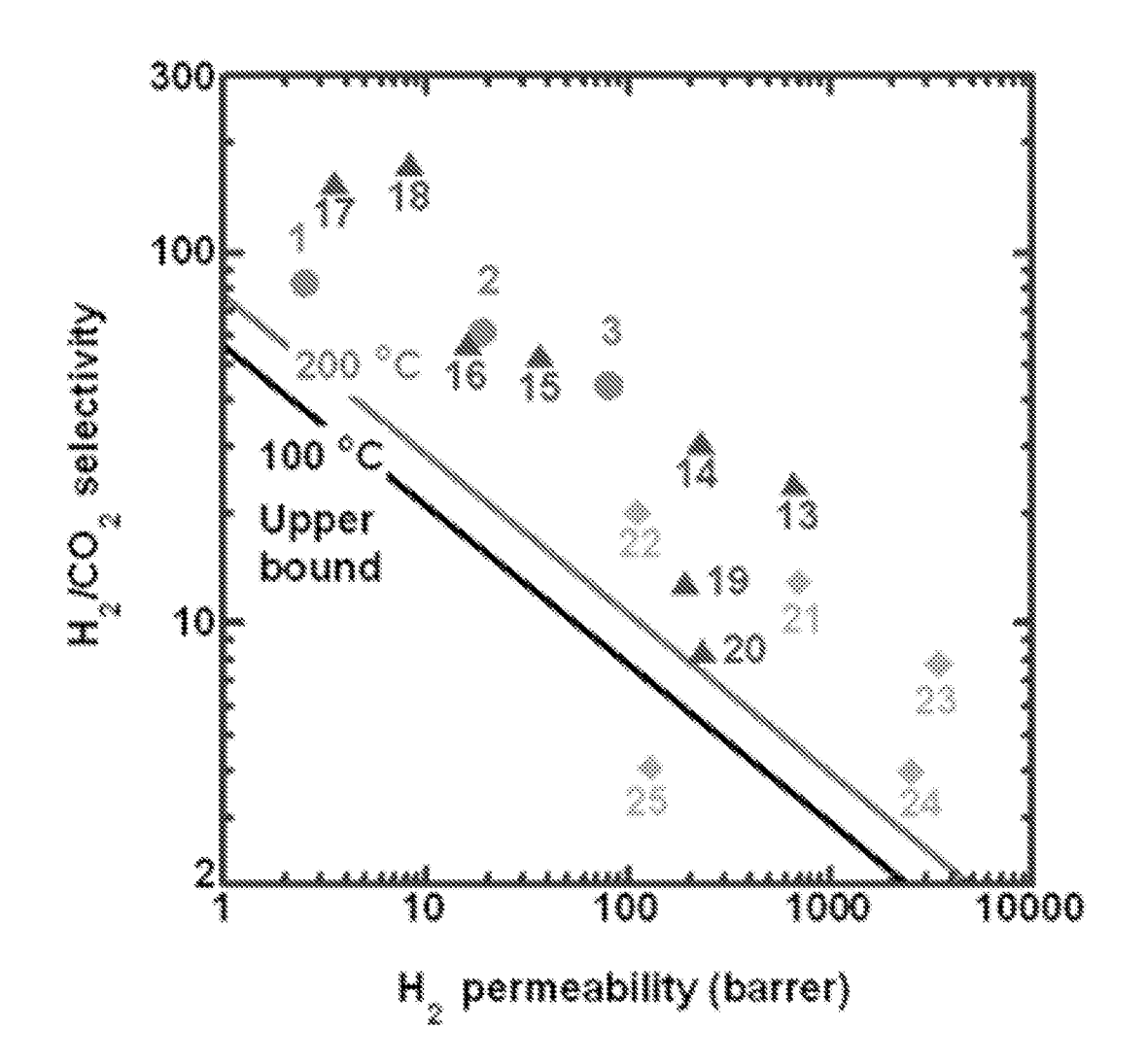
This study:

- 1. PSI500-100@100(P)
- 2. PBI550-100@100(P)
- 3. PBISSO-100@200(M)

CMS (T, < 700 °C):

- 4. PBI-PPA600@150(M)
- 5. PBI600@100(P)
- 6. Cellophane600@30(P)
- 7. Yorlon675@35(P)
- 8. MTI aramide675/035(P)
- Cellulose600@25(P)
- 10. Metal oxide-PFA525@100(P)
- 11. Matrimid500@150(P)
- 12.PPG-Cellulose550@25(P)

FIG. 14D



This study:

- PBI500-100@100(P)
- 2. PBISSO-100@100(P)
- 3. PBISSO-100@200(M)

CMS (7, ≥ 700 °C):

- 13. Polyimide700@200(P)
- 14. Cellulose700@90(M)
- 15.PBI900@100(M)
- 16. Torlon925@35(M)
- 17.MTI aramide925@35(M)
- 18. CANAL-TB900@100(M)
- 19.PABZ-6FDA850@35(P)
- 20. Polyester800@150(P)

ALD-engineered membranes:

- 21.Pd/Al₂O₂@188(P)
- 22.PBI/AI₂O₂@200(M)
- 23.217-000100(18)
- 24. PIM-1/A1,O₃(035(P)
- 28.88Z-43@200(P)

FIG. 14E

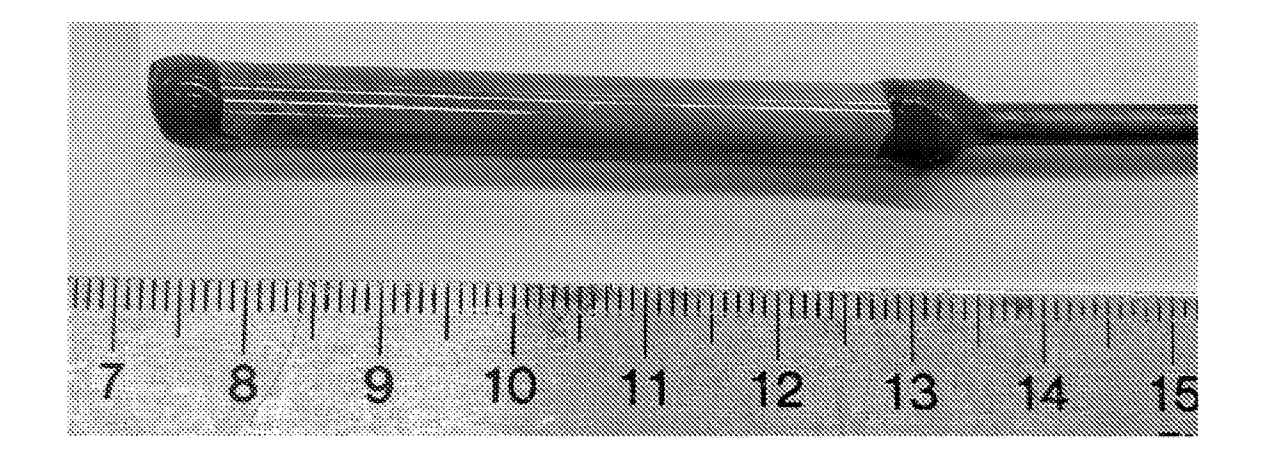


FIG. 15A

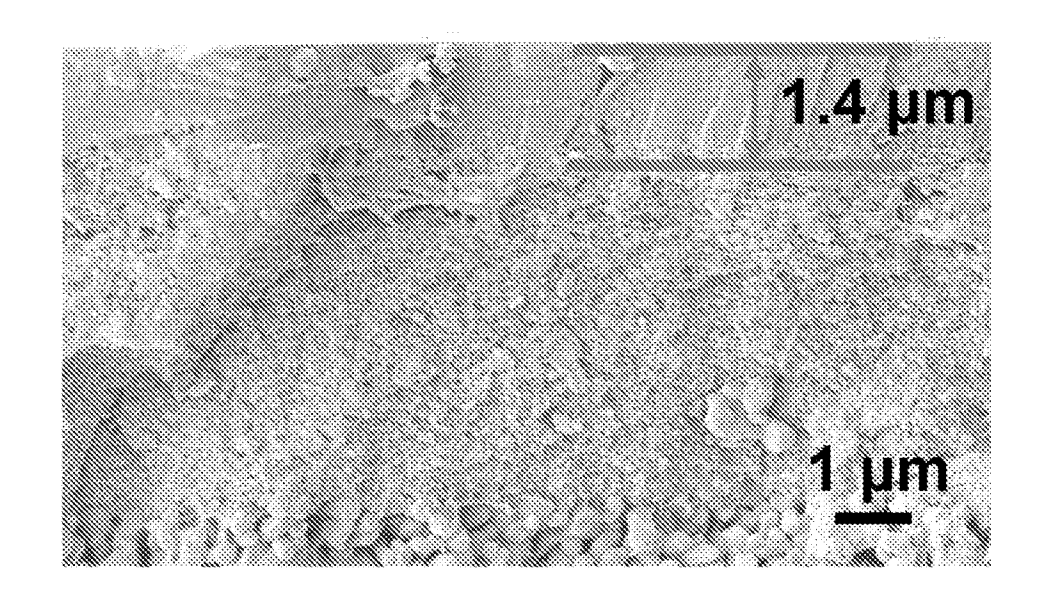


FIG. 15B

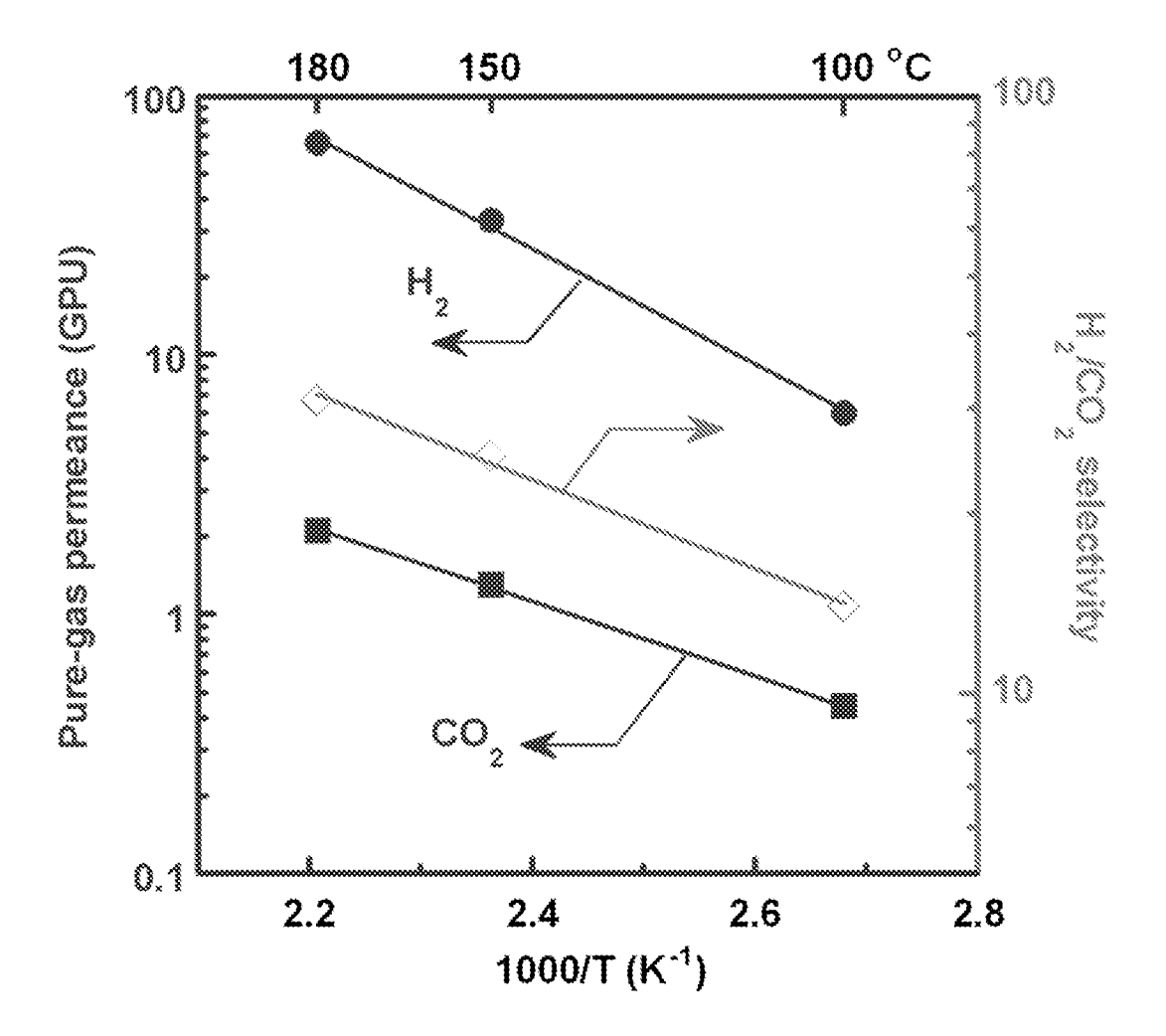
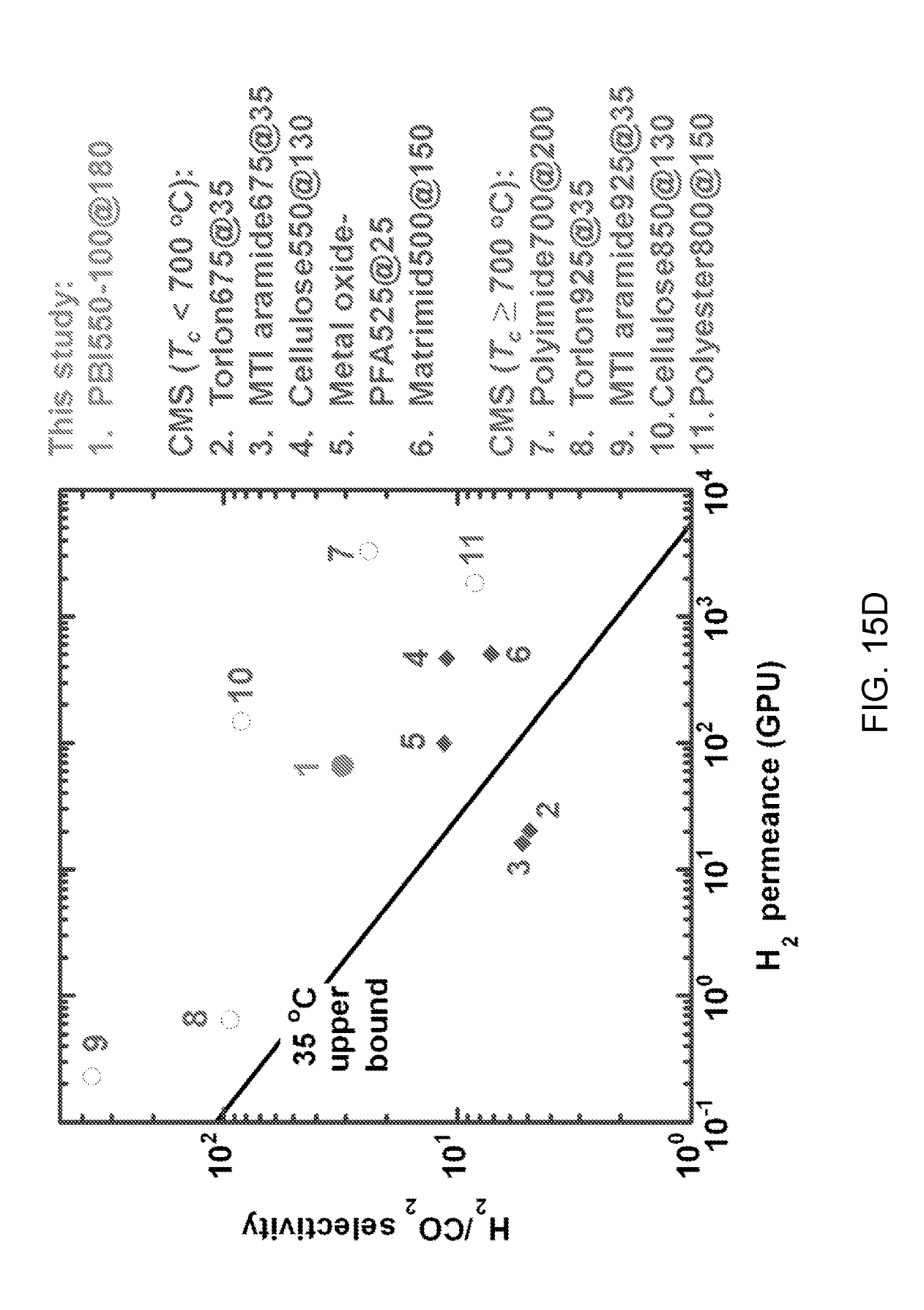


FIG. 15C



41 / 59

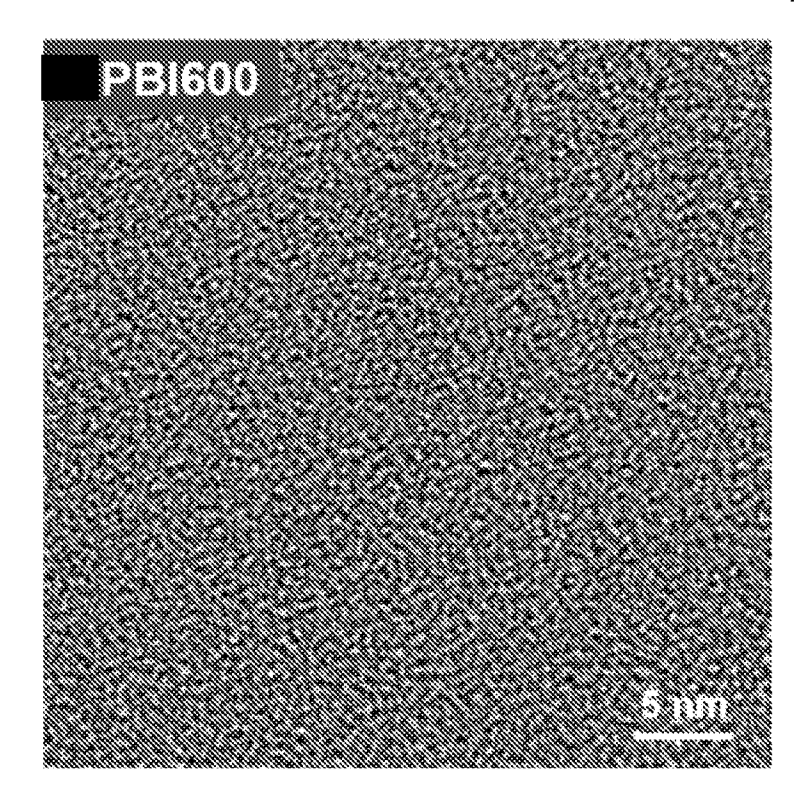


FIG. 16A

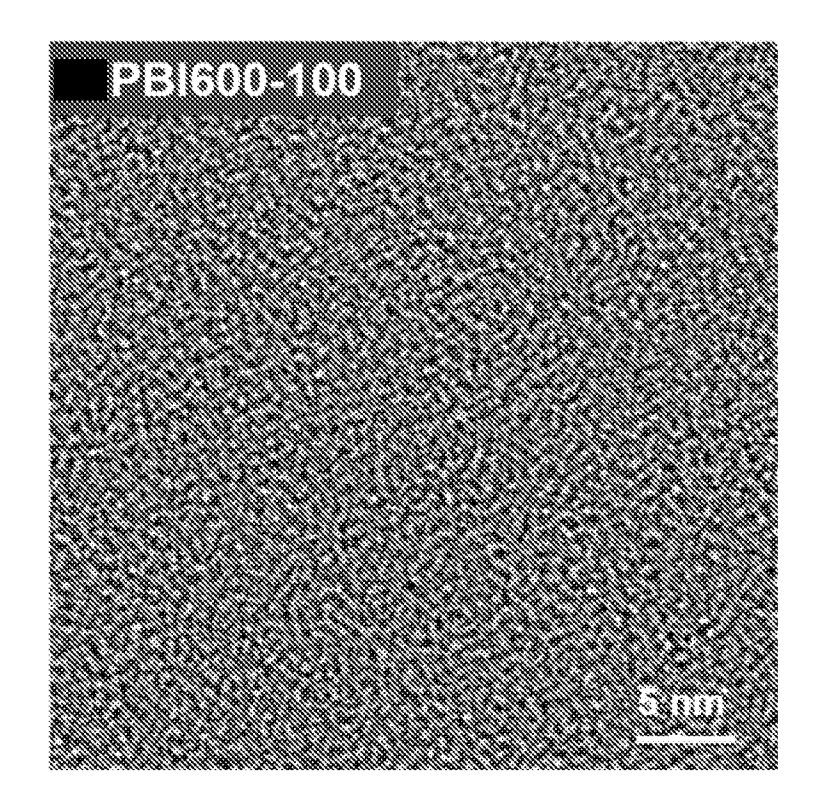


FIG. 16B

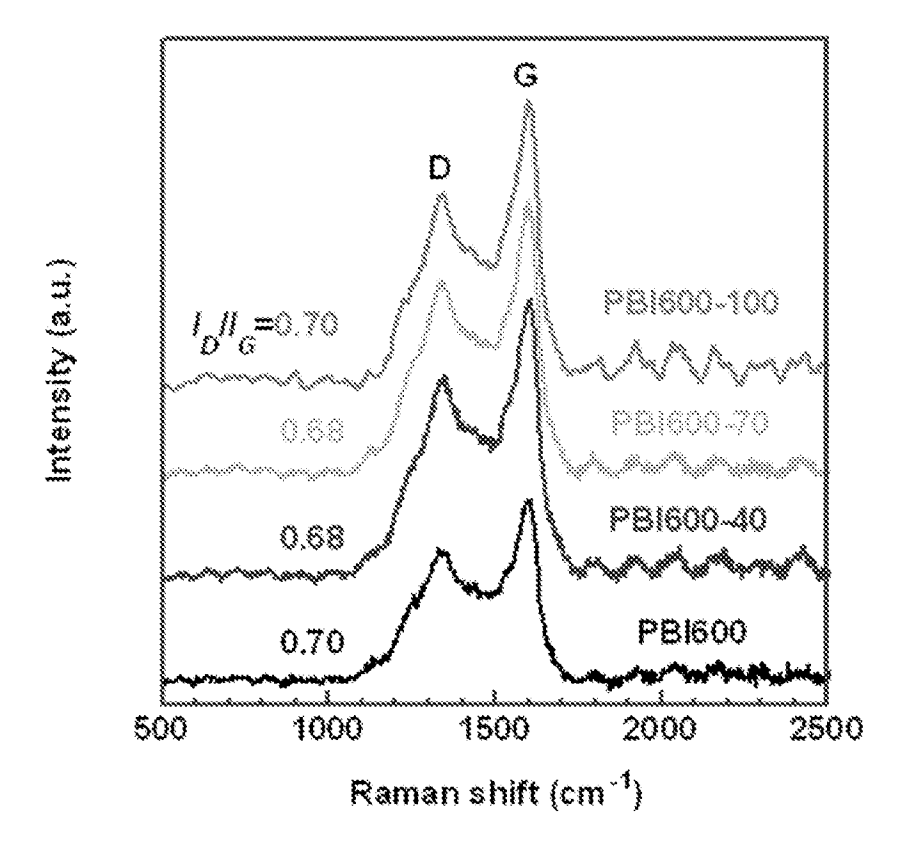


FIG. 17A

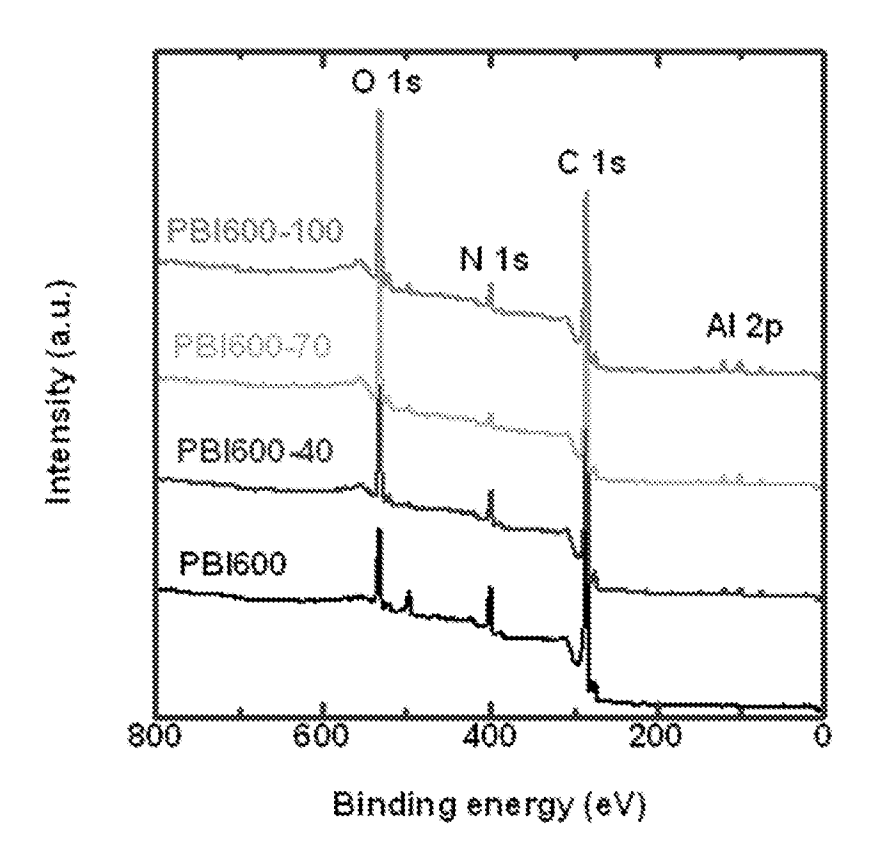
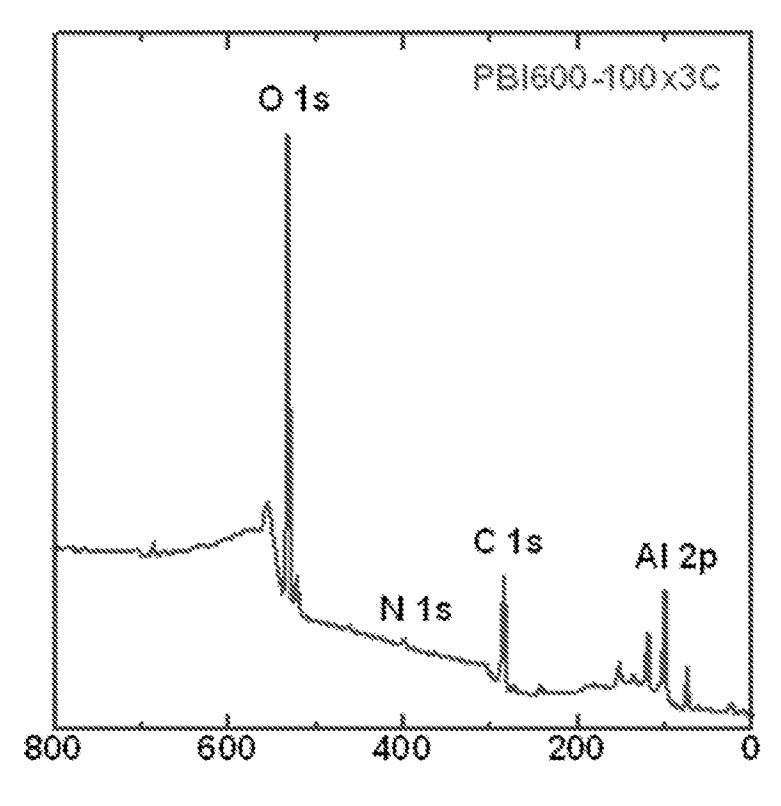
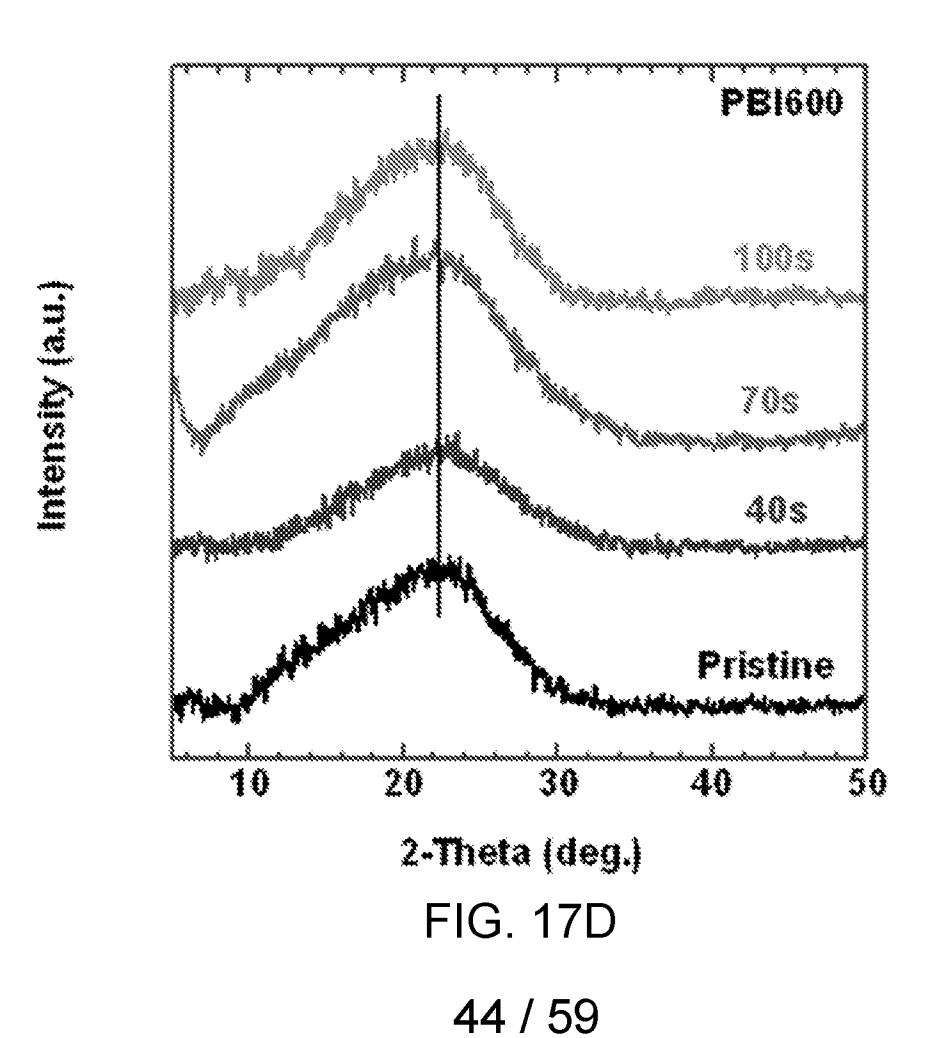
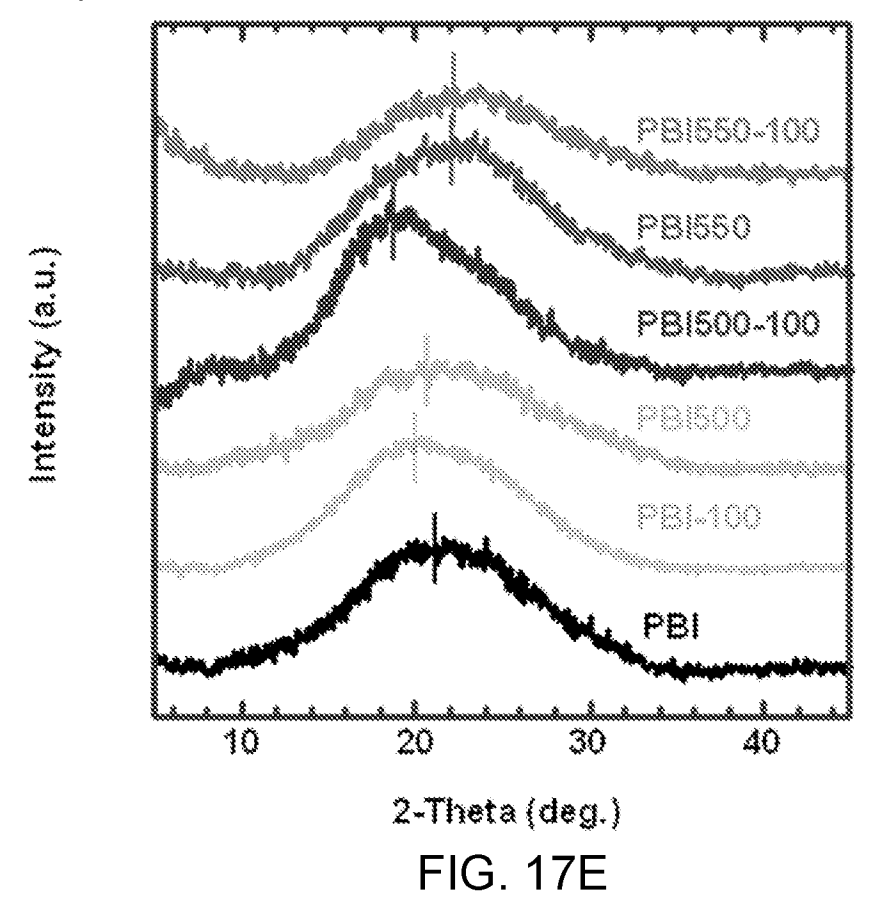


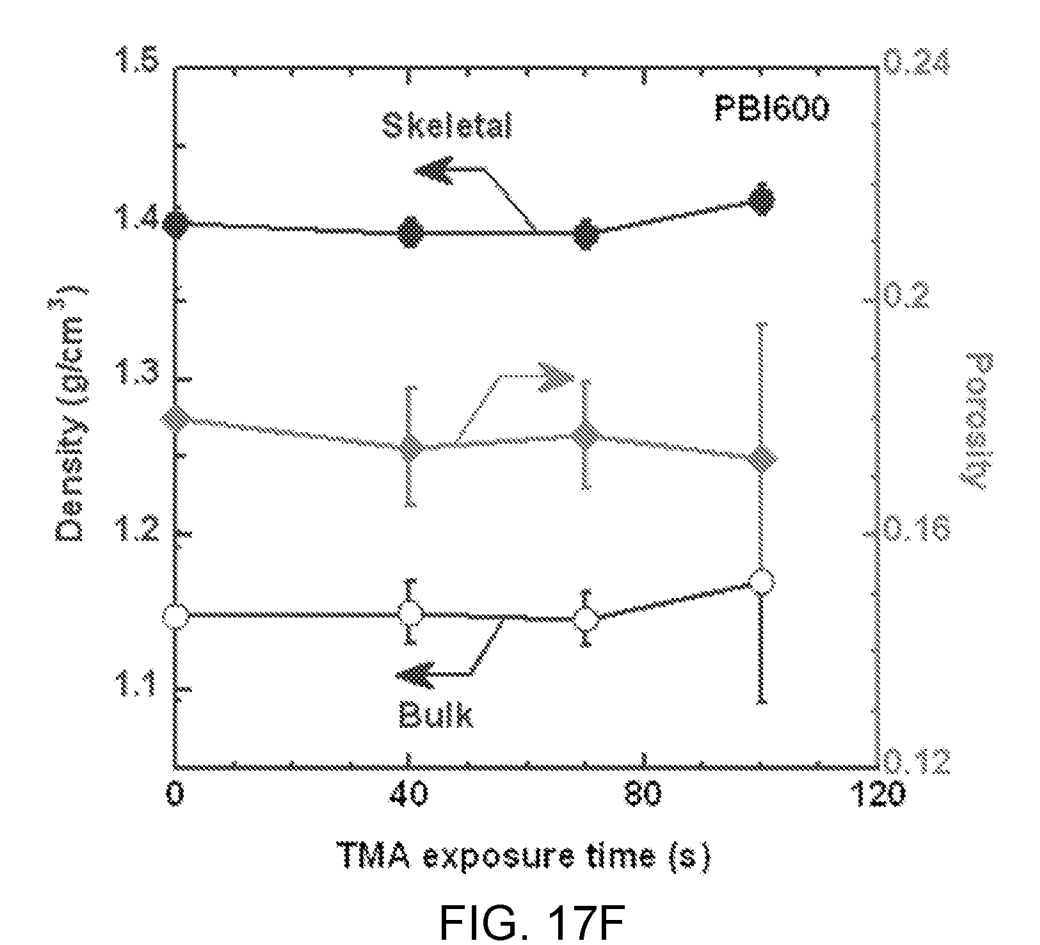
FIG. 17B



Binding energy (eV) FIG. 17C







45 / 59

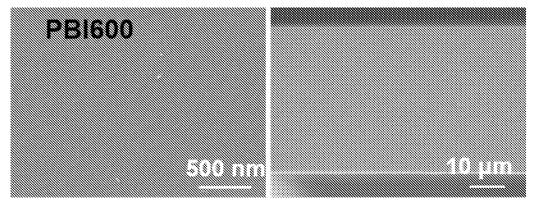


FIG. 18A

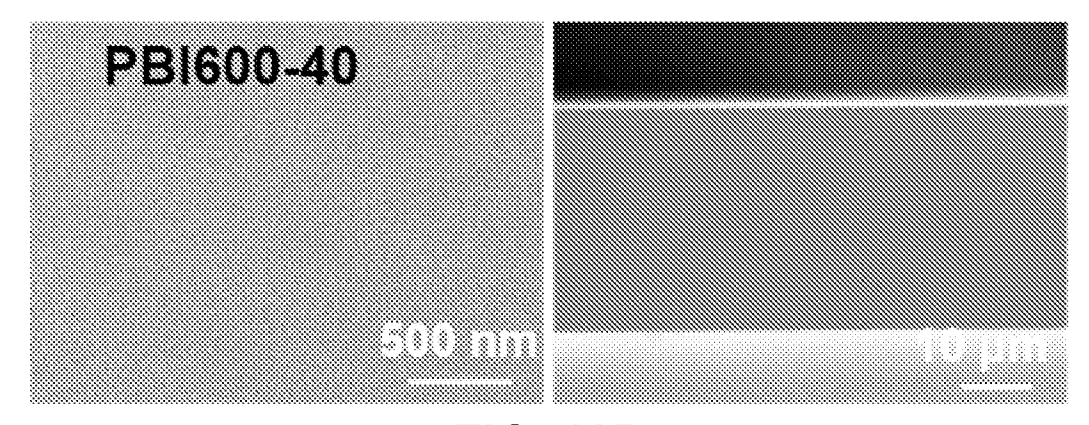


FIG. 18B

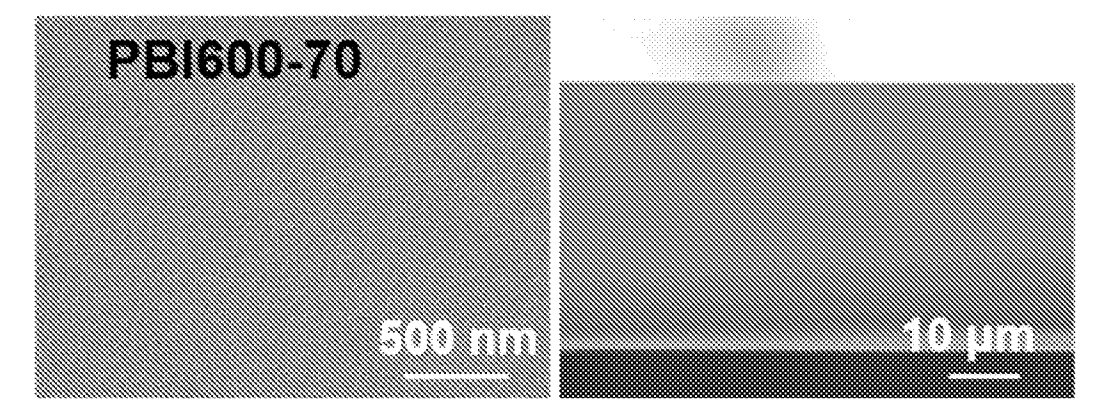


FIG. 18C

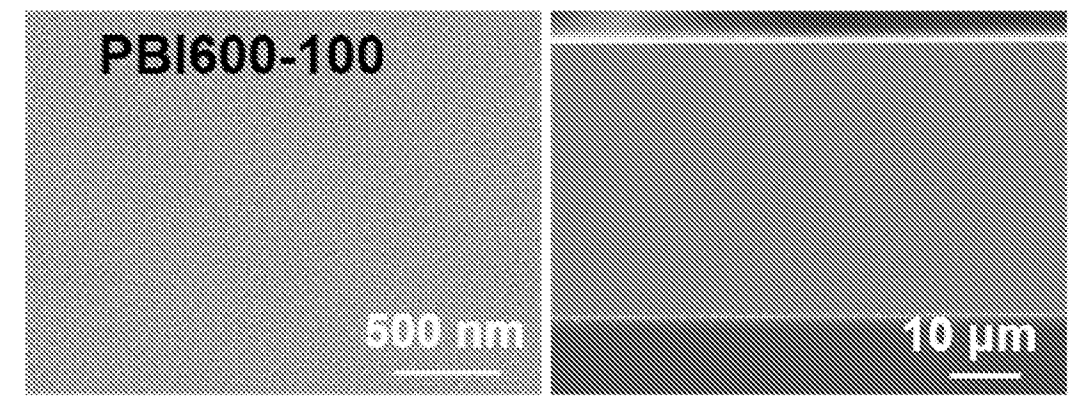


FIG. 18D

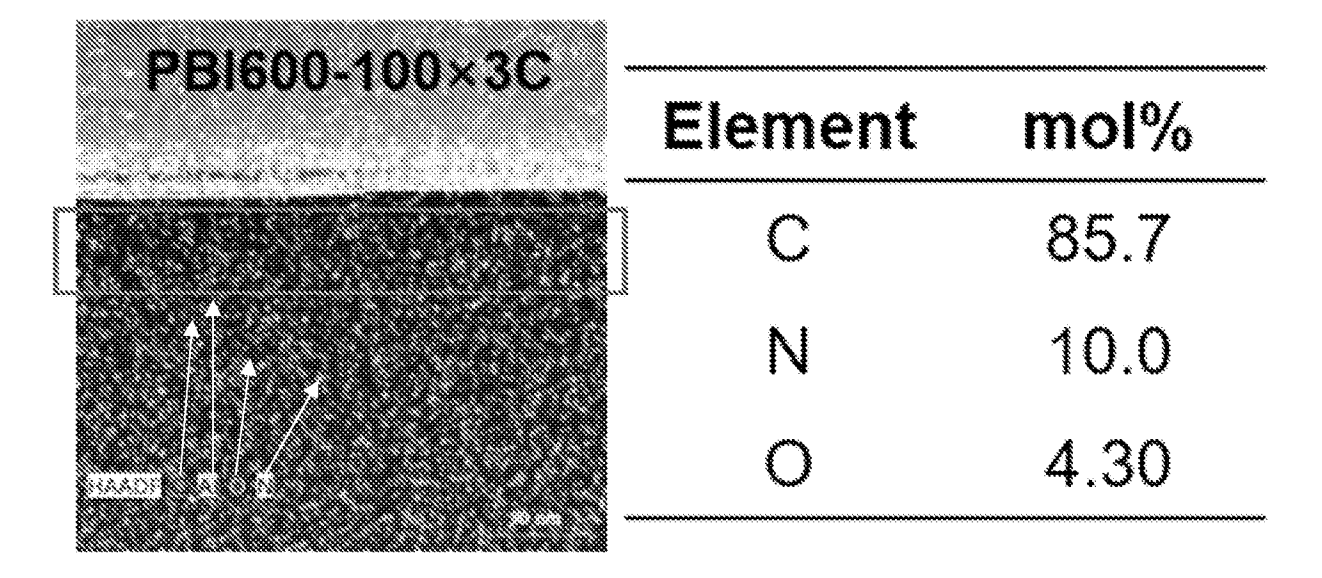


FIG. 19A

PBI600-100×3C	Element	mol%
	O	83.8
	AI	16.2

FIG. 19B

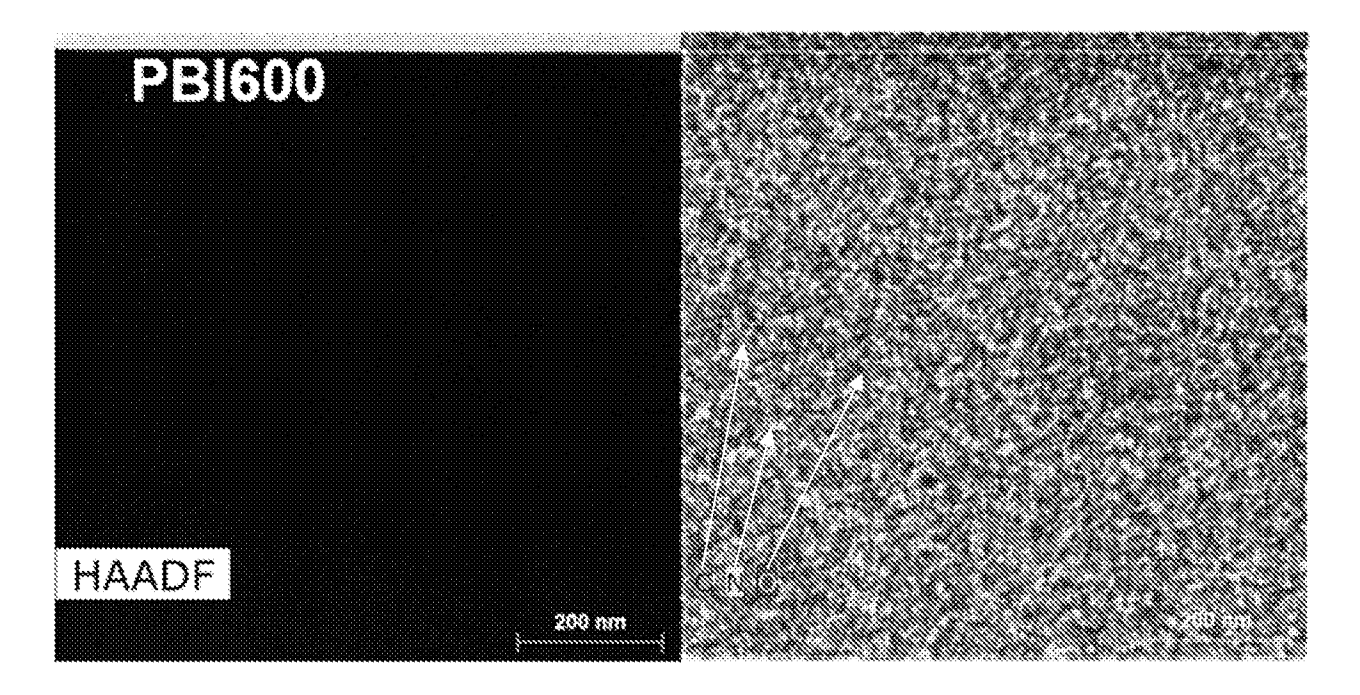


FIG. 19C

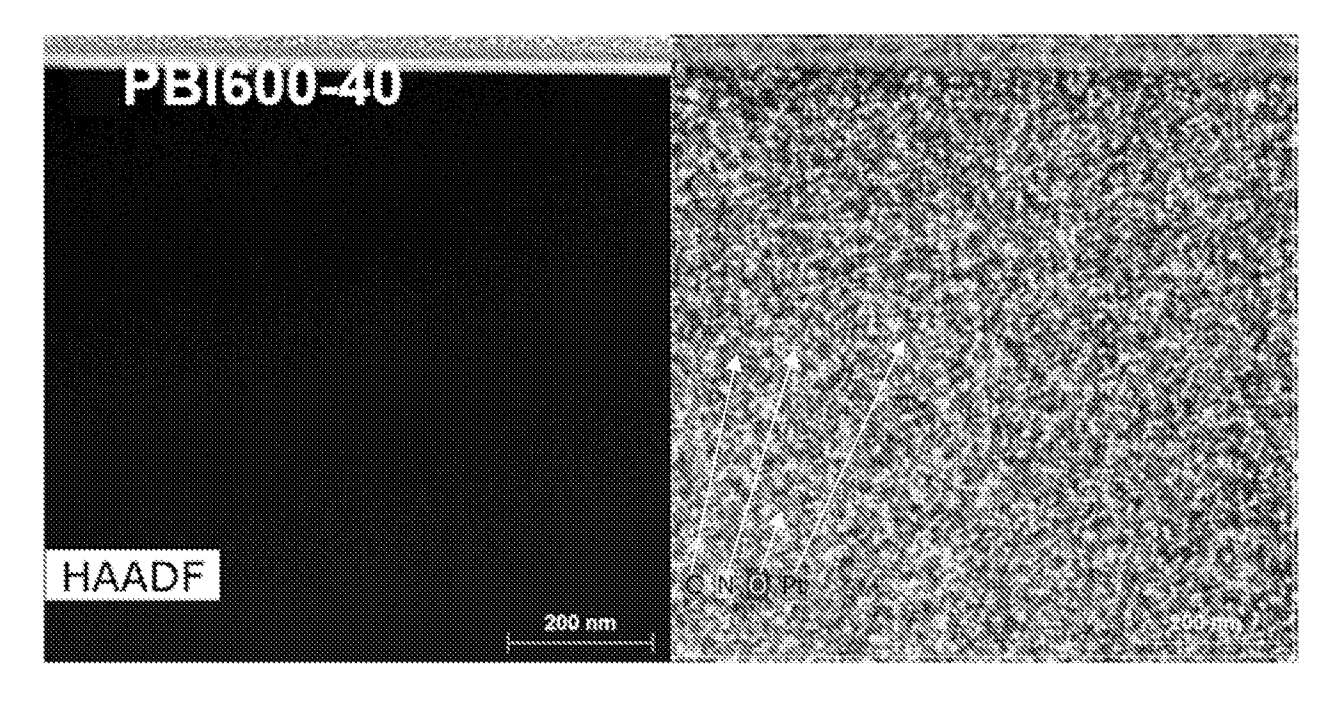


FIG. 19D

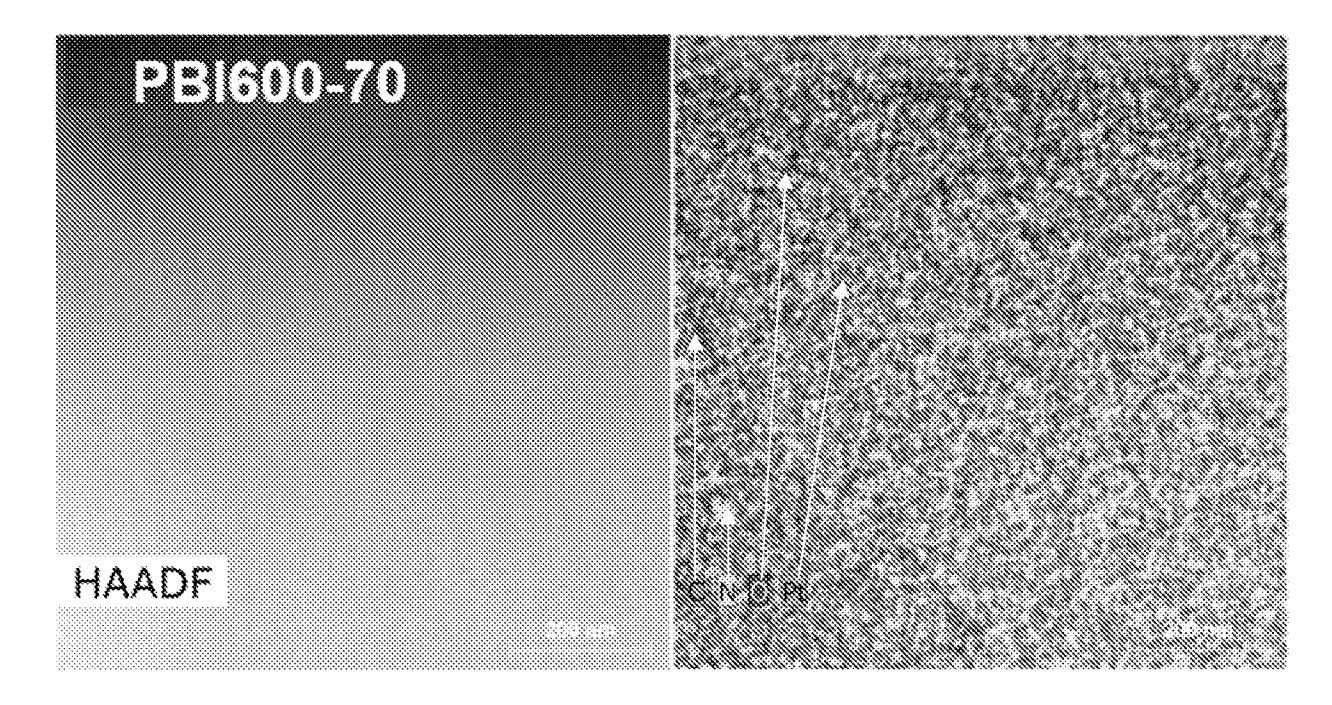


FIG. 19D

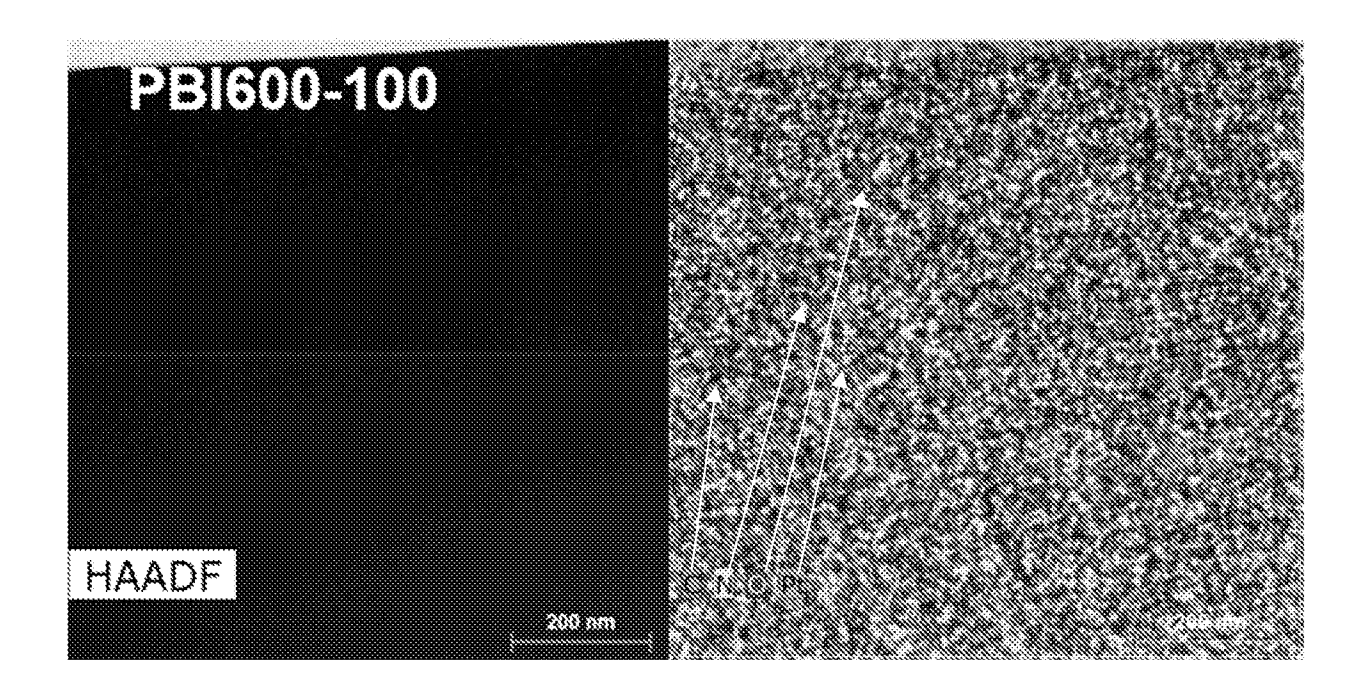


FIG. 19F

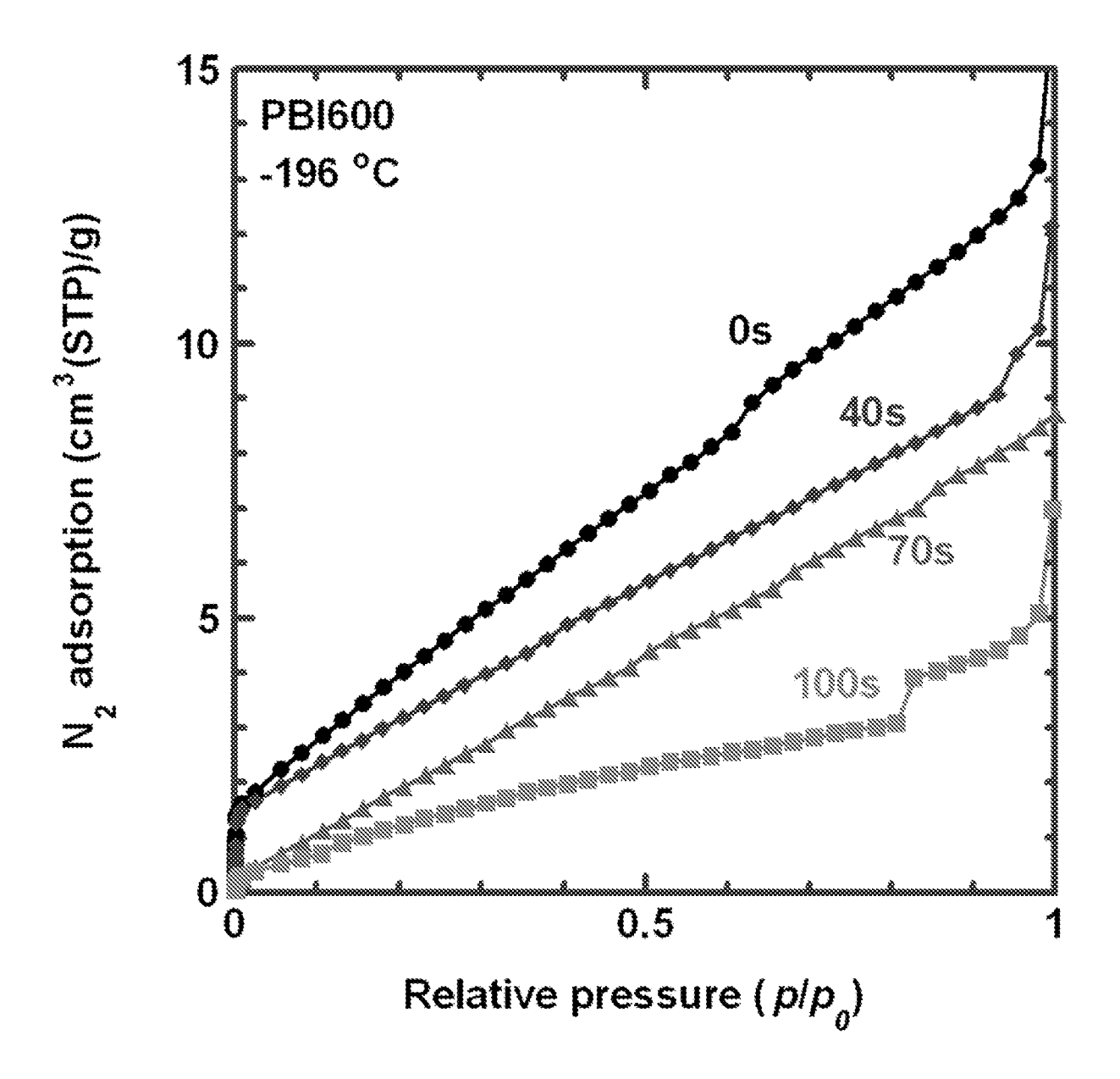


FIG. 20

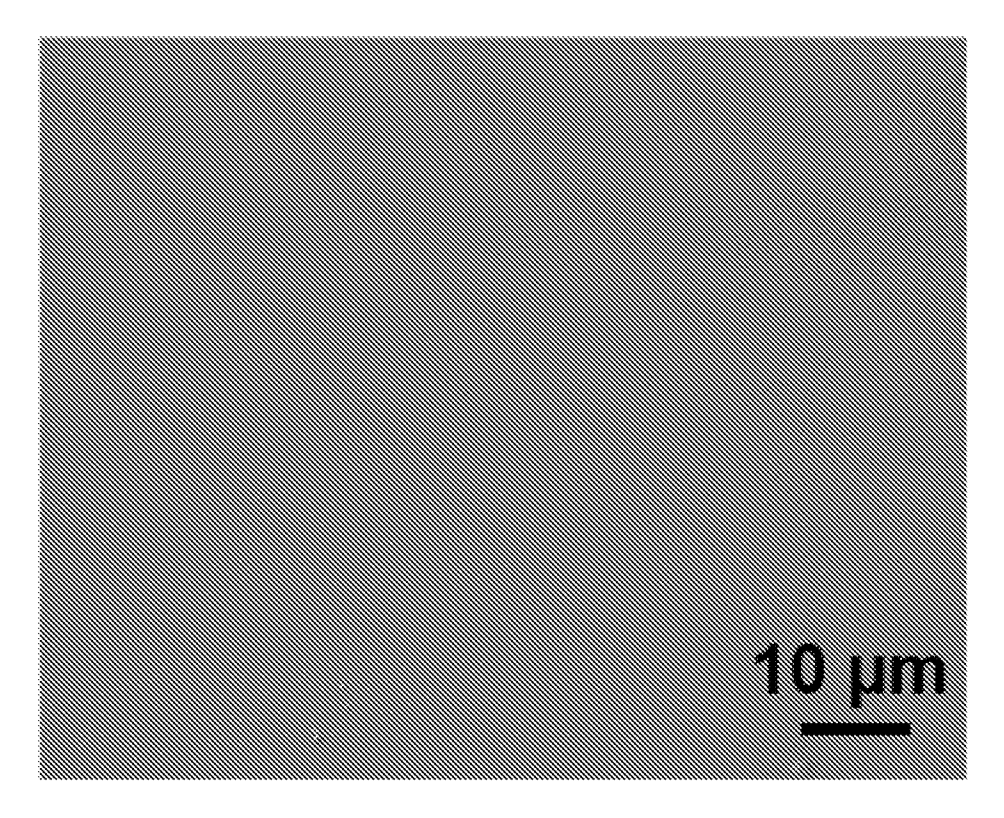


FIG. 21A

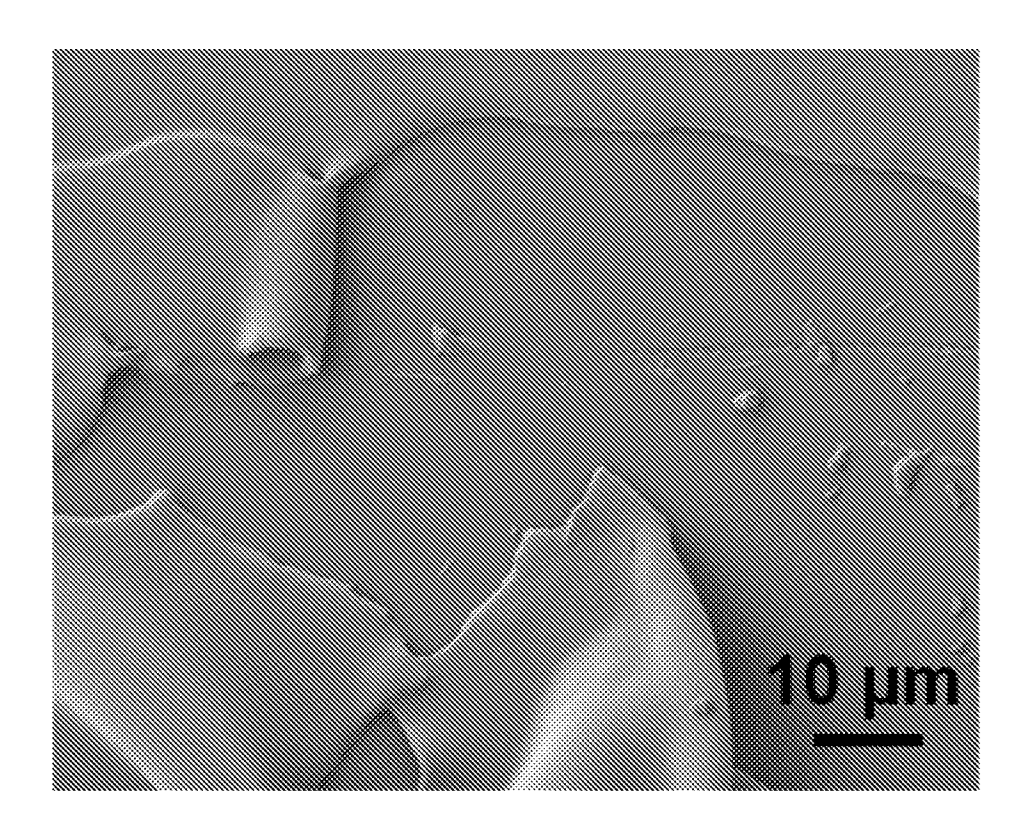
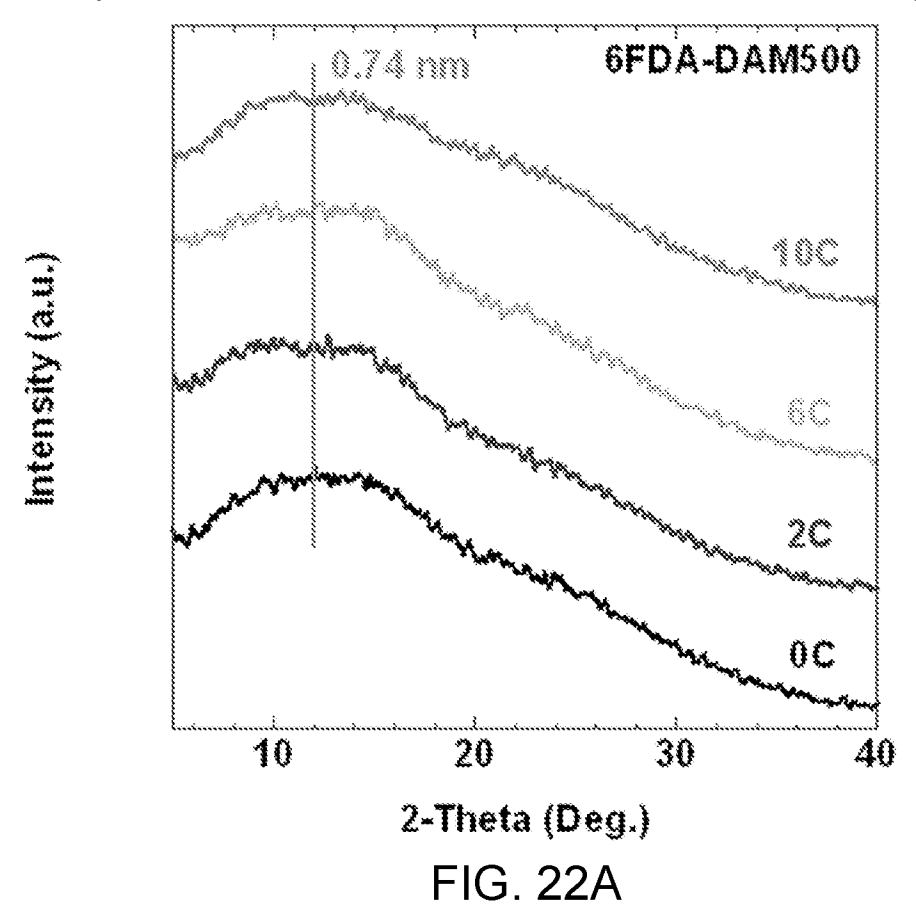
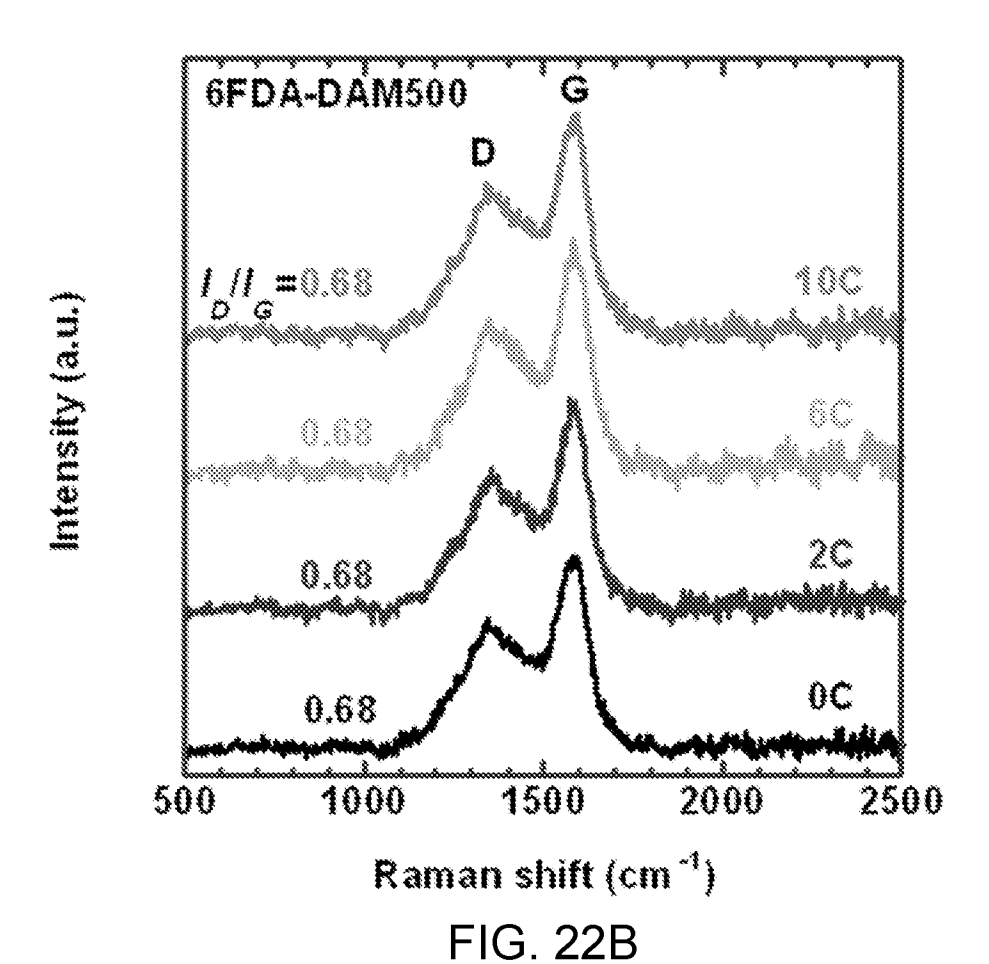


FIG. 21B

51 / 59





52 / 59

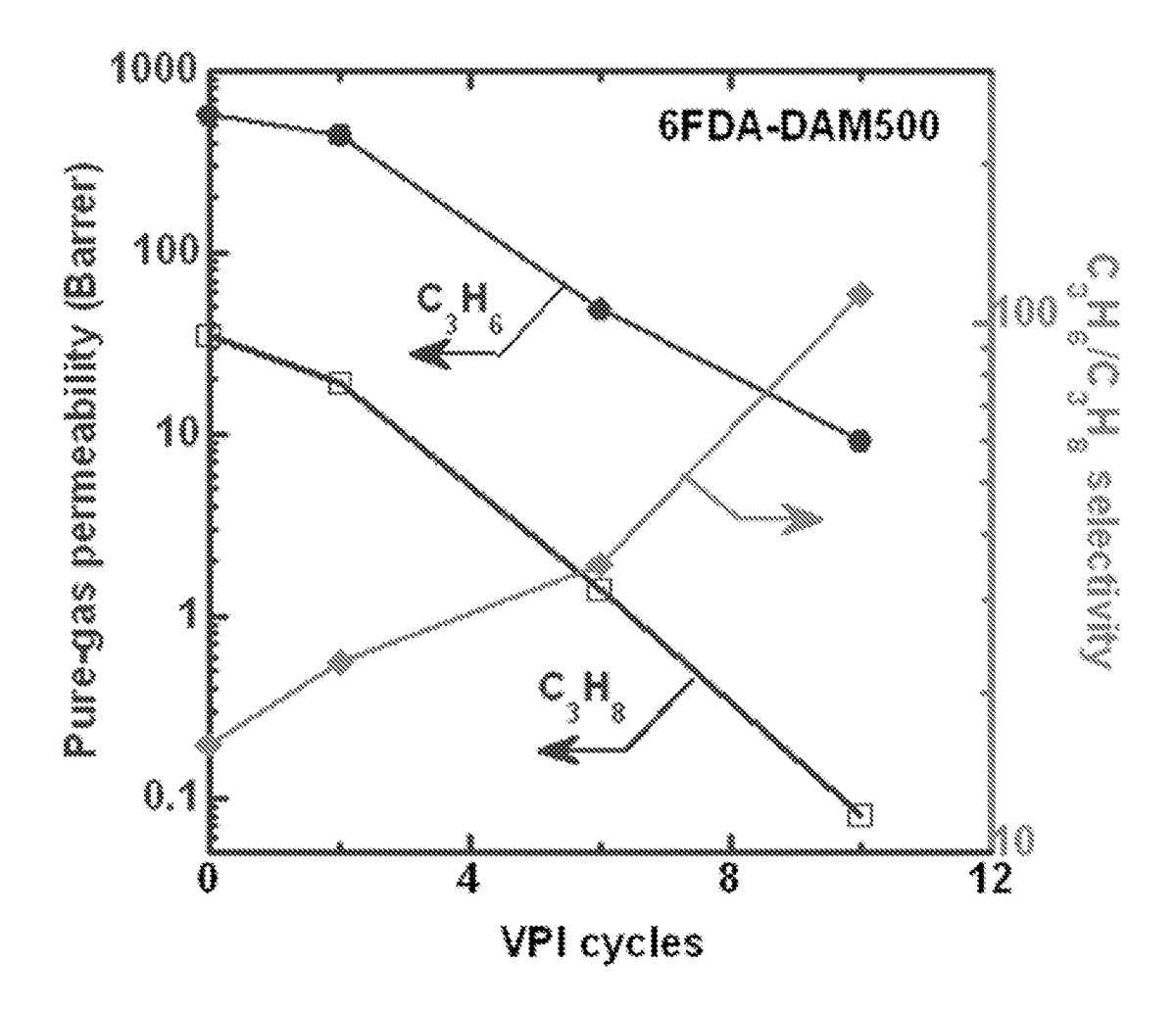
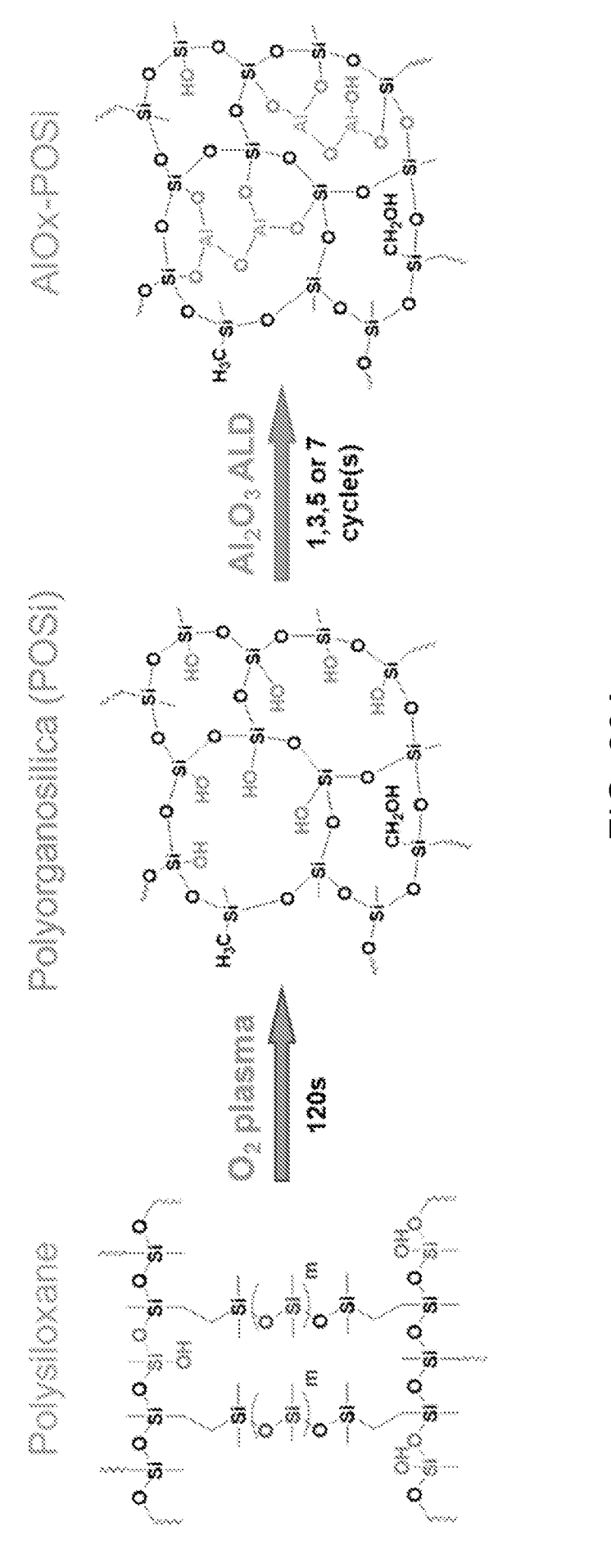


FIG. 22C



54 / 59

WO 2025/111491 PCT/US2024/056939

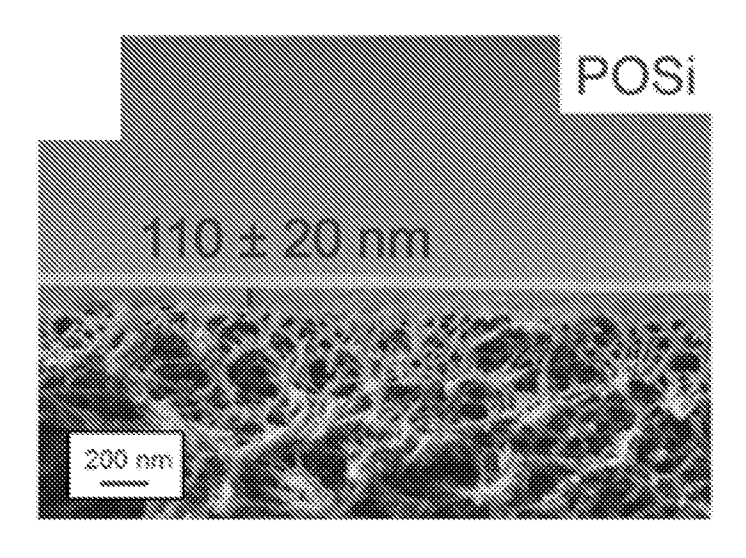
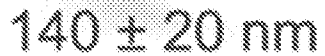


FIG. 23B

POSI-3C



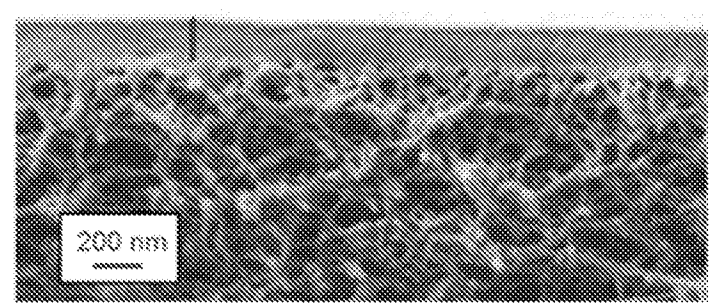


FIG. 23C

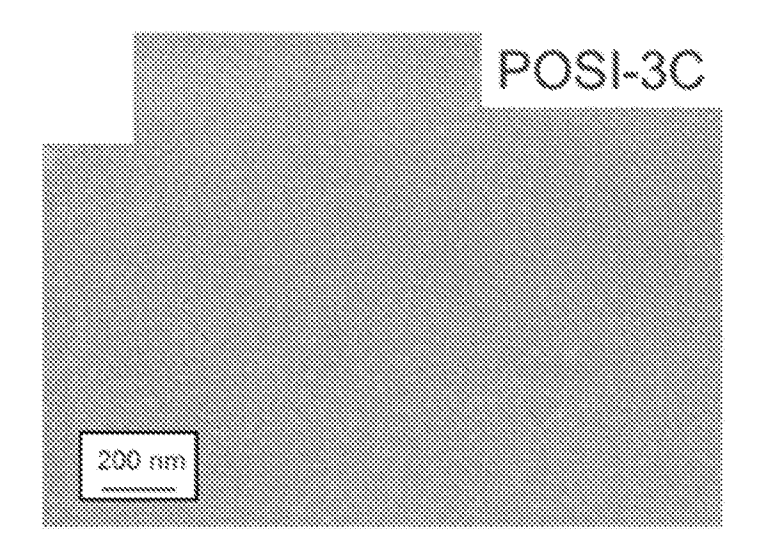


FIG. 23D

55 / 59

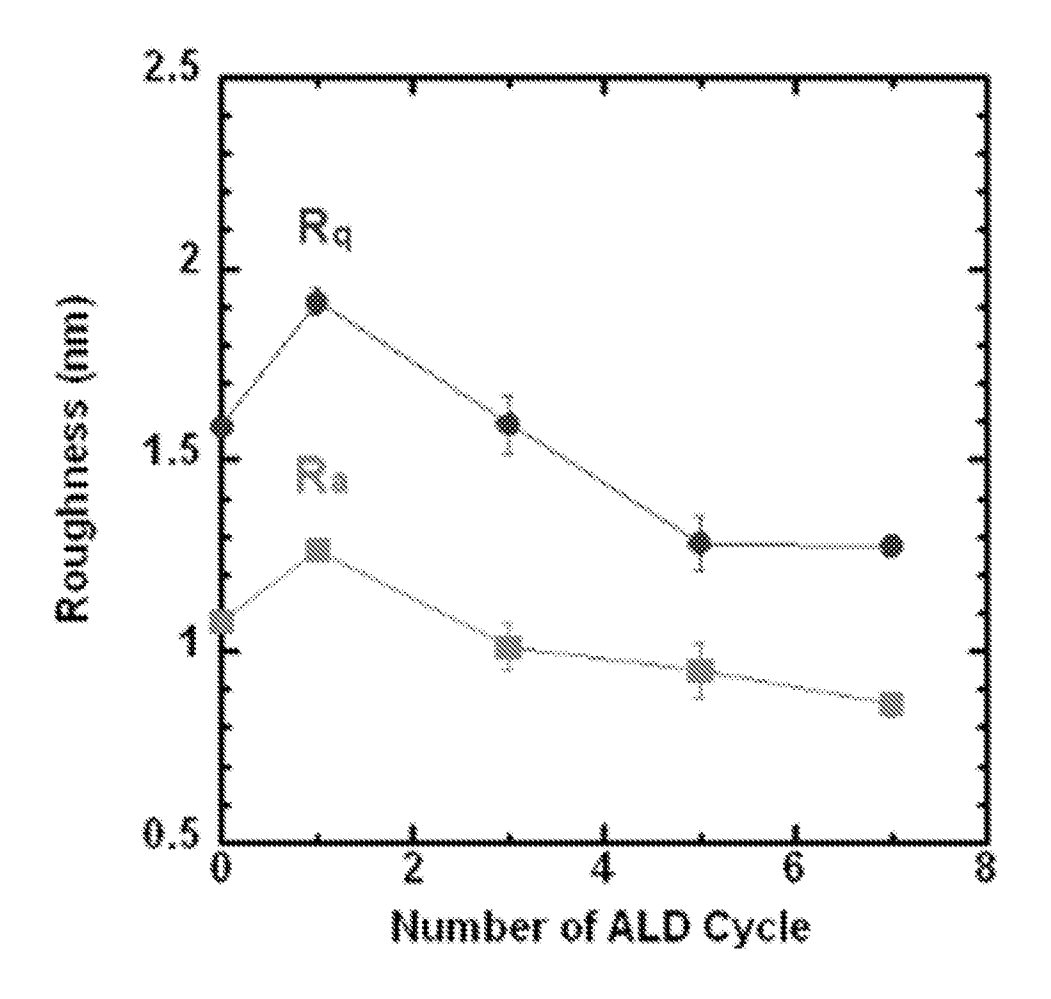
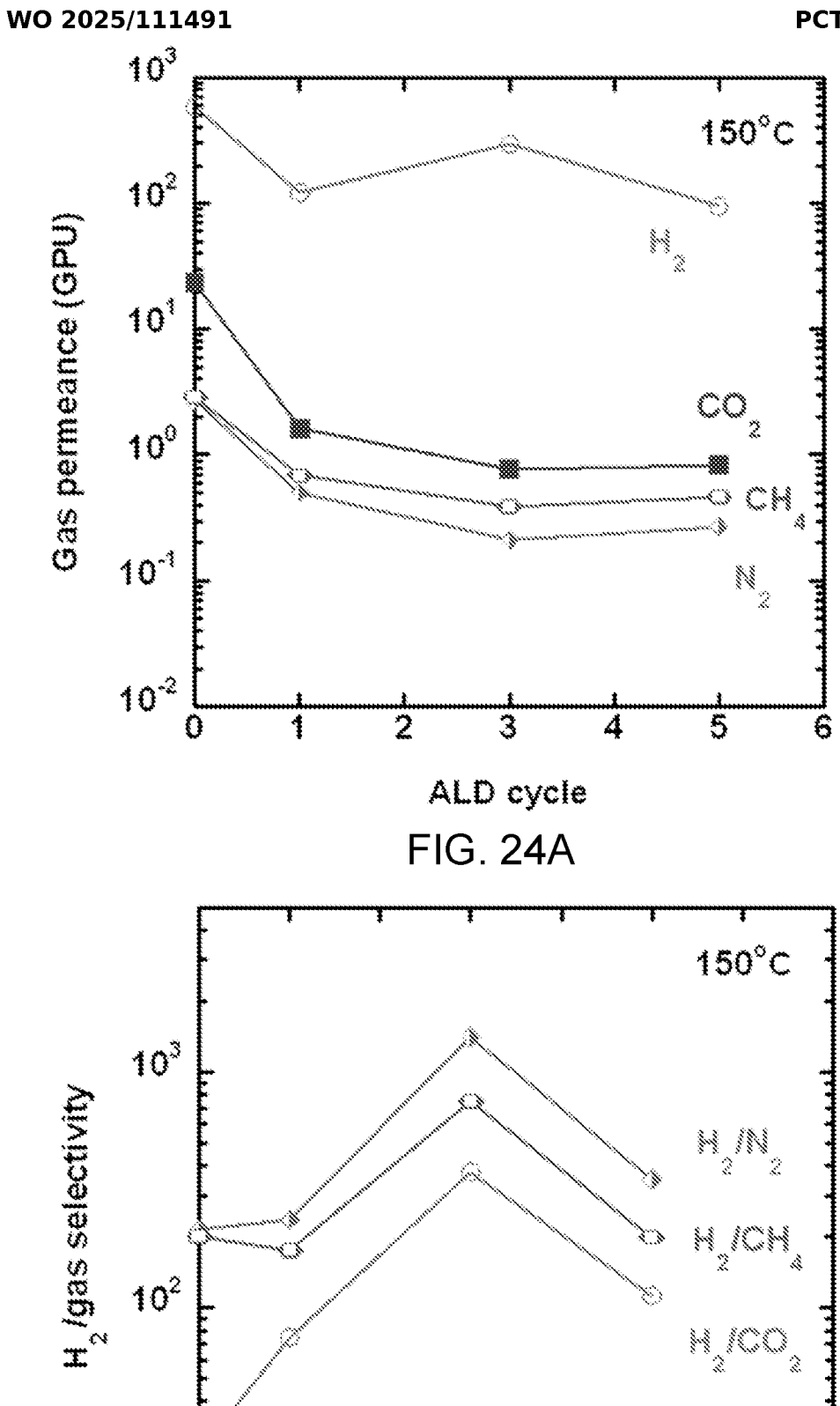


FIG. 23E

101

Ö



ALD cycle FIG. 24B

4

3

5

6

2

57 / 59

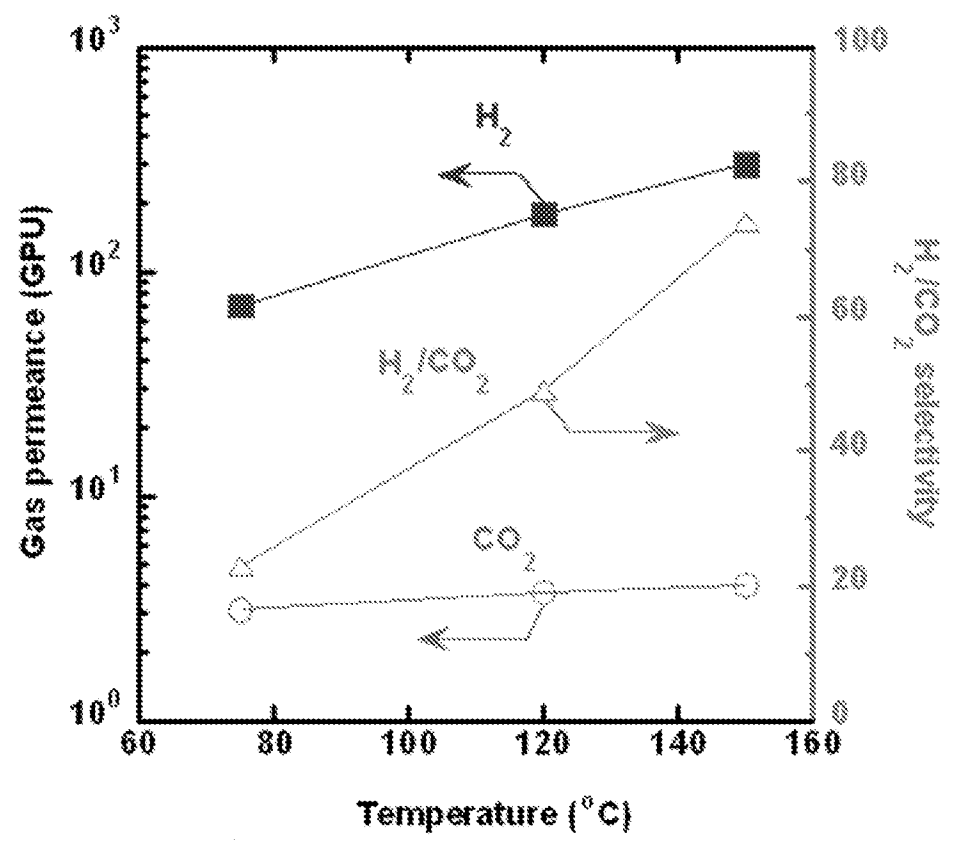


FIG. 25A

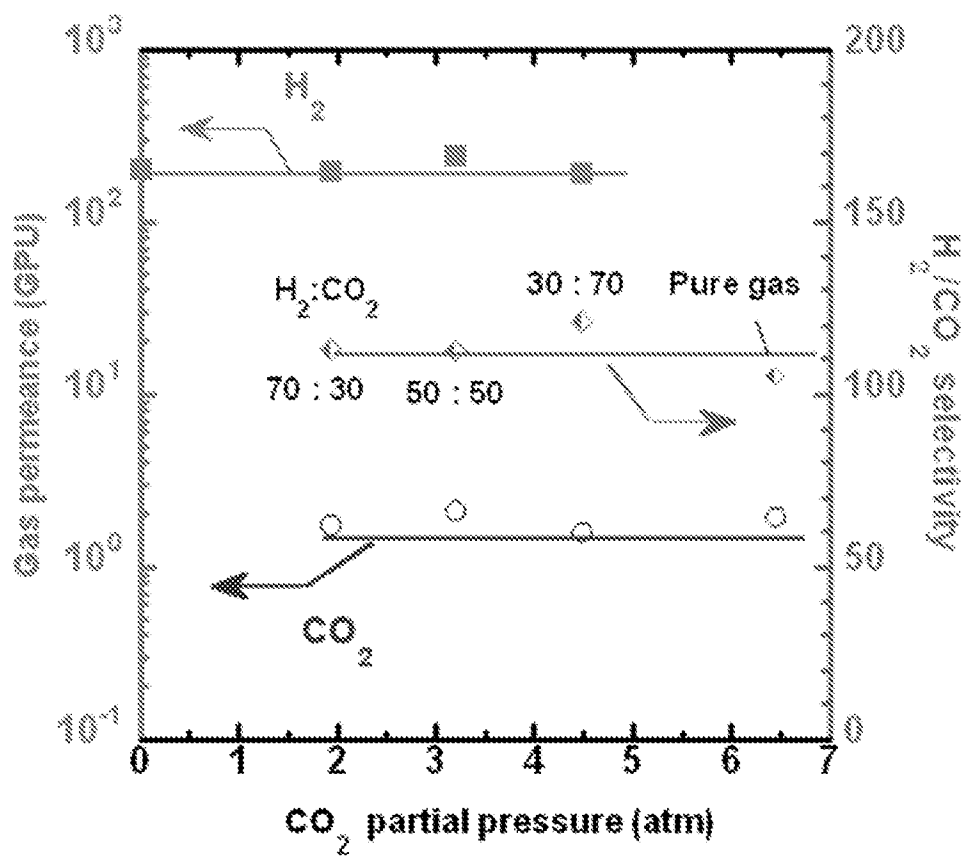
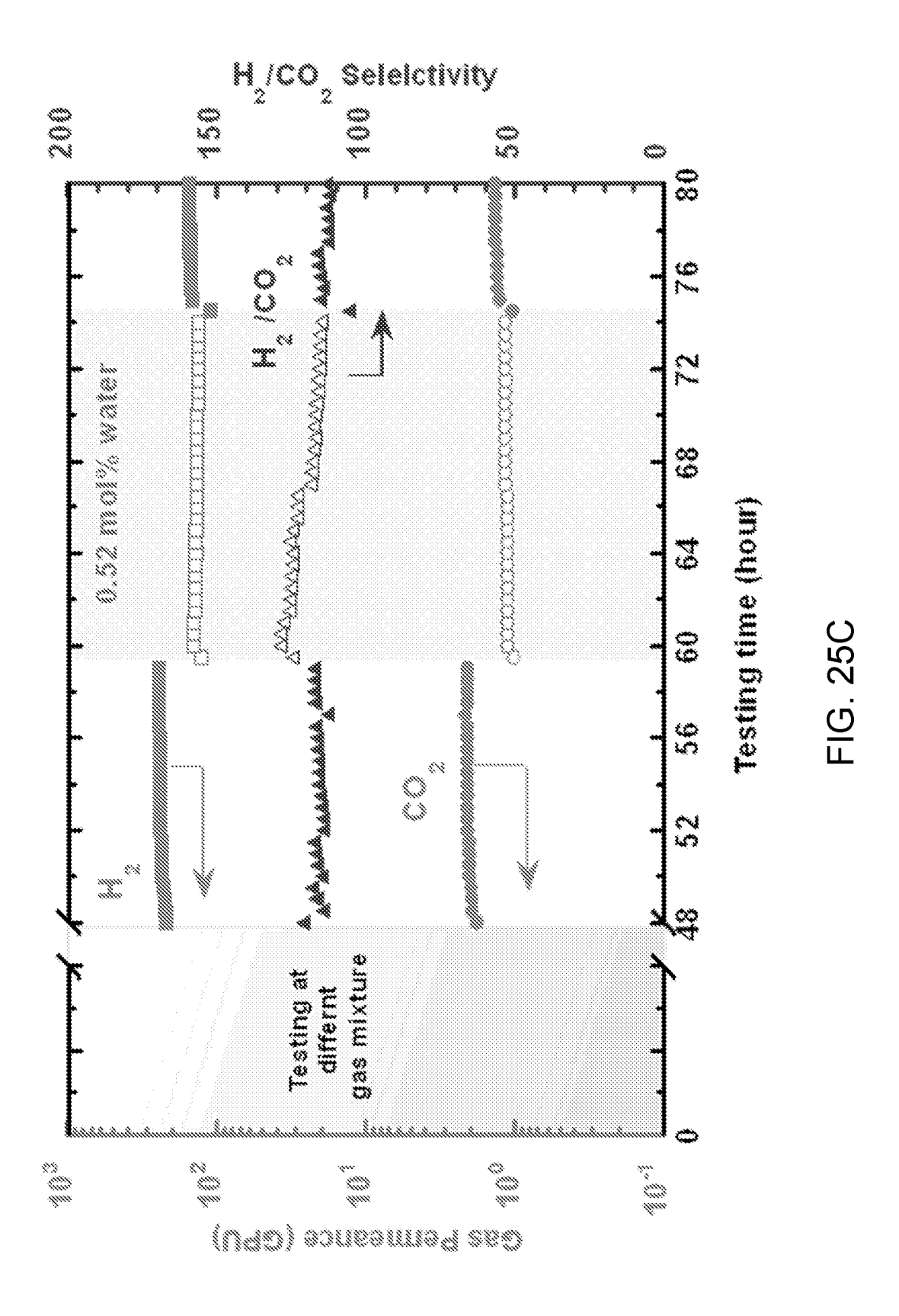


FIG. 25B



59 / 59

International application No.

TAINA MATOS

Telephone No. **571-272-4300**

PCT/US2024/056939

A. CLASSIFICATION OF SUBJECT MATTER

IDC: R01D 60/14 (2025 01): R01D 71/02 (2025 01): R01D 71/38 (2025 01): R01D 60/10 (2025 01): R01D 60/12 (2025 01)

	PC: B01D 09/14 (2023.01); B01D 71/02 (2023.01); B01D 71/38 (2023.01); B01D 09/10 (2023.01); B01D 09/12			
		301D 69/147; B01D 69/14111; B01D 69/106; B01D 12833; B01D 2323/21813; B01D 2323/30; B01D 232.		D 2325/02832; B01D
Acc	ording to	International Patent Classification (IPC) or to both na	ational classification and IPC	
B.	FIEL	DS SEARCHED		
Mir	imum do	cumentation searched (classification system followed	by classification symbols)	
	See Se	arch History Document		
Doc		on searched other than minimum documentation to the arch History Document	e extent that such documents are included in	the fields searched
Elec	etronic da	ta base consulted during the international search (nan	ne of data base and, where practicable, searc	th terms used)
		arch History Document		
C.	DOC	UMENTS CONSIDERED TO BE RELEVANT		
Cat	egory*	Citation of document, with indication, where	appropriate, of the relevant passages	Relevant to claim No.
	X	US 2005/0221103 A1 (MAEDA et al.) 06 October 2 entire document	2005 (06.10.2005)	1-4, 8
		KR 10-0717575 B1 (M COTEC et al.) 15 May 2007	7 (15.05.2007)	
	X	see machine translation		1, 5
	Y 	see machine translation		6, 7, 9
		ESMAIELZADEH et al., Construction of proton excirradiation based on novel fluorine functionalizing s silica bionanocomposite, Ultrasonics Sonochemistry 20 January 2025]. Retrieved from the internet: https://doi.org/10.1007/j.nc.2015.00/	ulfonated polybenzimidazole/cellulose/ y, Volume 41, March 2018 [retrieved on	
	Y	entire document		6, 7, 9
*	Special c	ocuments are listed in the continuation of Box C.	See patent family annex. "T" later document published after the international date and not in conflict with the application.	ational filing date or priority
"A" "D" "E"	to be of particular relevance document cited by the applicant in the international application		"X" document of particular relevance; the c considered novel or cannot be considered	on laimed invention cannot be
"L"	filing date		"Y" document of particular relevance; the claimed invention cannot be considered to involve an inventive step when the document is combined with one or more other such documents, such combination	
"O"	O" document referring to an oral disclosure, use, exhibition or other means		being obvious to a person skilled in the a "&" document member of the same patent fan	rt
"P"	documen	t published prior to the international filing date but later than ty date claimed	& document member of the static patent ran	iiiy
Date	of the act	ual completion of the international search	Date of mailing of the international search	report
		21 January 2025 (21.01.2025)	25 February 2025 (25.0	2.2025)
Name	and mai	ling address of the ISA/US	Authorized officer	
		SIONER FOR PATENTS OP PCT, ATTN: ISA/US		

Alexandria, VA 22313-1450 UNITED STATES OF AMERICA

P.O. Box 1450

Facsimile No. **571-273-8300**

International application No.

PCT/US2024/056939

Box No. III Observations where unity of invention is lacking (Continuation of item 3 of first sheet)

This International Searching Authority found multiple inventions in this international application, as follows:

This application contains the following inventions or groups of inventions which are not so linked as to form a single general inventive concept under PCT Rule 13.1. In order for all inventions to be examined, the appropriate additional examination fees need to be paid.

Group I: claims 1-9 are drawn to polymer-based membranes.

Group II: claims 10-15 are drawn to methods of making a polymer-based membrane.

Group III: claims 16-19 are drawn to systems.

Group IV: claims 20-23 are drawn to methods of separating one or more gas(es) from a mixture.

The inventions listed in Groups I-IV do not relate to a single general inventive concept under PCT Rule 13.1, because under PCT Rule 13.2 they lack the same or corresponding special technical features for the following reasons:

The special technical features of Group I, polymer-based membranes, are not present in Groups II-IV; the special technical features of Group II, methods of making a polymer-based membrane, are not present in Groups I, III and IV; the special technical features of Group III, systems, are not present in Groups I, II and IV; and the special technical features of Group IV, methods of separating one or more gas(es) from a mixture, are not present in Groups I-III.

Additionally, even if Groups I-IV were considered to share the technical features of a polymer-based membrane comprising; optionally, a substrate; optionally, an interlayer disposed on the substrate; and

i) a polymer film comprising a plurality of polymer chains; and a metal oxide layer disposed on at least a portion or all of an exterior surface or surfaces of the polymer film, wherein at least a portion of the polymer chains are immobilized and/or crosslinked by metal oxide groups of the metal oxide film, or ii) a carbonized polymer film comprising a plurality of micropores or a polyorganosilica film comprising a plurality of ultramicropores; and a plurality of a metal oxide domains disposed on at least a portion or all of an exterior surface or surfaces of at least a portion, substantially all, or all of the micropores or ultramicropores, and a method, these shared technical features do not represent a contribution over the prior art as disclosed by an article entitled "Effect of Al2O3 on Nanostructure and Ion Transport Properties of PVA/PEG/SSA Polymer Electrolyte Membrane" to Mohamed et al. (hereinafter, "Mohamed").

Mohamed teaches a polymer-based membrane (abstract, cross-linked poly(vinyl) alcohol (PVA)/poly(ethylene) glycol (PEG) membranes) comprising: optionally, a substrate (optional); optionally, an interlayer disposed on the substrate (optional); and i) a polymer film comprising a plurality of polymer chains (page 11, first paragraph, PVA/10 wt.% PEG samples, which can possibly have a stronger effect on the immobilization of the long polymer chains); and a metal oxide layer disposed on at least a portion or all of an exterior surface or surfaces of the polymer film (abstract, Al2O3; page 11, last paragraph, Al2O3 provided more H+ transport sites on the surface of the membrane), wherein at least a portion of the polymer chains are immobilized and/ or crosslinked by metal oxide groups of the metal oxide film (page 11, first-last paragraphs, A small Al2O3 filler particle can increase the conductivity of PVA/10 wt.% PEG samples, which can possibly have a stronger effect on the immobilization of the long polymer chains... Al2O3 provided more H+ transport sites on the surface of the membrane), or ii) (optional) a carbonized polymer film comprising a plurality of micropores or a polyorganosilica film comprising a plurality of ultramicropores; and a plurality of a metal oxide domains disposed on at least a portion or all of an exterior surface or surfaces of at least a portion, substantially all, or all of the micropores or ultramicropores (remains optional as ii) is optional), and a method (abstract, create novel polymer-based materials).

The inventions listed in Groups I-IV therefore lack unity under Rule 13 because they do not share a same or corresponding special technical feature.

International application No.

PCT/US2024/056939

Box No. III Observations where unity of invention is lacking (Continuation of item 3 of first sheet)					
1. As all requestions.	As all required additional search fees were timely paid by the applicant, this international search report covers all searchable claims.				
2. As all sear of additions	chable claims could be searched without effort justifying additional fees, this Authority did not invite payment al fees.				
	me of the required additional search fees were timely paid by the applicant, this international search report covers claims for which fees were paid, specifically claims Nos.:				
	d additional search fees were timely paid by the applicant. Consequently, this international search report is restricted ation first mentioned in the claims; it is covered by claims Nos.: 1-9				
Remark on Protest	The additional search fees were accompanied by the applicant's protest and, where applicable, the payment of a protest fee. The additional search fees were accompanied by the applicant's protest but the applicable protest fee				
	was not paid within the time limit specified in the invitation. No protest accompanied the payment of additional search fees.				

International application No.

PCT/US2024/056939

C. DOC	UMENTS CONSIDERED TO BE RELEVANT	
Category*	Citation of document, with indication, where appropriate, of the relevant passages	Relevant to claim No.
	MOHAMED et al., Effect of Al2O3 on Nanostructure and Ion Transport Properties of PVA/PEG/SSA Polymer Electrolyte Membrane, Polymers, Vol. 14, 26 September 2022 [retrieved on 27 December 2024]. Retrieved from the internet: <url: 14="" 19="" 2073-4360="" 4029="" https:="" www.mdpi.com="">.</url:>	
A	entire document	1-9
A	360/14/19/4029>.	1-9